Doctoral Dissertations

Graduate School

5-2004

The Development of Optical Nanosensor Technology for Single Cell Analysis

Paul Misiko Kasili
University of Tennessee - Knoxville

Recommended Citation

To the Graduate Council:

I am submitting herewith a dissertation written by Paul Misiko Kasili entitled "The Development of Optical Nanosensor Technology for Single Cell Analysis." I have examined the final electronic copy of this dissertation for form and content and recommend that it be accepted in partial fulfillment of the requirements for the degree of Doctor of Philosophy, with a major in Life Sciences.

<div style="text-align: right;">Tuan Vo-Dinh, Major Professor</div>

We have read this dissertation and recommend its acceptance:

Jeffrey M. Becker, Robert C. DeNovo, Russ F. Knapp

<div style="text-align: right;">Accepted for the Council:</div>

<div style="text-align: right;">Carolyn R. Hodges</div>

<div style="text-align: right;">Vice Provost and Dean of the Graduate School</div>

(Original signatures are on file with official student records.)

To the Graduate Council:

I am submitting herewith a dissertation written by Paul Misiko Kasili entitled "The Development of Optical Nanosensor Technology for Single Cell Analysis." I have examined the final electronic copy of this dissertation form and content and recommended that it be accepted in partial fulfillment of the requirements for the degree of Doctor of Philosophy, with a major in Life Sciences.

<div align="right">

Tuan Vo-Dinh Ph.D.
Major Professor

</div>

We have read this dissertation
and recommended its acceptance:

Jeffrey M. Becker Ph.D.

Robert C. DeNovo DVM, MS

Russ F. Knapp Jr. Ph.D.

<div align="right">

Acceptance for the Council:
Anne Mayhew
Vice Provost and Dean of Graduate Studies

</div>

(Original signatures are on file with official student records)

The Development of Optical Nanosensor Technology for Single Cell Analysis

A Dissertation Presented for the
Doctor of Philosophy Degree
The University of Tennessee, Knoxville

Paul Misiko Kasili
May 2004

DEDICATION

This dissertation is dedicated to my father, the late Prof. Edward G. Kasili, and mother, Speranza K. Kasili for their great inspiration and encouragement, for teaching me the value of education, discipline and hard-work, and my sisters Brenda and Angela for their moral support and for believing in me and being there for me.

ACKNOWLEDGEMENTS

"All Those Who Made This Ph.D. Possible."

First and foremost, I would like to thank God for blessing me with the knowledge, wisdom, will, discipline, strength, and courage that made it possible for me complete my Doctor of Philosophy degree in Biomedical Sciences.

I would like to thank Dr. Tuan Vo-Dinh, a great scientist and mentor, to have given me the great opportunity to work with him, for his guidance, patience, encouragement, support and his open door policy.

I would like to thank the members of the Advanced Biomedical and Technology Group, Oak Ridge National Laboratory (1998 – present), for their immeasurable assistance in my graduate career, especially Dr. Joel Mobley and Dr. Brian Cullum.

I would like to thank my beloved wife Serene Williams-Kasili for believing in me and for her unwavering support, our son Eric Kasili, for his great smiles –truly a bundle of joy!

Finally, I extend my deepest gratitude to my family and friends (AJ Blige, Paul Waya), for their prayers, encouragement and support.

ABSTRACT

Advances in modern biosciences and optical biosensor technology have provided exciting new insights and capabilities. The integration of these fields has witnessed revolutionary advances, which include the development of optical nanosensors. *Optical nanosensors* are devices based on a direct spatial coupling between biologically active molecules and a signal transducer element interfaced to electronic equipment for signal amplification, acquisition and recording. Optical nanosensors consist of biorecognition molecules covalently immobilized onto the nanotips nanoscale optical fiber that serves as the transducing element. By combining the specificity of biorecognition molecules and the excellent sensitivity of laser-based optical detection, optical nanosensors are capable of detecting and differentiating biochemical constituents of complex systems enabling the provision of sensitive and specific identification of specific molecular events inside living cells.

This work explores and focuses on the development and application of novel optical nanosensors for single living cell analysis. In this context, single cell analysis involves the application of optical nanosensor technology to observe and possibly map molecular events inside single living cells. Previous studies have focused on the bulk response of cells and this largely increases the probability of missing critical underlying mechanisms specific to the single cell. The ability to perform single cell analysis can dramatically improve our understanding of basic cellular processes e.g., signal transduction as well as improving our knowledge of the intracellular transport and the fate of therapeutic agents at the single cell level. This is important not only

because of the capability to perform minimally invasive analysis, but also to overcome the problem of ensemble averaging. This capability to overcome ensemble averaging has the potential to yield new information that is not available from population averaged cellular measurements.

This work involves the development and application of optical nanosensors for specific and sensitive chemical and protein analysis within single living cells. The ability of these sensors to successfully perform chemical and protein analysis at the single cell level, lay in their design specifications, size, specificity, sensitivity and eliminating interferences. With regard to their specifications, their size was in the nanometer regime, which is relative to the scale of a single mammalian cell (~ 10 μm) to allow non-invasive-to-minimally-invasive measurements in single living cells. In addition, they incorporated biological recognition molecules to achieve specificity and finally, near-field evanescent wave excitation and detection to achieve high sensitivity. High specificity and sensitivity allowed for precise and accurate identification of physicochemically detectable substances in complex matrices to eliminate any potential interference.

The optical nanosensor intracellular measurement process is straightforward and begins with a sparsely distributed cell culture in a petri dish to allow viewing of single cells using an inverted fluorescence microscope. The optical nanosensor is secured onto the manipulating arms of the microscope and gently manipulated toward the single cell, interacting with the cell, penetrating but not disrupting cellular membranes. The optical nanosensor is briefly incubated in a single living cell and the

laser is turned on and excitation light is launched into the optical nanosensor and propagated to the near field of the nanotip where the target analyte is excited by evanescent optical waves. The fluorescence signal generated when the target analyte is excited is collected by the optical set-up of the inverted fluorescence microscope, passes through spectral and spatial filters before detection with a sensitive photon counting photomultiplier tube (PMT). The PMT signal is amplified and recorded via a universal counter interfaced to a personal computer (PC). Data acquisition and recording are controlled using an integrated custom-written program, built on LabView platform.

During in vitro and in vivo measurements, the optical nanosensor response is determined in terms of the sensitivity, specificity, linear dynamic range, response time, nanosensor stability, and reproducibility. In the course of experimental measurements, it was evident that optical nanosensors have characteristics including fast response times (msec range), sensitivity (pM range), selectivity, and excellent reproducibility. In addition to the above figures of merit, optical nanosensors demonstrated biocompatibility with no observed detrimental effects on the cell under investigation in control growth conditions. This demonstrated the utility of optical nanosensor technology for minimally invasive measurement of cellular reactions without altering or destroying the chemical make-up of the cell. This work also illustrates the potential of optical nanosensors in playing an important role in elucidating and enhancing our understanding of cell signaling and transduction pathways in real-time.

PROJECT OVERVIEW

By convention, we take the cell to the analysis tools, but in this work, we use a radical approach and take the analysis tools into the cell. The main objective of this dissertation project was to conduct fundamental research with the aim to develop an innovative approach for using *Optical Nanosensor Technology for Single Cell Analysis*. More specifically, this dissertation addresses the capability of optical nanosensors to analyze the workings of individual cells without causing physiological or biological damage that may have resultant biochemical consequences. This dissertation entitled, *"Development and Applications of Optical Nanosensor Technology for Single Living Cell Analysis,"* is divided into two major sections, the *Developmental Section* and the *Application Section*. The *Developmental Section* involves the development, optimization, evaluation, and characterization of optical nanosensors. The *Application Section* is further divided into three sub-categories corresponding to one of three-immunochemical assay formats used, which include, *Direct Immunoassay Format* used for chemical analysis, *Indirect Immunoassay Format*, and *Peptide Substrate Immunoassay Format*, used for protein analysis. These assay formats are based on the type of biorecognition molecule used and biosensing technique. The *direct immunoassay format* used to detect and identify fluorescent species, registers primary immunocomplex formation at the transducer surface by optical changes in fluorescent properties. The advantage of this format is that measurement of the antibody-antigen interaction can be accomplished quickly without any need for additional antibodies or markers. *Indirect Immunoassay format*

used to detect and identify poorly-to-non-fluorescent species, mainly proteins with very weak fluorescent properties involves the use of primary (capture) and secondary (reporter) antibody. Capture antibody is immobilized onto the transducer element and binds the target molecule to form a primary immunocomplex. Shortly afterwards, the primary immunocomplex is complexed to a labeled reporter antibody that binds to a different epitope on the target molecule, for colorimetric or fluorometric detection. Finally, the *peptide substrate immunoassay format* is used to detect and identify protease or enzymatic activity. The substrate consists of a tetrapeptide sequence that a specific enzyme recognizes and cleaves, complexed to a fluorescent molecule. The way this immunoassay works is the fluorescence emission of the fluorescent molecule is quenched by the tetrapeptide sequence. Once cleaved, the fluorescent molecule can be excited and fluorescence emission detected and measured.

Corresponding to the two preceding major sections, this dissertation is divided into six parts each having its own abstract, introduction, description of experimental methods and materials, the results obtained and a summary (discussion), except for Part two which describes the technical aspects involved in the development of the optical nanosensor. Parts three, five, and six, correspond to a publication, an accepted manuscript and a submitted manuscript respectively.

Part one is the introduction to the dissertation and discusses the importance of single cell analysis and the optical nanosensor and the importance of optical nanosensors for single cell analysis. It also explains why the optical nanosensor offers the ability to monitor with spacio-temporal resolution cellular activity in a single

living cell at the single cell level. Part two describes the nanofabrication, optimization, characterization and evaluation of the optical nanosensor. Part three focuses on the first application of the optical nanosensor for the measurement of the carcinogen Benzo[a]pyrene in single living cells using the direct immunoassay format. Part four demonstrates the application of the optical nanosensor for the *in vitro* and pseudo *in vivo* measurement of apoptosis. Part five describes the application of the optical nanosensor for the measurement of caspase-9 activity in single living cells, with emphasis on nanosensor development. Part six focuses on the application of the optical nanosensor for the measurement of apoptosis in single living cells with emphasis on photosensitizer induced apoptosis. Part six also discusses the figures of merit, which are criteria used to determine why optical nanosensors are best suited for single cell analysis. In addition, a comprehensive summary discusses both the advantages, limitations and potential of the optical nanosensor and the possible outcomes together with future direction of this work.

TABLE OF CONTENTS

LIST OF FIGURES

Part One

Introduction to Single Cell Analysis: *Analyzing One Cell At A Time*

1.0 The Cell: The Basic Unit of Life

The main aim of this dissertation project is to try answering the fundamental question, "*Can we probe the workings of cells without causing physiological of biological damage that may have resultant biochemical consequences?*" [1]. As we have gained a better understanding the overall nature of bulk cell assays over time, and achieved a greater understanding of many macroscopic biological processes, we have been led to ponder the purpose of an increasingly smaller important entity, the basic unit of life, the single cell. The cell is the fundamental unit of life, a very small compartment with the capability to replicate itself. It is full of proteins, which support its life, replication, and interactions with other cells as well as its environment. Proteins are molecules made up of amino acids arranged in a specific order determined by the genetic code and are essential for all life processes.

Since the mid-1940's, biomedical researchers have made enormous progress in identifying and understanding proteins and how they interact in many cellular processes. Much of this research was "basic", scientific research that sought to discover how systems work and develop a base of knowledge that other scientists can use in order to achieve practical goals, such as treatments or cures for diseases[2, 3].

In the 1950's, scientists started to develop the current picture of the cell as a complex and highly organized entity. They found that a typical cell is like a miniature body containing tiny "organs," called organelles. One organelle is the command center, others provide the cell with energy, while still others manufacture proteins and additional molecules that the cell needs to survive and to communicate with its

2

environment. The cell components are enclosed in a plasma membrane that not only keeps the cell intact, but it also provides channels that allow communication between the cell and its external environment [2, 3].

1.1 The Importance of Single Living Cell Analysis

In recent years, many details of the biochemical mechanisms involved in the normal cell cycle have been discovered. Scientists have found that cell signaling pathways are regulated by highly complex interactions between proteins in biochemical pathways. To understand cellular function, most scientists study parts of specific biochemical pathways, such as the cell cycle, that involve individual molecules, cells, groups of cells, and whole organisms. The ultimate goal is to be able to put all the parts together to understand normal cellular activities and how they function in normal cellular activities or how they malfunction in diseases. These studies are usually performed using bulk cell assays that are blind to heterogeneity of cells and the fact that cells in a population behave asynchronously to external stimuli. A good example is the apoptosis pathway. The differences between cells in their ability to activate caspases involved in apoptosis pathway contribute to their responsiveness of any given cell within a population to apoptotic stimuli. Therefore, to study and understand molecular mechanisms that underlie such differences it is necessary to measure caspase activity in intact individual living cells [4-6]. By measuring caspase activity in single living cells, it should be possible to test hypotheses and determine the molecular mechanisms that underlie cell-to-cell

variability in response to apoptotic stimuli. In this context, it is important to understand the dynamic relationships between chemicals and molecular events in living cells in the context of a cell as a system rather than a collection of organelles and individual processes. The information obtained from such studies can be used to accurately map biological behavior and function and in the process be used to effectively pursue drug discovery. It is also important to analysis cellular components such as proteins in their native form and environment. Protein analysis techniques often involve exposing proteins to pretreatment conditions such as solubilization, denaturation and reduction. Exposing proteins to such conditions can cause modification that can end up causing artifacts in the results [7]. In addition, it is important to have the ability to monitor slight differences in the amounts of protein and other biomolecules within the smallest possible detection volumes down to the single cell level for diagnostic and technological purposes. This can be invaluable in the sense that it would permit studies that would be otherwise difficult to perform, such as, performing experiments in primary human cells from surgical specimens that are only available in very small numbers.

Accurate cellular studies can be performed if we did not have to study parts or components of a cell and then piece all the parts together like a jigsaw puzzle in order to study cell-signaling pathways. This means that we require technologies capable of performing sensitive and specific biochemical analysis within single living cells. Technologies for performing sensitive and specific biochemical analyses at the single cell level are mainly important for understanding intracellular signaling pathways that

control cell function and behavior. Such technologies should have the capability of penetrating cell membranes without disrupting or terminating cellular reactions. Disruption of the cell membrane can lead to significant changes in the parameter of interest which can occur during the course of cell lysis, resulting in an inaccurate view of the actual physiologic state of a cell [7, 8]. Cell lysis leads to disruption of the plasma membrane, which can result in order of magnitude changes in the concentrations of the analyte or proteins of interest. In addition, compartmentalized enzymes can be released and activated leading to a high background that can potentially obscure the detection of the target analyte or protein. If we could "go easier" on the cells, this information might become available to researchers.

This work focuses on the development and application of optical nanosensor technology for possibly determining all of the many molecular interactions, their components, and the order in which they occur during a biochemical-signaling pathway. The main aim of this work is to identify and possibly catalogue components in the apoptosis pathway. The hope is to yield information of the processes of apoptosis that can potentially aid researchers seeking to study or treat diseases in which cellular processes go awry and are only armed with bulk cell assay information that is not representative of what is happening at the single cell level. This information can also be used by scientists seeking to learn more about the ways single cells respond to external signals, which are often conveyed when molecules bind to special receptors in cell membranes or when molecules traverse the cell membrane. The fundamental knowledge developed through single cell analysis studies can lead

to new ways to diagnose, treat, cure, or even prevent diseases such as Alzheimer's Disease (AD), which involves neuronal apoptosis, or cancer, which involves a defect in the apoptosis machinery of a cell.

Single cell analysis involves monitoring the activities of single cells, preferably live, in their physiological conditions. These types of studies are important due to the enhanced sensitivity of single living cells to their environment. The results obtained from such studies are important because they can give an additional dimension to standard cellular assays that rely on population-averaged studies that are blind to heterogeneity and the presumed existence of subpopulations. Studies on single cells are crucial to determine the activities and functional relationships of signaling molecules within the complex cellular networks that comprise biological systems. However, to accurately measure the complex interrelationships of the elements in the biological systems, measurements must be performed on individual cells with their signaling pathways intact. Therefore, continued progress in understanding cellular physiology requires technologies capable of biochemical measurements in solitary living cells with spacio-temporal control over the regions of cells interrogated, techniques that do not compromise the integrity of the cell membrane or cause physiological damage with biochemical consequences. The disruption of the cell membrane can lead to significant changes in the parameter of interest, resulting in an inaccurate view of the actual physiologic state of the cell. This means that the accurate measurement of many cellular properties will require a technique that is minimally invasive and does not disrupt the cell, and perhaps no

recent technology has greater potential for this application the optical nanosensors [2, 3].

1.2 Optical Nanosensors

1.2.1 What Is An Optical Nanosensor?

An optical nanosensor is a measurement device consists of two components: a bioreceptor and a transducer. The bioreceptor is a biomolecule that recognizes the target analyte whereas the transducer converts the recognition event into a measurable optical signal. The uniqueness of optical nanosensors is that the two components are integrated into one single sensor. Figure 1.1 shows the basic principle of optical nanosensors. This combination enables one to measure the target analyte without using reagents. For example, the Benzo(a)Pyrene (BaP) can be measured directly within a single living cell by an optical nanosensor which is made specifically for BaP measurement by inserting the nanosensor in the cell. This is in contrast to the conventional assay in which many steps are used and each step may require a reagent to treat the cells. The simplicity and the speed of measurement is the main advantages of optical nanosensors. One major requirement for optical nanosensors is that the bioreceptor molecule has to be immobilized in direct spatial coupling to the transducer. The immobilization is done either by physical entrapment or chemical attachment. Only minute quantities of bioreceptor molecules are needed, and they are used repeatedly for measurements. The transducer element should be capable of converting the biorecognition event into a measurable optical signal and this is done
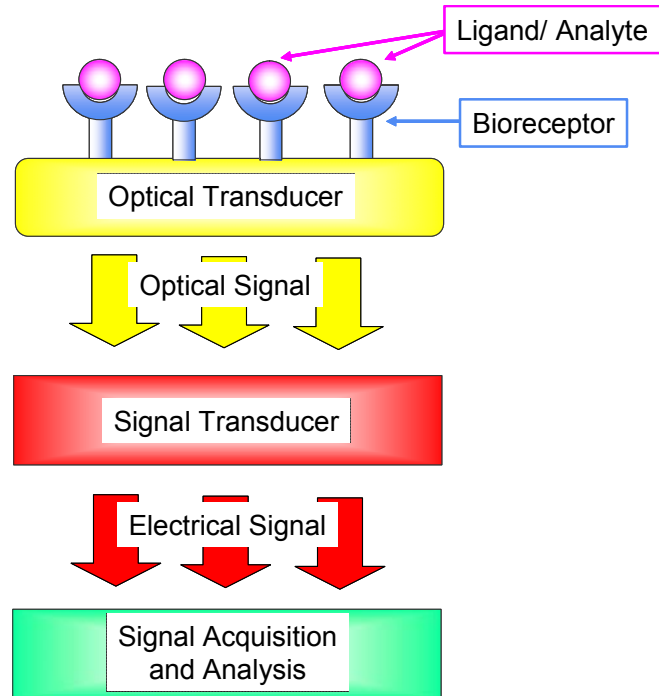
Figure 1.1 shows the basic principle of optical nanosensors. The analyte is bound by the bioreceptor (antibody) immobilized onto the optical transducer element. Molecular recognition leads to the production of an optical signal (fluorescence) which is detect by an signal transducer (photomultiplier tube). This signal is converted to a measurable electrical signal, which is acquired and analyzed and processed.

.

by measuring the change that occurs in the course of the bioreceptor reaction. The working requirements of optical nanosensors for single cell analysis include: relevance of output signal to measurement environment, accuracy and repeatability, sensitivity and spatial resolution, dynamic range, speed of response (temporal resolution), and insensitivity to electrical and other environmental interference

In the last decade, optical nanosensors have attracted much interest for their unique and novel optical properties. From the standpoint of practical applications, by confining one or more dimensions to the nanometer scale, optical nanosensors display extreme photonic interactions due to the highly enhanced role of interfaces such as quantum confinement and efficient energy transfer over nanometer distances. Optical nanosensors are small devices placed directly on or in a sample and designed to produce an optical signal that can be correlated in a specific way with the presence and concentration of the target analyte. If the target analyte is present or absent in a sample under investigation, the optical nanosensor should accordingly follow the variation in both directions and should deliver analytical information similar to or at a rate greater than the rate of change of the system

In recent years, two conspicuous research groups have made tremendous contributions and technological advances in the development of optical nanosensors for single cell analysis, namely, the Kopelman group at the University of Michigan, and the Vo-Dinh group at the Oak Ridge National Laboratory. The difference between the optical nanosensor technologies developed by the two groups is the type of analysis performed. The Kopelman group develops chemical nanosensors that use

a chemical mechanism for the molecular recognition step in chemical analysis, while the Vo-Dinh group develops biochemical nanosensors (nano-biosensors) that use a biochemical mechanism for the molecular recognition step in biochemical.

1.2.2 Chemical Optical Nanosensors

The development and application of chemical nanosensors was first reported by Kopelman and coworkers 1992 [9, 10] who produced small chemical nanosensors that enabled optical, spectral and chemical imaging on a nanometer scale. The optical nanosensors developed were for intracellular pH measurements in single living cells. These nanosensors reduced the sample volume and detection limit a billion-fold, and simultaneously the response time by a factor of a thousand [9]. Kopelman and coworkers used a micropipette puller to pull multimode and single-mode fibers down to diameters of 100-1000 nm at the tip. The pulled nanotipss were then used in the production of pH nanosensors that consisted of a pH sensitive dye, acrylofluoresceinamine, attached to the optical nanotip [11, 12]. The response time of the sensor (300 ms) was found to be 100-fold faster than conventional fiber-optic chemical sensors and was shown to be stable and reversible with respect to pH changes. The first reported application of optical chemical nanosensors was to monitor the biological process organogenesis in live rat-embryos. In this study, pH nanosensors similar to the ones described above were inserted into the extra-embrionic space of a rat conceptus, with minimal damage to the surrounding viseral yolk sac, and pH measurements were made. Values of the pH in the extraembrionic

fluid of rat conceptuses ranging in age from 10 to 12 days were then compared for any differences [9, 10, 13]

Kopelman and coworkers also produced fluorescent optical nanosensors for the detection of zinc. This is a ratiometric sensor that was fabricated and incorporates two fluorescent dyes; one is sensitive to zinc and the other acts as a reference. The sensing components are entrapped within a polymer matrix by a microemulsion polymerisation process that produces sensors that are in the size region of 20 to 200 nm. Cellular measurements are made possible by the nanoscalel sensor size and the biocompatibility of the cellular matrix. These nanosensors are capable of inter- and intra-cellular imaging and are insensitive to interference from proteins. The small size and inert matrix of these nanosensors allows them to be inserted into living cells with minimal physical and chemical perturbations to their biological functions [14].

1.2.3 Biochemical Optical Nanosensors

Due to the complexity of biological systems and the biochemical interferences caused by nanoparticles delivered using liposomal delivery, gene gun bombardment or picoinjection into single live cells, there was a need for a specific and suitable delivery and measurement technique. The need for a biochemical sensors that could be used to non-invasively-to-minimally invasively probe complex biological systems such as that of the mammalian cell led to the development of antibody-based optical nanosensors (nano-biosensors). The first application of antibody-based optical nanosensors to the field of biochemical analysis was reported in 1996 by Vo-Dinh

11

and coworkers [15]. The antibody-based optical nanosensor is a novel and unique technology first developed by the Vo-Dinh group and has the capability to perform qualitative and quantitative measurements in single live cells. This nanosensor has previously been used to successfully measure two carcinogenic compounds, benzo [a] pyrene (BaP) and its metabolite benzopyrene tetrol (BPT) in single cells [16, 17]. Using these nanosensors, it was possible to probe individual chemical species in specific locations within single living cells [17, 18]. The ability to monitor *in vivo* processes within living cells can dramatically improve our understanding of cellular function at the single cell level potentially revolutionizing cell biology [19].

The fabrication of these optical nanosensors involves a four-step process. First, a 600-micron diameter fiber optic was pulled down to 50 nm at the tip and coated with approximately 100-200 nm of silver to prevent light leakage and maximise the delivery of light to the distal end of the optical nanosensor, in essence creating quantum confinement. Following the silver metal coating procedure, the nanofibers are silanized to facilitate the immobilization of antibodies. The silanized nanotips are activated to allow covalent coupling and immobilization of antibodies. This binding procedure first called for the activation of the silanized nanotips with a solution of carbonyl diimidazole (CDI), followed by incubation of the activated nanotips with the antibody of interest for 12 hours at 4 °C. Once the antibodies are bound, the optical nanosensors are ready for studies such as to testing for the retention of antibody binding as well as sensitivity and absolute detection limits.

In previous studies, *in-vivo* measurements of single cells using optical nanosensor have been performed [18, 20-25]. In one such study, antibody-based optical nanosensors for BPT were prepared and used for the measurement of intracellular concentrations of BPT in the cytosol of two different cell lines: [1] human mammary carcinoma cells; and [2] rat liver epithelial cells [18, 20] The cells in both lines are spherical in shape and have diameters of approximately 10 microns. Several hours prior to making a measurement, the culture media of the cells was spiked with a known amount of BPT. Then immediately prior to measurement, the culture media was aspirated and the cells rinsed several times and finally replaced with BPT free media. The results from this work, demonstrated that the concentration of BPT in each of the different cell lines was the same, suggesting that the means of transport of the BPT into the cells was the same in both cases (probably by diffusion). By performing similar measurements inside various subcellular compartments, it could be possible to obtain critical information about the location of BPT formation within cells and its transport throughout the cell during the process of carcinogenesis. It was also shown in this work that the insertion of a nano-biosensor into a mammalian cell does not effect the cell's normal function, as was evidenced by the monitoring of cell division prior to and following a measurement [19]. Additional tests were performed by placing the nano-biosensors in a measurement system like the one described for chemical nanosensors and inserting the distal end of the sensor into a solution of BPT. From these measurements, it was found that the antibodies had retained greater

than 95 % of their binding affinity for BPT and that the absolute detection limit for BPT using these sensors was approximately 300 zeptomoles (zepto = 10^{-21}) [18, 25].

1.3 Optical Nanosensors for Single Cell Analysis

1.3.1 Principles of Optical Nanosensors

Despite the wide variety of bioreceptors and optical transducer elements employed, they are all based on the same principle (previously shown in Figure 1.1): General principles of optical nanosensor). Bioreceptors can be biological molecules such as antibodies, enzymes, non-enzymatic proteins, peptide substrates or nucleic acids. Optical transduction describes the measurement technique e.g., absorption, fluorescence, phosphorescence, Raman, surface enhanced Raman scattering (SERS), refraction, dispersion spectrometry, etc. These spectroscopic techniques can be used to measure any of many different optical properties including the amplitude, energy, polarization, decay time and/or phase. The most commonly measured parameter of the electromagnetic spectrum is amplitude, as it can generally be correlated with the concentration of the analyte of interest easily. While amplitude is the most commonly measured, the other parameters can also provide a great deal of information about the analyte of interest as well. For instance, the energy of the electromagnetic radiation measured can often provide information about changes in the local environment surrounding the analyte, its intramolecular atomic vibrations (i.e. Raman or infrared absorption spectroscopies) or the formation of new energy levels (i.e. luminescence, UV-vis absorption). Therefore, the resulting interaction between the analyte and the

bioreceptor then produces an effect that can be measured via the transducer, which converts this effect into some type of measurable signal.

1.3.2 Optical Nanosensor Immunoassay Formats

One key characteristic in determining the utility of optical nanosensors is their ability to specifically measure the analyte of interest, without having other chemical species interfere with the measurement. The specificity is dependent on two factors, the type of biorecognition molecule and the target analyte (whether inherently fluorescent or not). These factors dictate the type of immunoassay that can be applied for analysis. In addition, the type of immunoassay format should allow measurements to be made in complex matrices such as that of mammalian cells. Two different types of immunoassay formats are described, *direct* and *indirect* immunoassay format, with the ultimate aim of single cell analysis (Figure 1.2). *Direct* and *indirect* immunoassay format register immunochemical complex formation at the transducer surface via optical changes. The advantage of a *direct* immunosensor is that measurement of the primary immunocomplex formation (antigen–antibody interaction) can be accomplished immediately without any need for additional antibodies or markers. For *indirect* immunoassay format, the measurement of the secondary immunocomplex formation (antigen–antibody-labeled antibody interaction) is accomplished immediately with additional antibodies or markers. The *direct* immnuoassay format consists of antibodies as biorecognition molecules where antibodies bind target molecules in the bio-sensitive layer of the sensor. The resulting interaction between
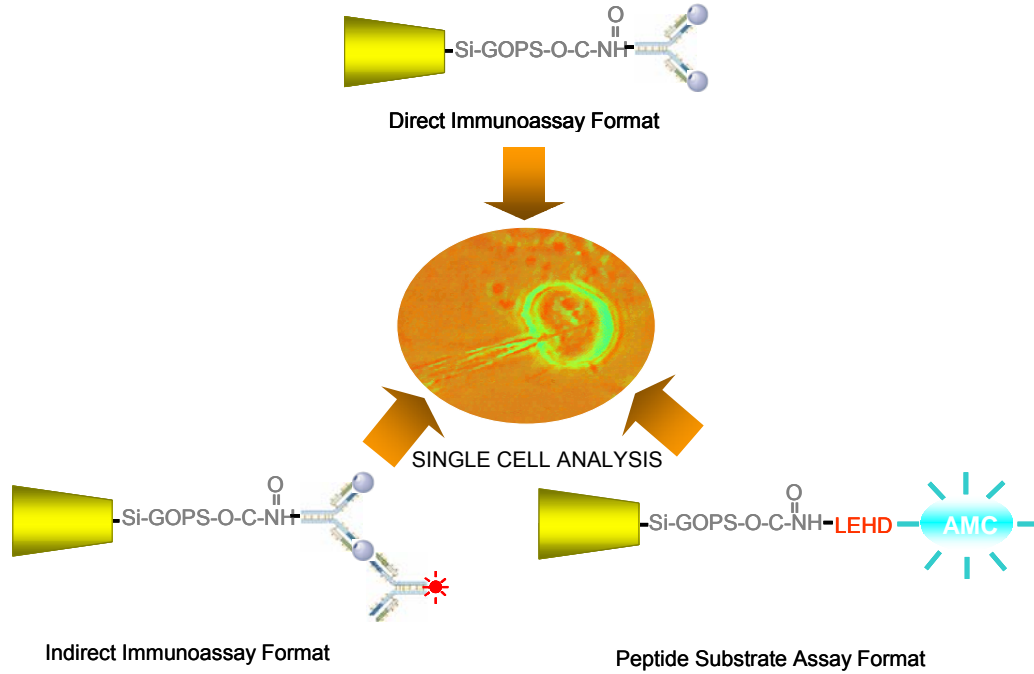
Figure 1.2 shows the *direct* and *indirect* immunoassay format used for single cell analysis. Immunochemical complex formation at the transducer surface was monitored via optical changes.

the antibody and target molecule produces a measurable fluorescent signal when excited by the appropriate wavelength. The direct assay format is the simplest, and often most sensitive, of the above assay formats. In a direct measurement format, the target molecule interacts with and binds to the immobilized antibody, at which time an optical property of the antigen is measured. This direct measurement technique is most often used in the analysis of molecules that are intrinsically fluorescent, due to the high sensitivity of the fluorescence technique [26]. The challenge associated with *direct immunoassay* format is the limitation to measuring intrinsically fluorescent target molecules, though this can be solved by using the *indirect* immunoassay format. The *indirect* assay format is a versatile and sensitive assay based on the capture of the analyte by one antibody (capture antibody) and the subsequent detection by secondary antibody (reporter antibody). The target antigen must have two epitopes and the capture and reporter antibodies must have different antigenic specificities. Many proteins in fact have repeating epitopes so this is not a major problem. The reporter antibody is labeled with a fluorescent molecule, such as Cy5 to facilitate detection of target analyte when the secondary immunocomplex is formed. The first step is to bind the antigen using the capture antibody immobilized to the surface of the transducer element. The second step is to bind fluorescent-labeled reporter antibody to the antigen forming a "sandwich like" structure. Once bound, the fluorescence intensity of the labeled reporter antibody is measured when excited by the appropriate wavelength. and correlated to the amount of target molecule that is present [19].

17

The third immunoassay format, tetrapeptide enzyme-substrate assay, consists of an enzyme substrate complexed to an indicator dye. Tetrapeptide enzyme subsrates can only be cleaved by specific enzymes. An activated target enzyme would recognize the sequence it specifically cleaves and the resulting interaction between the enzyme and the enzyme substrate complex would yield a fluorescent indicator dye that would fluoresce when excited by the appropriate wavelength. An illustration of this biosensing scheme is shown in Figure 1.3. In this work, optical nanosensors are for the first time used that employ an enzyme-substrate system that is specifically used to measure caspase activity in single cells. Tetrapeptide enzyme substrates are specifically used to measure enzyme activity. They consist of a synthetic peptide sequence complexed to a fluorescent molecule. During the enzymatic response, the activated enzyme cleaves the tetrapeptide sequence producing a fluorescent product that is readily measurable by fluorescence spectroscopy. This is based upon the enzyme having a region whose three dimensional structure has a specific geometrical configuration that exactly matches the three dimensional configuration of the substrate of interest. Enzymes accelerate the rate of chemical reactions and each enzyme has a unique shape that determines its function and is complementary to its substrate meaning one enzyme specifically works on one type of substrate. Enzyme-substrate-based optical nanosensors can be extremely sensitive and have extremely low detection limits [19]. The ultimate goal of single cell analysis studies is to offer insight into cell function when perturbations in the local environment have occurred
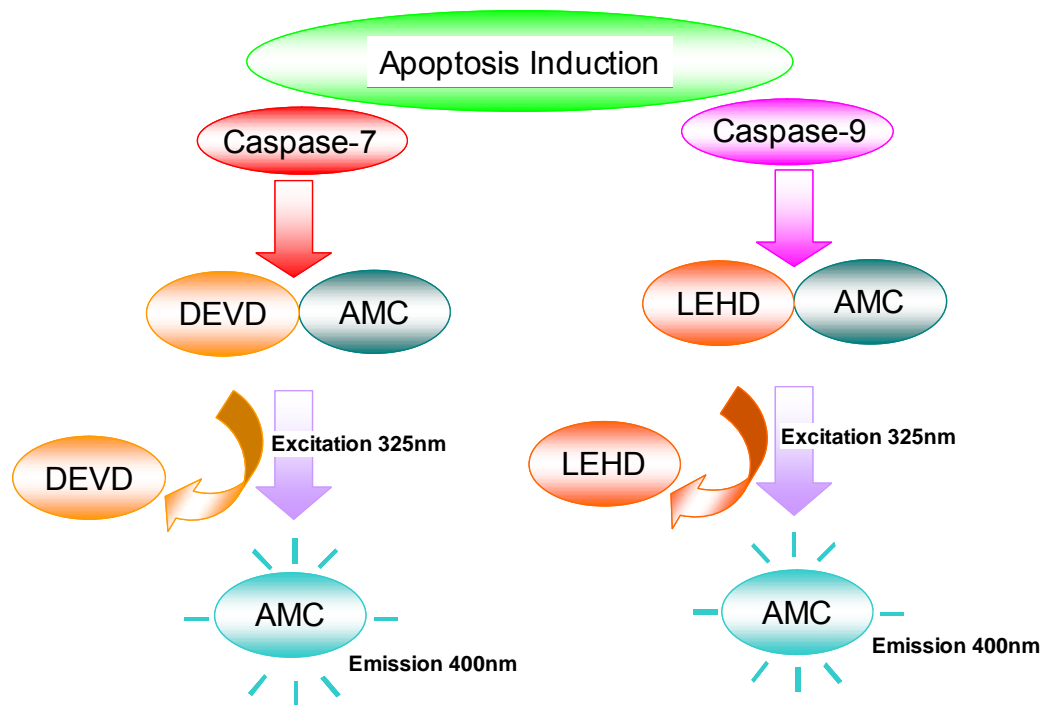
Figure 1.3 is an illustration of the tetrapeptide substrate immunoassay format. An activated target enzyme (caspase-9 or caspase-7) would recognize the sequence (LEHD = Leucine-Glutamate-Histidine-Aspartate OR DEVD = Aspasrtate-Glutamate-Valine-Aspartate) it specifically cleaves and the resulting interaction between the enzyme and the enzyme substrate complex would yield a fluorescent indicator dye (AMC = 7-amino-4-meathylcoumarin) that would fluoresce when excited by 325 nm Helium-Cadmium laser.

with the cellular machinery intact. Optical nanosensors can be implemented in the direct chemical analysis of single cells whereby the internal environment of an individual cell is directly monitored by correlating the binding of antigen to antibody based on a fluorescent intensity signal as a function of time or concentration of the analyte. Previous methods used to analyze single cells are too slow requiring times of the order of seconds to remove the cell contents for analysis during which concentrations of metabolites of interest could undergo order-of-magnitude changes. Optical nanosensors have the capability to quantitate reactions that occur in sub-second times without altering or destroying the chemical makeup of the cell. This will also enable measurement of cellular processes, such as apoptosis and the functioning of proteins in their native environment and form.

References

1. Zandonella, C., *Cell Nanotechnology: The Tiny Toolkit.* Nature, 2003. **423**: p. 10-12.
2. Behbehani, M., *Cell Physiology Source Book*, ed. N. Sperelakis. 1995, San Diego: Academic Press. 490-494.
3. Morris, C., *Cell Physiology Source Book*, ed. N. Sperelakis. 1995, San Diego: Academic press.
4. Tsien, R., *Intracellular signal transduction in four dimensions: from molecular design to physiology.* Am J Physiol Cell Physiol, 1992. **263**: p. C723-C728.
5. Giuliano, K., Post, PL., Hahn, KM., Taylor, DL., *Fluorescent protein biosensors: measurement of molecular dynamics in living cells.* . Annu Rev Biophys Biomol Struct., 1995. **24**: p. 405-34.
6. Jankowski, J., Tratch, S., Sweedler, JV., *Assaying single cells with capillary electrophoresis.* Trends Anal. Chem., 1995. **14**: p. 170-176.
7. Luzzi, V., Lee, C.L., Allbritton, N.L., *Localized sampling of cytoplasm from Xenopus oocytes for capillary electrophoresis.* Anal Chem, 1997. **69**(23): p. 4761-4767.
8. Li, H., Sims, C.E., Wu, H., Allbritton, N.L., *Spatial Control of Cellular Measurements with the Laser-Micropipet.* Anal. Chem., 2001. **73**.
9. Tan, W., Shi, ZY., Smith, S., Birnbaum, D., and Kopelman, R., *Submicrometer Intracellular Chemical Optical Fiber Sensors.* Science, 1992. **258**(5083): p. 778-781.
10. Tan, W., Shi, ZY., Smith, S., and Kopelman, R., *Development of Submicron Chemical Optic Sensors.* Anal. Chem, 1992. **64**(23): p. 2985-2990.
11. Munkholm, C., D.R. Walt, and F.P. Milanovich, *Preparation of Co2 Fiber Optic Chemical Sensor.* Abstracts of Papers of the American Chemical Society, 1987. **193**: p. 183-ANYL.
12. Munkholm, C., D.R. Parkinson, and D.R. Walt, *Intramolecular Fluorescence Self-Quenching of Fluoresceinamine.* Journal of the American Chemical Society, 1990. **112**(7): p. 2608-2612.
13. Tan, W.H., et al., *Submicrometer Intracellular Chemical Optical Fiber Sensors.* Science, 1992. **258**(5083): p. 778-781.
14. Sumner, J., Aylott, JW., Monson, E., Kopelman, R., *A fluorescent PEBBLE nanosensor for intracellular free zinc.* Analyst, 2002. **127**(1): p. 11-16.
15. Alarie, J.P. and T. VoDinh, *Antibody-based submicron biosensor for benzo a pyrene DNA adduct.* Polycyclic Aromatic Compounds, 1996. **8**(1): p. 45-52.
16. Vo-Dinh, T., Alarie, JP., Cullum, BM., Griffin, GD., *Antibody-based nanoprobe for measurement of a fluorescent analyte in a single cell.* Nat Biotechnol, 2000. **18**(7): p. 764-767.
17. Kasili, P.M., Cullum, B.M., Griffin, G.D., and Vo-Dinh, T., *Nanosensor for In-Vivo Measurement of the Carcinogen Benzo [a] Pyrene in a Single Cell.* Journal of Nanoscience and Nanotechnology, 2003. **2**(6): p. 653-658.

18.   Cullum, B., Griffin, GD., Miller, GH., Vo-Dinh, T., *Intracellular measurements in mammary carcinoma cells using fiber-optic nanosensors.* Anal Biochem, 2000. **277**(1): p. 25-32.

19.   Vo-Dinh, T., and Cullum, BM., *CRC Handbook for Biomedical Photonics.* Nanosensors for Single Cell Analysis, ed. T. Vo-Dinh. 2003, Newyork: CRC Press. 14.

20.   Cullum, B.M., et al., *Intracellular measurements in mammary carcinoma cells using fiber-optic nanosensors.* Analytical Biochemistry, 2000. **277**(1): p. 25-32.

21.   Cullum, B.M. and T. Vo-Dinh, *The development of optical nanosensors for biological measurements.* Trends in Biotechnology, 2000. **18**(9): p. 388-393.

22.   Cullum, B.M. and T. Vo-Dinh, *Optical nanosensors and biological measurements.* Biofutur, 2000. **2000**(205): p. A1-A6.

23.   Vo-Dinh, T.G., G. D.; Alarie, J. P.; Cullum, B. M.; Sumpter, B. and Noid, D., *Development of Nanosensors and Bioprobes.* J. Nanoparticle Research, 2000. **2**: p. 17.

24.   Vo-Dinh, T., et al., *Antibody-based nanoprobe for measurement of a fluorescent analyte in a single cell.* Nature Biotechnology, 2000. **18**(7): p. 764-767.

25.   Cullum, B., Vo-Dinh, T., *The development of optical nanosensors for biological measurements.* Trends Biotechnol, 2000. **18**(9): p. 388-393.

26.   Vo-Dinh, T., et al., *Antibody-Based Fiberoptics Biosensor for the Carcinogen Benzo(a)Pyrene.* Applied Spectroscopy, 1987. **41**(5): p. 735-738.

Part Two

Development of Optical Nanosensors

2.0 Overview

This chapter discusses the design and development of two classes of optical nanosensors (i) antibody based optical nanosensors and (ii) enzyme substrate based optical nanosensor. Antibody based optical nanosensors are used for two immunoassay formats, *direct* and *indirect* immunoassay format. *Direct* immunoassay format involves the use of antibodies on a solid-state platform to capture a target analyte (antibody-antigen), while *indirect* immunoassay format involves the use of a set of antibodies to capture and identify a target analyte (antibody-antigen-[labeled[antibody) forming a sandwich type structure. The immobilized capture antibodies bind one epitope of the target analyte, while the reporter antibodies bind another epitope of the target analyte. The enzyme substrate based technique as the name implies utilizes a enzyme substrate that is recognized by a specific enzyme, cleaved and generates a fluorescent product tat is detected. This section is divided into 5 sub-sections involving the *(i) introduction (ii) principle of operation (iii) nanofabrication (iv) characterization (v) optimization and (vi) evaluation.*

2.1 Introduction to Optical Nanosensors

Optical nanosensors are in general nanoscale devices consisting of two components, a biorecognition molecule and an optical signal transducer element in direct spatial coupling. The biorecognition molecule recognizes the target analyte and the transducer converts the recognition event into a measurable signal. The uniqueness of optical nanosensors lies in their size, novel optical properties, and the

two components (biorecognition molecule and transducer element) integrated into one single nanosensor. With dimensions in the nanometer range, the photonic interactions of optical nanosensors exhibit dramatic changes. Key contributory factors include confinement of light within the nanosensor and efficient energy over nanoscale distances, due the highly enhanced role of interfaces. The finely tailored scale of the optical nanosensors provides a high surface area-to-volume ratio, which is important for surface chemistry to facilitate immobilization of biorecognition molecules. At the nanoscale, in contrast to conventional assay in which many steps are used and each step may require a reagent to treat the sample, the optical nanosensor offers simplicity and speed of measurement. The general principle of an optical nanosensor is illustrated in Figure 2.1. The most important part is the biosensing element (biorecognition molecule) at which the molecular recognition process takes place, since this defines the overall selectivity of the entire nanosensor. The sensing-element surface is functionalized facilitate covalent immobilization process and to prevent interfering substances from reaching the sensing-element surface. The target analyte recognition process takes place at the surface of the biosensing element leading to change in an optical property that can be transformed into an electrical signal by an optical signal transducer e.g., photon counting photomultiplier tube (PMT). The optical signal transducer can improve the sensitivity of detection of the physicochemical interaction. The electrical signal from the optical
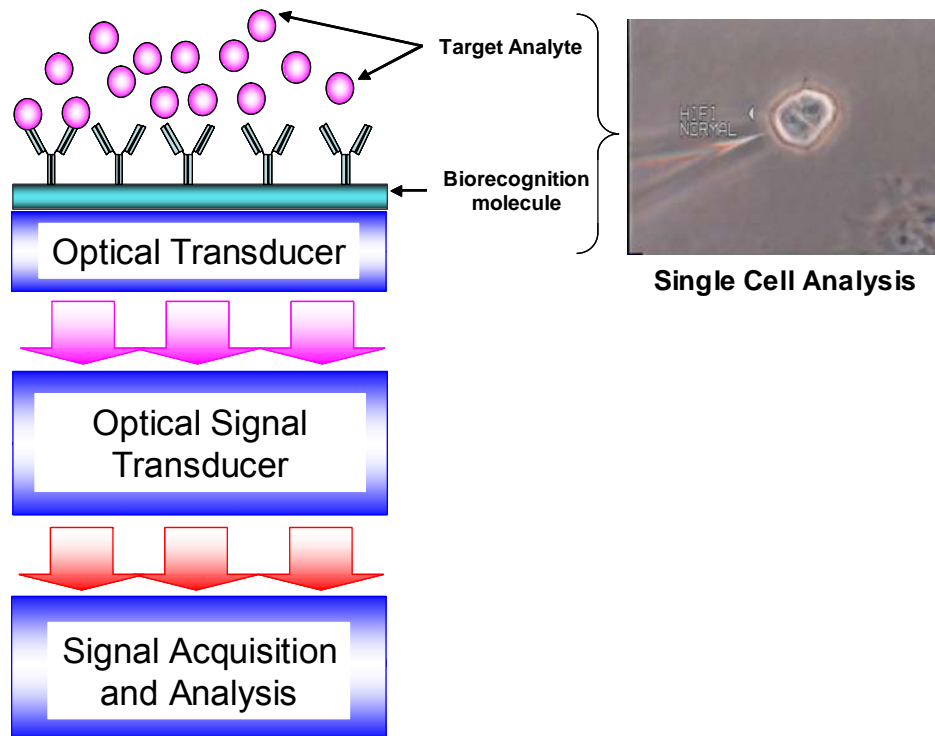
Figure 2.1: Schematic representation of biosensing principle: The interaction of between the analyte and biorecognition molecule secured on the optical transducer is designed to produce an effect that can be converted by the optical signal transducer to a measurable electrical signal. Inset is an image of an optical nanosensor and single living MCF-7 cell

2.1.2 Description of Optical Nanosensors

Optical nanosensors can be defined as analytical devices containing a sensing element of biological origin, which is either integrated within or in intimate contact with an optically transparent transducer element. The optical transducer in intimate contact with the sensing element in used to convert the biological recognition, association or dissociation, event into a measurable signal [27]. The end goal is to produce a continuous electronic signal, which is directly proportional to the fluorescence signal generated when the target chemical or biomolecule in a sample are excited. The sensing element of biological origin may be biocatalytic e.g., enzymes, or affinity systems e.g., antibodies. Figure 2.2 shows a diagrammatic representation of an optical nanosensor

2.1.3 Optical Nanosensor Principle of Operation

The type of physical transducers used to create optical nanosensors form the basis of their characterization. Optical nanosensors for example, are fabricated from optical fiber, which is optically transparent enabling optical measurements. They use fluorescence of light by a product formed or reactant depleted involving the biorecognition molecule. Optical nanosensors are used to relate the fluorescent intensity produced during the product formation or reactant depletion to the presence or absence of analyte. Some types of molecules when illuminated with light corresponding to the region of absorbance are promoted from ground state to excited state. At excited state, they can release energy by emitting light of a longer
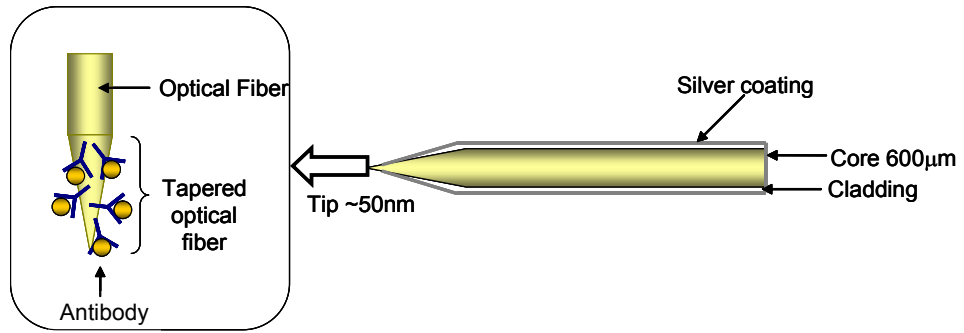
Figure 2.2 shows a diagrammatic representation of an optical nanosensor

wavelength and less energy. This phenomenon is known as fluorescence and is described in Figure 2.3 by the Jablonski diagram. Fluorescence can be defined as an optical phenomenon that occurs when a molecule of substance is irradiated and absorbs energy in the form of a photon. The absorbed energy produces a change in the electronic state of the molecule, where the electron is moved to a higher energy level, singlet state. This is a temporary short-lived state and the electron returns to its normal ground state by emitting a photon of less energy (light at different wavelength). Due to the loss of energy, the emitted fluorescent radiation has a longer wavelength than that of the absorbed light. The distribution in the wavelength that the molecule absorbs is known as the absorption spectrum, and the distribution in the wavelength emitted is known as fluorescence emission spectrum [28].

2.2 The Fluorescence Phenomenon

Fluorescence has three major advantages over other light-based investigation methods: high (i) sensitivity, (ii) speed of detection, and (iii) safety. Sensitivity is an important factor mainly because the fluorescence signal generated is proportional to the concentration of target analyte under investigation and relatively small changes in concentration within living cells that can have significant physiological effects can be detected and measured. Fluorescent techniques have the capability to reliably and accurately determine concentrations only as low as pico- and even femtomolar. In some cases, quantities less than an attomole ($<10^{-18}$ mole) have been detected [29]. Fluorescence measurements can also be used to monitor very rapid changes in

29
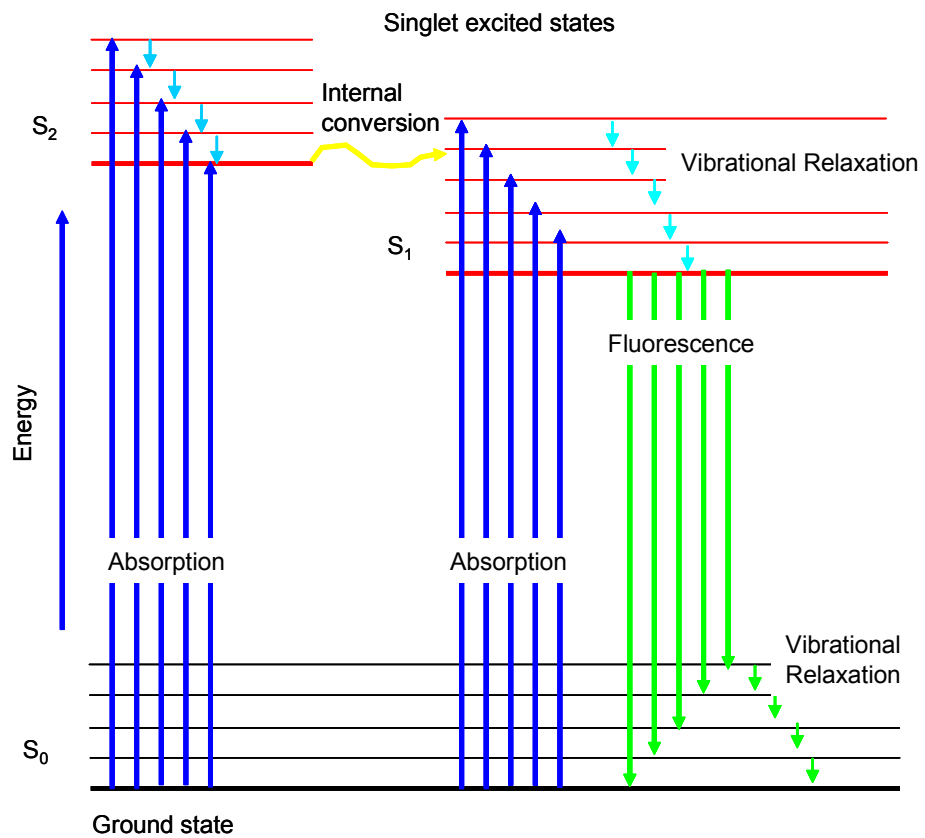
Figure 2.3 Simplified Jablonski Diagram illustrating the processes involved in the creation of an excited electronic singlet state by optical absorption and subsequent emission of fluorescence.

concentration that occur within nanoliter to femtoliter volumes. Fluorescent measurements detecting changes in fluorescence intensity on the order of picoseconds can be detected if necessary. Furthermore, since fluorescence is a non-invasive technique, it does not interfere with a sample. The excitation light levels required to generate a fluorescence signal are low, reducing the effects of photo-bleaching, and single living cells can be investigated with no adverse effects on its natural physiological behavior. The point of safety implies that samples are not affected or destroyed in the process, and no hazardous byproducts are generated during fluorescent measurements [29].

Fluorescence is an established and powerful technique for studying molecular interactions in analytical chemistry, biochemistry, cell biology, photochemistry, and environmental science whilst boasting phenomenal sensitivity [30]. The levels of fluorescence from a single fluorophore are extremely low (hundreds to thousands of photons per second). The fluorescence generated is observed by imaging the fluorescent signal through a pinhole onto a photomultiplier tube (PMT), with which we can count the number of photons detected. This should give us a very high signal to noise ratio, and allow us clearly to determine when the fluorophore binds to the fluorescent molecules, and when it associates or dissociates. In this work, as in other optical sensors, one partner of the reaction is immobilized on the waveguide surface and binding a fluorescent complementary partner is monitored. The excitation light is guided through the wave-guide leading to an excitation of those molecules that are in close proximity to the wave-guide surface within the evanescent field and the emitted

fluorescence is monitored using PMT. Fluorescence signal is collected by the objective, and passes through spectral and spatial filters before detection with a PMT. The PMT signal is amplified and plotted vs. time on a PC to form electropherograms. Depending on the assay principle, fluorescent signal intensity is recorded as a function of time and as a function of concentration.

2.3 Components of Fluorescence Measurement System

The Fluorescence measurement systems consist of the following components; a light source emitting selected wavelengths to excite the fluorophore. (selected light sources are obtained by using lasers), optical fiber that serves as the waveguide to deliver light to the sensing region, the biorecognition element which is in direct contact with the optical device and target analyte to be analyzed, optics or an optical system to collect and convey the light emitted by the fluorophore to a photodetector e.g., photomultiplier tube (PMT), a photodetector for detecting the emitted light, device for signal amplification, data processing and output.

The following section describes the basic physics behind the relationship between total internal reflection and evanescent optical waves. This will be followed by a description of the three-immunoassay formats: Direct, Indirect and tetrapeptide substrate, respectively, used in this work

2.4 Optical Nanosensor Principle of Operation

Optical nanosensor based on evanescent fluorescence were developed and used in the work. They work via evanescent optical waves produced by total internal reflection (TIR). TIR is an optical phenomenon that occurs when light energy propagating in a dense medium e.g., silica, meets an interface with a less dense medium e.g., cytosol of a cell. However, some of the light energy propagates a short distance (a few hundred nanometers) into the cytosol of a cell, generating an evanescent wave. Evanescent optical waves travel into restricted regions of materials with exponentially diminishing energy. With evanescent optical waves, there is no free-beam propagation and the laser energy can be confined to a layer less than half the wavelength of the excitation source providing for near-field excitation. The evanescent optical waves produced enable detection of particular components of complex biomolecular assemblies with exquisite sensitivity and selectivity. If this energy is not absorbed, it passes back into the glass. However, if a fluorescent molecule is within the evanescent wave it can absorb photons and be promoted from ground to excited state. The fluorescence signal is produced at the nanotips when the components of the immunocomplex or complex biomolecular assemblies are excited with evanescent optical waves lie in the near-field of the optical nanosensor. This means that it is possible to capture fluorescence with a very low background of excitation light creating a high signal-to-noise ratio. Optical nanosensors utilize the formation of an evanescent field, which provides a highly localized excitation area in

the near field of the optical nanosensor, for the excitation of fluorescent molecules

[31, 32]

2.5 Total Internal Reflection and Evanescent Wave Theory

Total internal reflection and evanescent wave theory explains that if a material of a higher refractive index borders a medium of lower refractive index, corresponding to Newton's and Snell's law, the light is reflected and refracted at the border between the two media. In the case of the optical nanosensor, the light is totally internally reflected, it is kept within the high refractive index material layer by multiple reflections on both interfaces sides and guided through the optical fiber. The critical angle (θ) is the minimum angle at which total internal reflection takes place and no light passes through the low refractive index layer except at the nanotip. Using Snell's law the critical angle can be calculated using the equation [33]. Thus the critical angle is defined by the equation;

$$\sin\theta = \frac{n_2}{n_1}$$

At TIR, no wave exists traveling through the higher index medium. However, a wave results at the nanotip, along the interface and decaying exponentially. Thus at the interface of the nanotip, a electromagnetic field (evanescent field) is created. The

penetration depth of the evanescent field depends on the refractive indices of the media and the critical angle, calculated by Snell's law [33, 34]

2.6 Penetration Depth (d_p) of Evanescent Wave Interaction

A diagrammatic representation of the penetration depth (dp) of evanescent wave interaction is shown in Figure 2.4. The near-field light oozing out from the probe irradiates an area through the tip of the aperture creating an evanescent field. The evanescent field provides a highly localized excitation area (distances $<0.5\lambda$).The binding interaction event takes place and the analyte is excited by the evanescent wave on the surface of the waveguide. Using the penetration depth equation, the penetration depth (dp) of the evanescent wave of different laser wavelengths can be calculated. The following penetration depths were calculated for Helium-Neon laser (632.8nm) δ = 351.6nm, Argon-Ion laser (514nm) δ = 285.6nm, Argon Ion laser (488nm) δ = 271.1nm and Helium-Cadmium (325nm) δ = 180.6nm. From the equation to calculate the d_p, it can be seen that greater differences in refractive indices (n_1 and n_2) allow greater angles of incidence for the light guide, due to the effect of the critical angle. The thinner the guiding layer (the high refractive index layer, n_2) the greater the number of reflection incidences whereas d_p becomes shorter. The result of both effects is an increase of the interacting area of the evanescent wave[33]. In optical nanosensors, this increases the sensitivity if the device. The penetration depth (d_p) is given by the following equation;
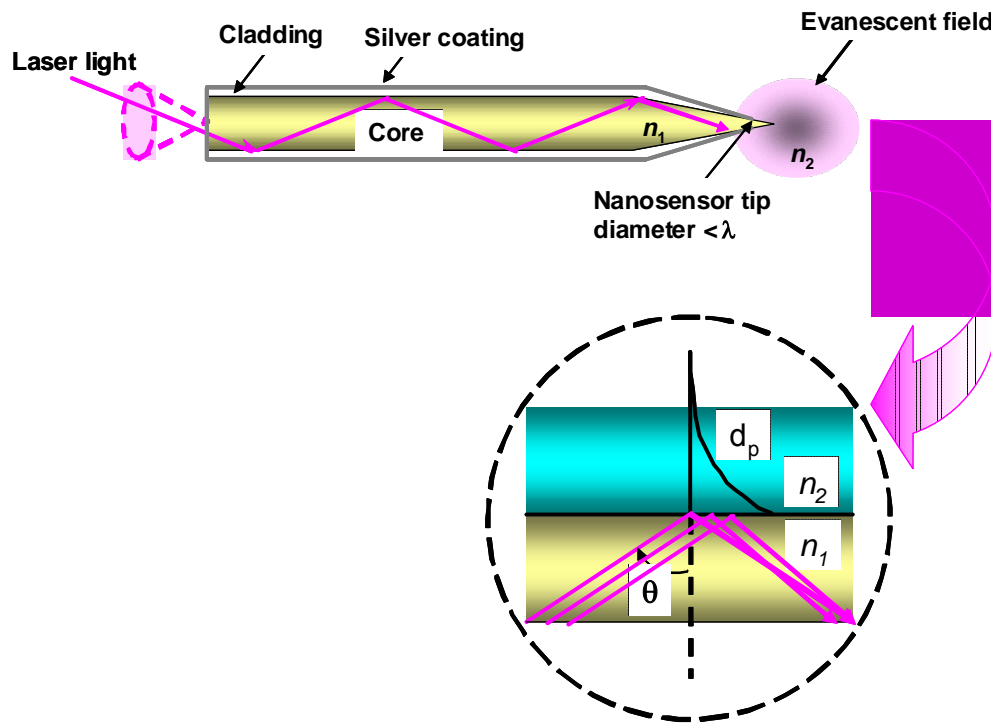
Figure 2.4 shows the formation of an evanescent field at the nanotip when laser light is launched into the optical nanofiber. Inset is a representation of the penetration depth (d_p) of the evanescent wave which is dependent of the wavelength of light transmitted through the core.

$$d_p = \frac{\lambda}{2\pi(n^2_1 \sin^2\theta - n^2_2)^{\frac{1}{2}}}$$

2.7 Nanofabrication of Optical nanosensor

The nanofabrication of optical nanosensors involves a number of parameters each of which must be optimized for efficient and effective experimental design. One important parameter is the method of choice for attachment of biorecognition molecule. Some of the issues to be considered in choosing an appropriate support and the associated attachment chemistry include: the level of scattering and fluorescence background inherent in the support material and added chemical groups; the chemical stability and complexity of the construct; the amenability to chemical modification or derivatization; surface area; loading capacity and the degree of non-specific binding of the final product. [35]. The solid support selected for immobilization of biorecognition molecule was silica-based optical fiber for the following reasons. Silica-based optical fiber is a readily available and inexpensive support medium, possessing a relatively homogeneous chemical surface whose properties have been well studied and which is amenable to chemical modification using very versatile and well developed silanization chemistry [36]. Although silanized proteins can be covalently linked to an unmodified silica surface, most attachment protocols involve chemically modifying the silica surface to facilitate attachment of the biorecognition molecule [37].

Figure 2.5 outlines the multi-step nanofabrication process. Briefly, the nanofabrication process involves the following steps: (i) fiber preparation, polishing and pulling process, (ii) silver deposition process, (iii) protein immobilization chemistry and (iv) immunochemical assay formats for single cell analysis. The immobilization of the biorecognition molecule is very important for the performance of the optical nanosensor itself due to the influence on the stability, activity and reproducibility of the sensing layer. The biological recognition molecules are linked to the sensor surface by covalent immobilization which is achieved by modifying the silica surface using a four step process, that involves washing, silanization, activation and finally protein immobilization. Covalent attachment is more stable than physical absorption or photo-immobilization. Preparation of two-dimensional surfaces usually involves treatment silane couplng reagents for silanol modifications [35, 38]. Silanol modifications are chemically stable, and ussually eliminate undesired steric interference from the support, and are hydrophilic enough to be freely soluble in aqueous solution and not produce non-specific binding to the support [35]).

The surface density of the optical nanosensor is an important parameter because a low surface coverage will yield a correspondingly low conjugation signal, and decrease the conjugation rate, while reasonably high surface densities may yield a high conjugation signal [35]. The relatively high surface area to volume ratio of the optical nanosensors greatly increases the loading capacity of biorecognition molecules such as antibodies. The surface area permits relatively large amounts of antibody to be linked to the surface resulting in strong signal intensities and a good

```
┌─────────────────────────────────────────────────────┐
│ Cleaving fiber 8″, Polish fibers 30μm Al₂O₃          │
└─────────────────────────────────────────────────────┘
                         ↓
┌─────────────────────────────────────────────────────┐
│ Pulling of Optical Fibers (600 μm → 50/ 100 nm)      │
└─────────────────────────────────────────────────────┘
                         ↓
┌─────────────────────────────────────────────────────┐
│ Silver Coating    (~ 100 → 200 nm)                    │
└─────────────────────────────────────────────────────┘
                         ↓
┌─────────────────────────────────────────────────────┐
│ Silanization of Fiber    (GOPS)                       │
│                       Glycidoxypropyltrimethoxysilane │
└─────────────────────────────────────────────────────┘
                         ↓
┌─────────────────────────────────────────────────────┐
│ Activation of Fiber         (CDI)                     │
│                          Carbonyldiimidazole          │
└─────────────────────────────────────────────────────┘
                         ↓
┌─────────────────────────────────────────────────────┐
│ Protein Binding – e.g.mouse IgG for BaP              │
└─────────────────────────────────────────────────────┘
```
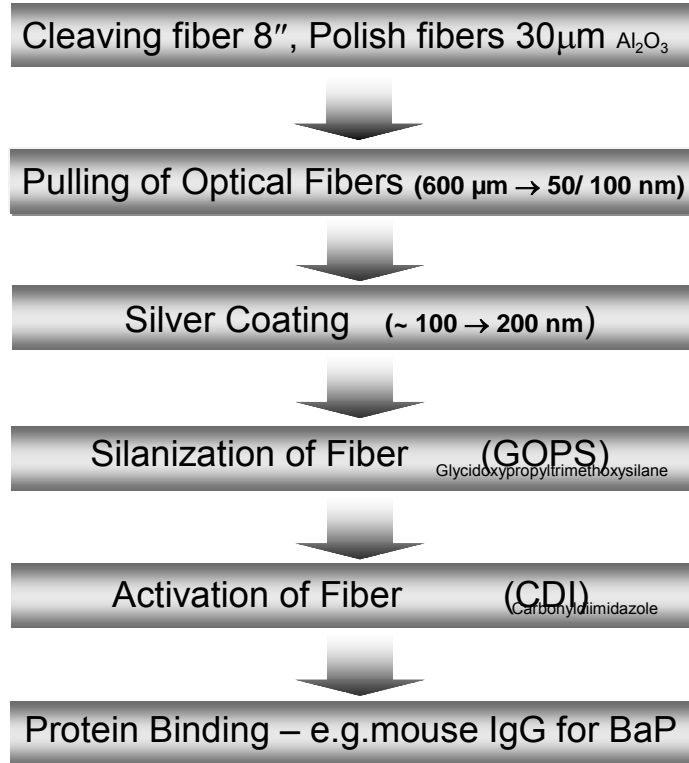
Figure 2.5 shows the multistep process involved in the nanofabrication process

specificity though at this scale, the optical nanosensor suffer from a limited dynamic range.

Immobilization of proteins to solid supports such as polystyrene or silica can be achieved using multiple methods. Based on previous laboratory experience and information in the literature, the linking reagents glycidoxypropyltrimethoxysilane (GOPS) and 1,1'- carbonyldiimadazole (CDI), and its associated bonding procedures was selected. This immobilization procedure has been thoroughly evaluated by Alarie *et al.,* [39] based on two criteria, the amount of antibody that can be loaded, and the retention of antibody activity, i.e., the ability of the immobilized antibody to recognize its specific antigen after immobilization as determined by the ratio of the moles of antigen bound to the moles of antibody immobilized. These criteria are important because in direct and indirect assays, sensitivity is directly proportional to antibody loading [40, 41]. In addition, the preservation of the antibody activity on bonding to the solid silica support influences both sensitivity and selectivity.

2.7.1 Cleaving, Polishing and Pulling

600μm diameter plastic clad optical fiber was used to construct the optical nanosensors. Optical fiber consists of a central core and median cladding made of fused silica (SiO_2), and an outer jacket made of a hard polymer. Lengths of optical fiber measuring eight inches are sectioned off a reel of optical fiber. The fiber tips are polished for about one to two hours to facilitate coupling of incident excitation radiation. The fibers are polished using a fiber polisher (UltraTech,, Santa Ana, CA)

with a 32 μ sized aluminum oxide (Al_2O_3) lapping paper. After polishing the fiber, the hard polymer jacket is manually stripped off using a sharp razor. The fibers are passed through a flame to remove parts of the jacket that were not stripped off with the razor. After cleaning the fibers with kimwipes, the fibers are drawn from 600 μm (core diameter) down to about 50 *n*m using Sutter P-2000 laser-based fiber puller (Sutter Instrument Company, Novato, CA). Figure 2.6 shows a digital image and a schematic profile of the fiber pulling instrument. Figure 2.7 details the fiber pulling process and the product of this process, a 50 nm diameter optical nanofiber.

2.7.2 Silver Deposition Process

The pulled optical nanofibers with a final tip diameter of about 50 nm were coated with 200 nm of silver metal (99.999% pure) using a thermal source vacuum evaporator (Cooke Vacuum Products, South Norwalk, CT) operating at 10^{-26} Torr achieving a final diameter of 250nm (Figure 2.8). The coating was deposited by placing the nanofibers on a rotating stage with the tips pointed away from the silver source at an angle of approximately 45°, thus preventing coating of the sensing region. The Thermal deposition system is equipped with a crystal for monitoring the metal thickness during the deposition process. This system has an on board computer which determines the thickness deposition rate which is typical 0.5 Å/s. Following the silver coating process, the optical nanosensor tips are functionalized to facilitate the immobilization of the biorecognition molecule.

TOP VIEW

Mirror

CO_2 Laser

Tension Mount   Tension Mount

Retro Mirror

Fiber Optic

Sutters Instruments P-2000
laser based fiber puller

SIDE VIEW

Stripped Optical
Fiber (without jacket)

Optical Fiber
(with jacket)

Retro Mirror

Clamps

Tension Mounts
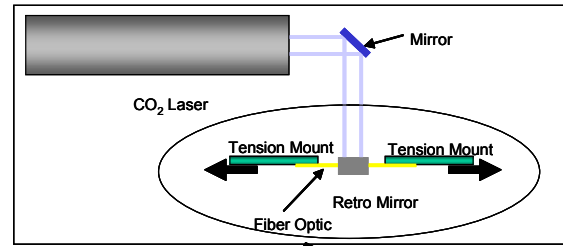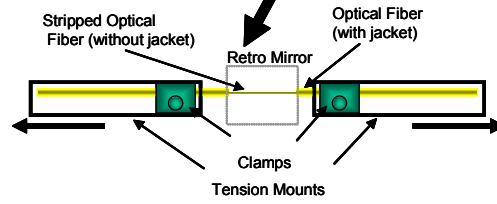
Figure 2.6 shows a digital image of the fiber-pulling instrument (LEFT) and a top-view and side-view diagrammatic profile of the fiber-pulling instrument.
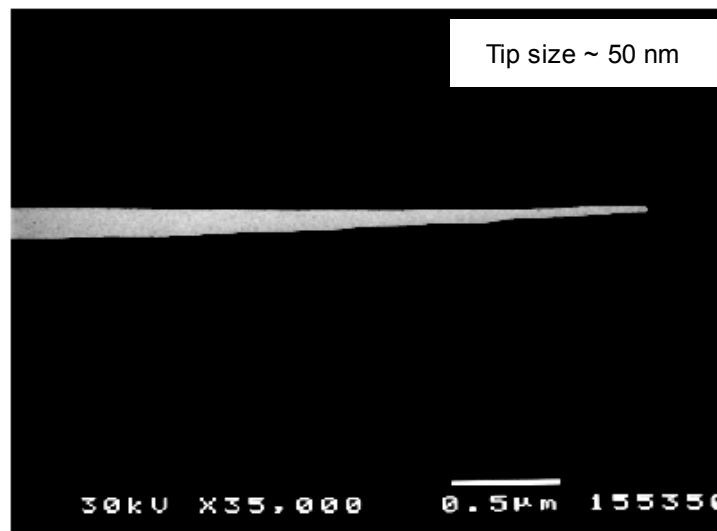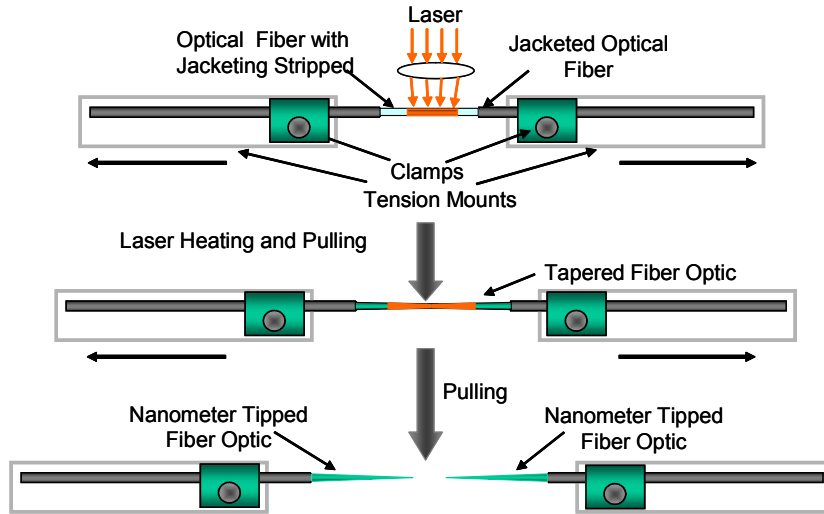
Figure 2.7 (above) shows the details the fiber pulling process and (below) the product of this process, a Scanning Electron Micrograph of a 50 nm diameter optical nanofiber
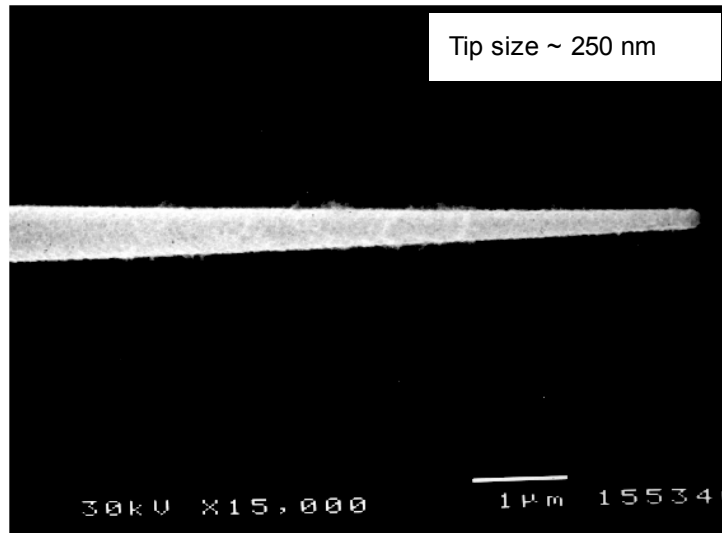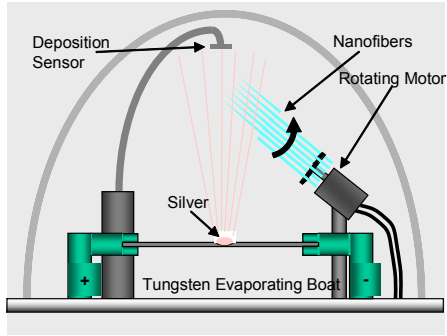
Figure 2.8 shows how the pulled optical nanofibers with a final tip diameter of 50 nm are coated with ~200 nm of silver metal using a thermal source vacuum evaporator (ABOVE) achieving a final tip diameter of 250nm. Above LEFT shows the 45° orientation of the nanofibers in the thermal deposition chamber during the silver coating process. Above RIGHT is an image of the thermal vacuum deposition chamber without the bell jar.

2.7.3 Protein Immobilization Chemistry

Immobilization of proteins onto SiO_2 surfaces is of great interest for many applications, particularly in developing biosensors. The immobilization of proteins by covalent coupling usually leads to very stable preparations. The covalent binding method is based on the attachment of proteins to solid SiO_2 supports. The reaction involves only functional groups of the protein that are not essential for its activity. The major aspects which have to be considered for the covalent immobilization of proteins are the following: Optical transduction principles that allow the use of the evanescent field has facilitated the development of optical nanosensors whereby/ in which one binding partner is immobilized on the transducer element followed by the binding of the target analyte. This generated evanescent field is used to excite the captured target analyte. Immobilization of protein onto solid-phase supports is thus an important/ essential step in the nanofabrication of optical nanosensors. The immobilization of antibodies/ protein on the surface of the transducer in optical nanosensors has to achieve the following criteria; (i) result in a reproducible amount of antibody on the surface, (ii) result in stable binding of the antibody to the optical transducer surface (iii) maintain the activity of the antibody and (iii) non-specific binding interactions.

Optical nanofibers are functionalized to facilitate covalent immobilization of protein. Figure 2.9 describes the antibody binding chemistry procedure performed to facilitate this process. Briefly, the silver coated nanotips were acid cleaned by
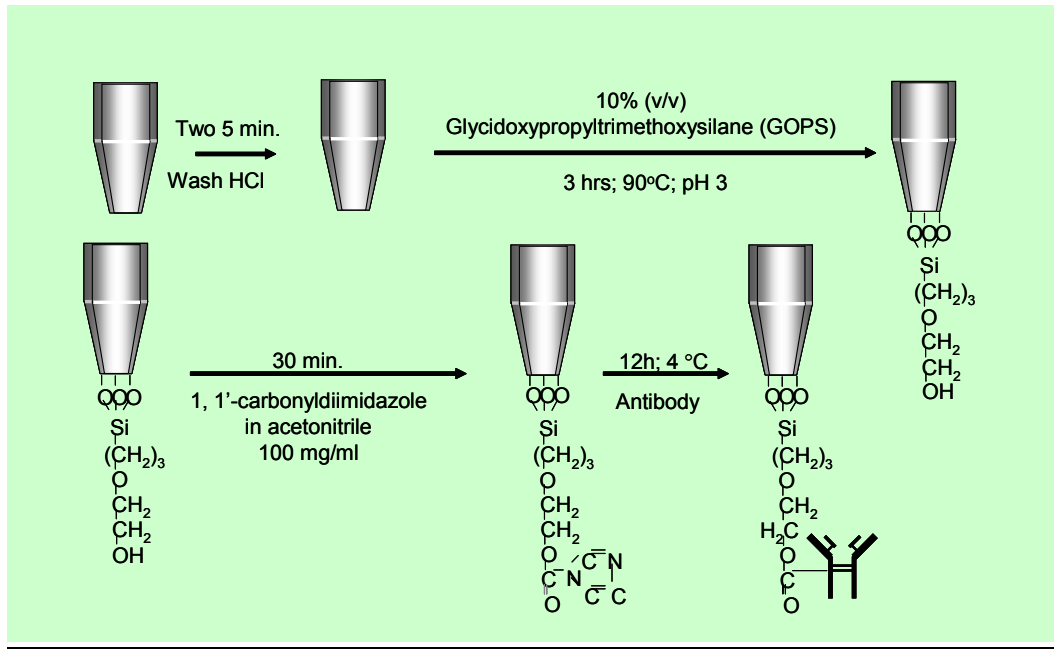
Figure 2.9 describes the multistep surface chemistry procedure performed to functionalize the optical nanofiber tips to facilitate protein immobilization onto the optical nanofibers

immersion in a 1:1 mixture of concentrated hydrochloric acid (HCl) and methanol for 30 minutes followed by rinsing several times in doubly distilled water. Next the substrates were allowed to air dry. The air-dried nanofibers were suspended in 20mL of 10% (v/v) aqueous (anhydrous acetonitrile) GOPS. The mixture is heated for 3h at 90°C with the pH maintained at 3 using 1M HCl. After the activation of the silica nanotips and direct GOPS attachment, the silica nanotips were dried overnight in a vacuum oven at 105°C. After drying in the vaccum oven, the nanotips were washed with anhydrous acetonitrile and then suspended in 20ml of acetonitrile and 2g of CDI added while stirring (30 minutes). Finally, they were washed with acetonitrile before immobilizing antibody. For the methods, the immobilization of 0.5-1.0 mg/ml of antibody was added to centrifugation vials. The nanotips were incubated for 12 hours at 4°C. The antibody bound to the activated aldehydic sites. The fiber tips were rinsed in PBS and remain in PBS overnight to hydrolyze and unreacted sites after the incubation step.

A 0.05 (or 0.5) mg/ml solution of specific antibody and control antibody in PBS was placed on the substrate coated with silane and cross-linker and allowed to incubate for one hour after which the substrate was rinsed and washed in PBS.

2.8 Optical Nanosensing Schemes for Single Cell Analysis

2.8.1 Immunochemical Assay Formats

This work describes the use of two basic immunoassay formats for single cell analysis based on biochemical interactions between the biorecognition molecule and

the target analyte. These two immunosensing formats can be distinguished as bioaffinity and biocatalytic reactions (Figure 2.10). Bioaffinity reactions involve antigen – antibody (Ag – Ab) interactions which take advantage of physicochemical changes that accompany complex formation e.g., changes in layer thickness, refractive index, light absorption or emission. Bioaffinity reactions are characterized by high specificity and high sensitivity that typifies an Ag – Ab reaction. Two different types of bioaffinity reactions have been described *direct* and *indirect* immunoassay. *Direct* immunoassay format register immunochemical complex formation at the transducer surface via optical changes such as fluorescence emission. The advantage of a *direct* immunoassay is that measurement of the antigen– antibody interaction can be accomplished immediately without any need for additional antibodies or markers (fluorescent tags). In contrast, i*ndirect* immunoassay format is based on the measurement of the antibody – antigen– antibody interaction can where one of the antibody partners in the immune interaction has a fluorescent label for detection. *Indirect* immunoassay format combine the high selectivity of an immunoreaction with the high sensitivity characteristic of the fluorescent label effect.

On the other had, biocatalytic reactions are important in biosensing applications in cases where the target analyte does is not inherently fluorescent. The biocatalytic reaction is based on the specific recognition of an enzyme substrate and its subsequent chemical conversion to the corresponding products. The biocatalytic reaction itself accomplishes specific binding between the active site of the enzyme and the substrate, conversion of the substrate to product, and release of the product
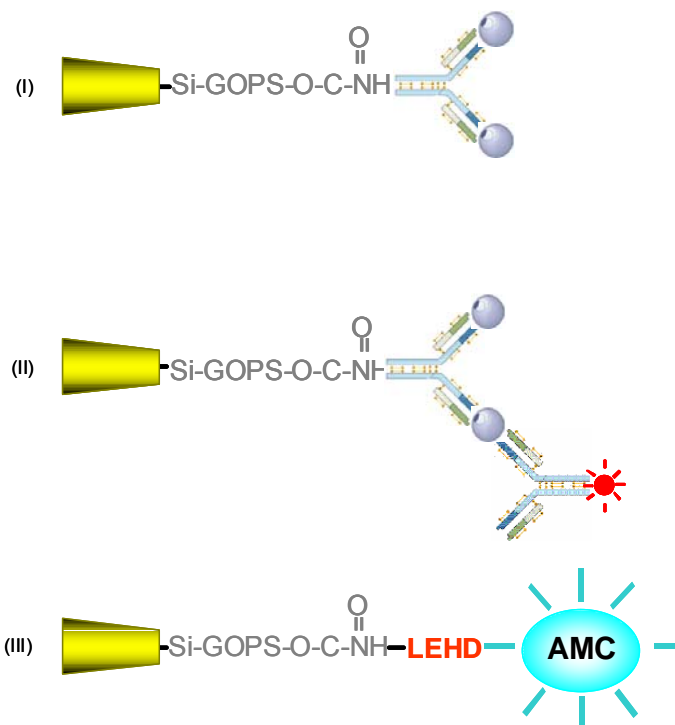
Figure 2.10: The two immunosensing formats can be distinguished as **Bioaffinity** immunoassays: (i) *direct* immunoassay format, (ii) *indirect* immunoassay format, and **Biocatalytic** immunoassay: (iii) tetrapeptide substrate format

from the active center, which in turn leads to regeneration of the binding affinity and catalytic state of the enzyme. A fluorescent molecule can be coupled to the substrate and upon release of product for the enzymes active center, the fluorescent molecule can be detected. This work exploits a tetrapeptide substrate coupled to a fluorescent molecule for he detection of specific enzymatic activity. The use of biocatalytic reaction facilitates both sensitivity and selectivity.

The two basic approaches to sensing *direct* optical interaction with an analyte, and *indirect* optical interaction with an analyte were applied to optical nanosensors. *Direct* optical interaction involves the use of primary antibody to bind a fluorescent target analyte, while the *indirect* approach used indicator dye bound to biological substrate molecules that change their optical properties after reacting with analyte.

2.8.2 Immobilization of Fluorogenic Tetrapepetide Substrate

This approach involves the immobilization of fluorogenic tetrapepetide substrate onto the optical nanosensor to measure the activity of caspases (-9 and −7). Caspase-9 and -7 are synthesized in the cytosol of mammalian cells as inactive zymogens, which become active through intracellular caspase cascades. By mapping the cleavage site of the substrates of caspase-9 and caspase-7, tetrapeptides Leucine-Glutamic acid-Histidine-Aspartic acid (LEHD) and Aspartatic acid-Glutamic acid-Valine-Aspartic acid (DEVD) consensus cleavage sites were identified. Conjugation to a fluorimetric moiety to DEVD provides a substrate for analyzing caspase like protease activity. The following figure shows the cleavage reactions central to

fluorimetric detection method. The fluorogenic tetrapeptide is immobilized. The fluorimetric assay detects emission of the molecule 7-amino-4-methylcoumarin (AMC) after cleavage from the AMC-substrate conjugate, LEHD-AMC and DEVD-AMC respectively (Figure 2.11).

2.9 Components of Intracellular Measurement System

The components of the intracellular fluorescent measurement system are shown in Figure 2.12. The components include three lasers, a Helium-Cadmium (HeCd) laser emitting at 325nm, Helium-Neon (HeNe) laser emitting at 632.8 nm, Argon (Ar) ion laser emitting at 488 nm and 514 nm, depending on the source required for excitation. Optical fiber for laser delivery. Band pass filters (UV fluorescence) were used to reject the laser-line and collect the fluorescence emission. Nikon inverted fluorescence microscope, fluorescence signal detector using a photomultiplier tube (PMT). Signal acquisition and recording using a custom written LabView software program and a PC. Calibration curves were prepared by measuring (over 50msec) the rates of fluorescence increase.

The measurement system is designed so that the output from laser source is directed into an optical nanosensor. The optical nanosensor acts as a waveguide, and the evanescent wave generated at the nanotip excites fluorophores that are associated with bound protein at the surface of the nanotip. Some fluorescence is collected and is filter and then detected by a PMT. Our system has been designed so that optical fibers
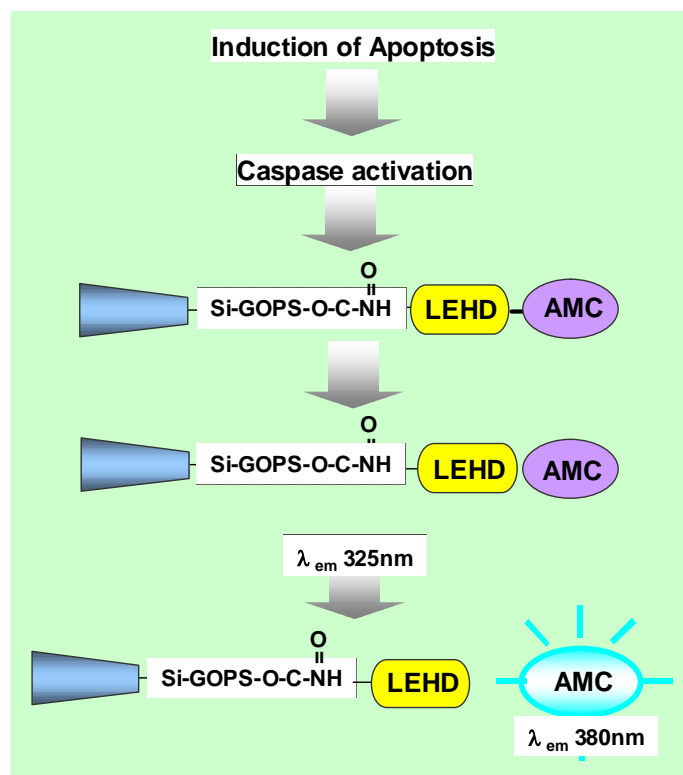
Figure 2.11 shows the cleavage reactions central to fluorimetric detection of caspase activity. The fluorogenic tetrapeptide substrate is immobilized onto the optical nanosensor (shown in blue) and the fluorimetric assay detects emission of the molecule 7-amino-4-methylcoumarin (AMC) after cleavage from the Leucine- Glutamic Acid- Histidine- Aspartic Acid AMC-substrate conjugate (LEHD-AMC).

HeCd Laser

Incubator

Nanosensor

Cell

197319792003

HP universal
counter

Data acquisition PC

PMT

HP power supply

Nikon inverted
fluorescence microscope
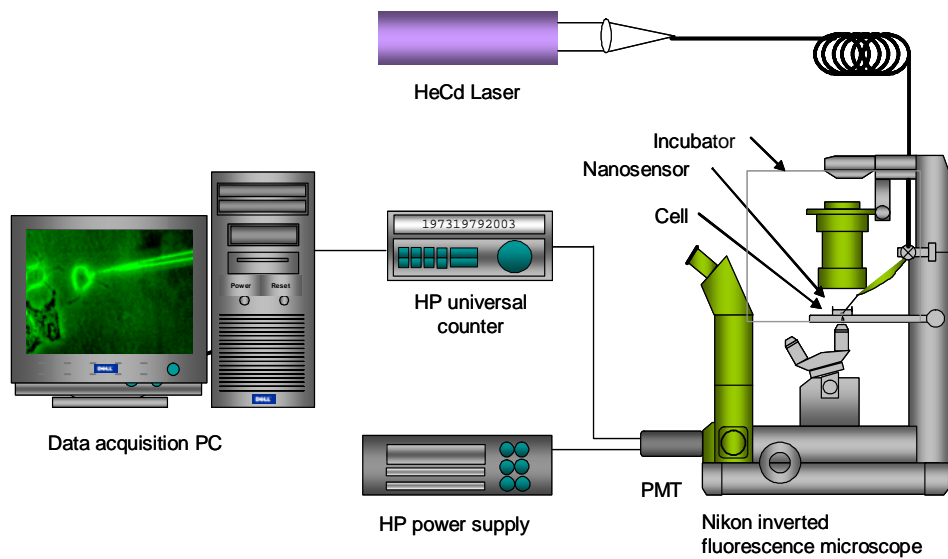
Figure 2.12 shows the components of the laser-induced fluorescence measurement system. The excitation source (HeCd laser) is interchangeable and are chosen and used depending on the excitation wavelength of the target analyte

that are used as sensing elements are inserted into a SMA connector/collar which, when inserted into the cell compartment, immediately aligns the proximal end of the fiber to assure high efficiency of transmission of light into and back from the waveguide. The system has been used for the development of methods of immobilization of antibodies, and as a sensing platform to develop methods for detection of BPT [18]. The results demonstrated that our system can selectively detect BPT at the femtomolar concentration level for a sample of 100 ul within a 50 ms of exposure of the sensor to sample and 10 sample accumulations. Perhaps most importantly, it is now clear that this system can be used for the sensitive and specific analysis of protein-ligand interactions at a solid interface.

2.10 Optimization of Optical Nanosensors

This section describes the optimization of optical nanosensors, which was performed to improve and maximize the efficacy of the production of uniform nanotips. Production of uniform nanotips is important minimize the variability from fiber to fiber and to enhance the reproducibility factor. Optimization of nanotips was achieved by fine-tuning the parameters, Heat, Velocity, Delay, and Pull Strength of the current state-of-the-art in micropipette puller technology, the P-2000 system (Sutter Instruments, Novato, CA). The P-2000 integrates a CO_2 laser-based heat source. The CO_2 laser has several features that make it amendable as a heat source of choice. These features include nominal emission wavelength of the laser approximates the resonant frequency of the SiO_2 lattice in glass, CO_2 laser heat is

clean and leaves no residue on the SiO_2 as do conventional heating filaments, and finally, laser heat can be turned off instantly, leaving no residual filament heat. The user can program the amount and distribution of heat supplied to the glass. The P-2000 system has microprocessor-controlled programmability with 100 separate programs, each program consisting of up to 8 command lines. Programmable parameters include; laser power level, scan width, trip velocity, delay/ laser on time, and hard pull strength (heat, filament, velocity, delay and pull). These programmable parameters were adjusted in order to draw nanotips of different tip diameters.

Drawn nanotips were evaluated using Hitachi S-4700 scanning electron microscope (SEM). In scanning electron microscopy an electron beam is focused into a small probe and is raster scanned across the surface of the nanotips. Several interactions with the nanotipse that result in the emission of electrons or photons occur as the electrons penetrate the surface. These emitted particles are collected with the appropriate detector and processed with image visualization software to yield measurement information about the nanotips. The Hitachi S-4700 is highly suited for this purpose because of its capability of high-resolution imaging with resolution of at least 3 nm.

Dozens of nanotips were drawn for the optimization study by varying the program parameters of the Sutter Instruments P-2000 fiber-pulling instrument. The optical nanosensor for this optimization study were prepared using a three-step process. Before this process, individual programs were written and write-protected in order to secure them from inadvertent changes. Eight inch pieces of PCS were

cleaved using a fiber cleaver. Both ends of the optical fiber were polished using 30μm Al_2O_3 lapping paper. The fibers were then secured on the tension mounts of the P-2000 Laser based fiber puller using clamps. For each program used, I pulled five eight-inch fibers resulting in a total of ten nanofibers for each program used. The nanofibers were labeled in order to keep track and link the fiber to the program after acquiring SEM images.

2.10.1 Experimental Procedure

600 μm plastic clad silica (PCS) optical fiber was purchased from Fiberguide Industries, Stirling, New Jersey. The benefits o PCS optical fiber include, cost effective, high numerical aperture (NA) for efficient light collection from extended sources, radiation resistant, laser damage resistant, dielectric nonmagnetic construction, broad operating wavelength range from 220nm to 700n, excellent laser beam delivery. PCS optical fibers were cut into 8 inch pieces and each end of the fiber was polished using Aluminium oxide lapping paper. The fibers were drawn to various tip diameters using Sutter P-2000 micropipette puller. The P-2000 works well with small diameter glasses such as PCS optical fibers. The programmable parameters laser power level, scan width, trip velocity, delay/ laser on time, and hard pull strength, were modified before each pulling to obtain nanotips of different diameters. After pulling the optical fiber to nanotips, they were coated with 99.999 % silver metal in silver thermal deposition chamber. After coating the nanotips with silver,

scanning electron microscope (SEM) images of the nanotips were acquired with Hitachi S-4700 SEM at theHigh Temperature Materials Laboratory, ORNL.

2.10.2 Results and Discussion

Table 2.1 shows the programmable parameters include; heat, trip velocity, delay/ laser on time, and hard pull strength (heat, filament, velocity, delay and pull) that were adjusted to draw nanotips of different tip diameters. This table shows the change in each parameter and the results obtained. Figures 2.13 show SEM micrographs of the nanotips acquired with Hitachi S-4700 SEM. From the results, it can be concluded that increasing the pull strength, decreases the tip diameters obtained. These results were used as guide in the production of uniform optical nanosensors to enhance the reproducibility factor between single cell measurements.

2.11 Characterization of Optical Nanosensors

The greatest challenge of developing nanoscale materials and structures lies in being able to look at what has been created and to determine the presence or absence of elements and their distribution. I devised a simple but straightforward method to characterize the optical nanosensor and in the process confirm protein immobilization chemistry. The optical nanosensors were characterized by immobilizing Cy-5 labeled antibody onto functionalized nanotips and detecting the presence or absence of Cy-5 labeled antibody. Cy-5 was used because of its intense fluorescence, low hydrophobicity, [42] and their high photostability which renders them useful for

Table 2.1shows the programmable parameters include; heat, trip velocity, delay/ laser on time, and hard pull strength that were adjusted to draw nanotips of different tip diameters

Sutter P-2000 Input Parameters					
Program	Heat (oC)	Velocity	Delay	Pull	Size (nm)
40	850	20	150	200	50
10	850	60	126	130	1000
3	850	60	126	160	500
9	850	40	126	170	400
22	850	40	126	180	300
19	850	20	126	190	200
18	850	20	126	200	100
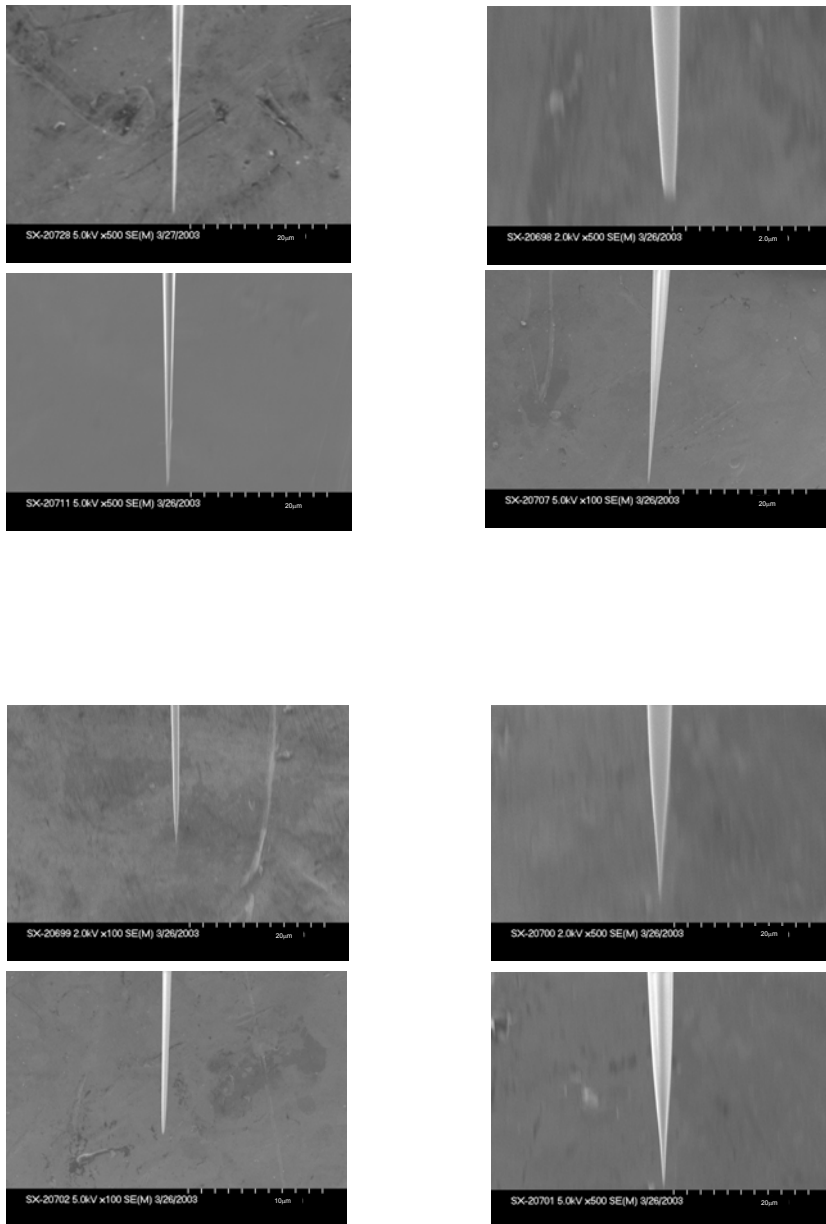
Figures 2.13 shows SEM micrographs of the nanotips of different tip diameters acquired with Hitachi S-4700 SEM. Note the different measurement scale on each micrograph.

single molecule fluorescence detection [43-45]. In this study, anti-cytochrome *c* was labeled according to the following protocol and immobilized on nanotips (antibody was labeled in a column and collected). 1mg of protein was labeled to a final average molar dye/ protein ratio of 8 (this assumes an average protein molecular weight of 155 KDa). Cytochrome c antibody was labeled according to the following protocol and immobilized on nanotips. Protein (1mg/ml in PBS) + Coupling buffer + Reactive Cy-5 dye. Mixture is incubated at room temperature for 30 minutes. Separation of labeled protein from non-conjugated (free) dye using a gel filtration column. Collection tubes used to collect labeled protein. One batch of functionalized nanotips were incubated in the labeled protein solution while the others were incubated in unlabeled protein solution. Interaction between the Cy-5 labeled and unlabeled antibody, with the nanotip was investigated. Interaction between the Cy-5 labeled antibody and the nanotip was investigated. Fluorescence signal produced when the antibody-antigen complex is excited; is converted to a measurable electrical signal

2.11.1 Experimental Procedure

Analytical grade materials were used as long as they were commercially available. Cy-5 labeling kit containing, buffers, Cy-5 monofunctional dye as well as PD-10 columns were purchased from Amersham Pharmacia Biotech. Cytochrome c antibody was purchased from Santa Cruz Biotechnology, Inc (Santa Cruz, CA).

2.11.2 Labeling of Cytochrome c with Cy5

In the standard procedure, the contents of 1 vial (to label 1 mg of protein) of Cy-5 monofunctional dye was dissolved in 50 µL of DMSO. Cytochrome c antibody was dissolved in buffer provided, typically at 1 mg/mL protein concentration. 10 µL of dye/DMSO mixture was pipetted into 200 µL cytochrome c solution under slow vortexing. After 30 min incubation at 25°C in the dark the reaction was terminated by freezing at -4°C. For separation of unbound dye, 300 µL of 100 mM NaH_2PO_4 (to suppress further labeling after thawing) was added to a frozen sample and the sample was incubated in a 25°C water bath until thawed. The sample was loaded on a PD-10 column (10 mL bed of Sephadex G-25M), which had been pre-equilibrated in buffer. After washing the column with buffer A (2 *1 mL) the labeled protein was eluted by adding 2 mL of buffer to the column top. Another 10 mL of buffer was added to elute all unbound dye, and the column was regenerated with 20 mL of buffer. Higher Cy-5 dye concentrations can be achieved by dissolving 2 vials of Cy-5 dye in 50 µL of DMSO.

2.11.3 Immobilization of Labeled Anti-Cytochrome c

Preparation of anti-cytochrome *c* optical nanosensors involved the construction of nanofibers and functionalizing the nanotips to facilitate antibody immobilization. PCS optical fibers were pulled using the laser based fiber puller, from 600 µm diameter to 50 nm diameters. The pulled fibers were coated with silver metal in silver thermal deposition chamber. After coating the nanotips with silver, the

nanotips were functionalized as described previously to allow the immobilization of Cy5 labeled anti-cytochrome *c*. The measurements were performed using labeled antibody for the experimental and unlabeled antibody for the control.

2.11.4 Results and Discussion

Figure 2.14 is a schematic representation of the fluorescence excitation and measurement procedure used for Cy5 detection during the characterization study of optical nanosensor. Figure 2.15 shows the results of the characterization study, which involved the detection of Cy5 labeled anti-cytochrome *c* immobilized on the nanotips. This study involved two treatment groups, optical nanosensor with Cy5 labeled anti-cytochrome *c* and without Cy5 labeled anti-cytochrome *c*. These results show a difference of an order of magnitude in the fluorescent intensity measurements. This difference is significant enough to determine the successful immobilization of Cy5 labeled anti-cytochrome *c*.

2.12 Characterization of Optical Nanosensor: -AFM measurements

In addition, we attempted to determine the distribution of antibody using a recently acquired an atomic force microscope (AFM). AFM is a method of measuring surface topography on a scale from angstroms to 100 microns. The technique involves imaging a sample through the use of a probe, or tip, with a radius of 20 nm.
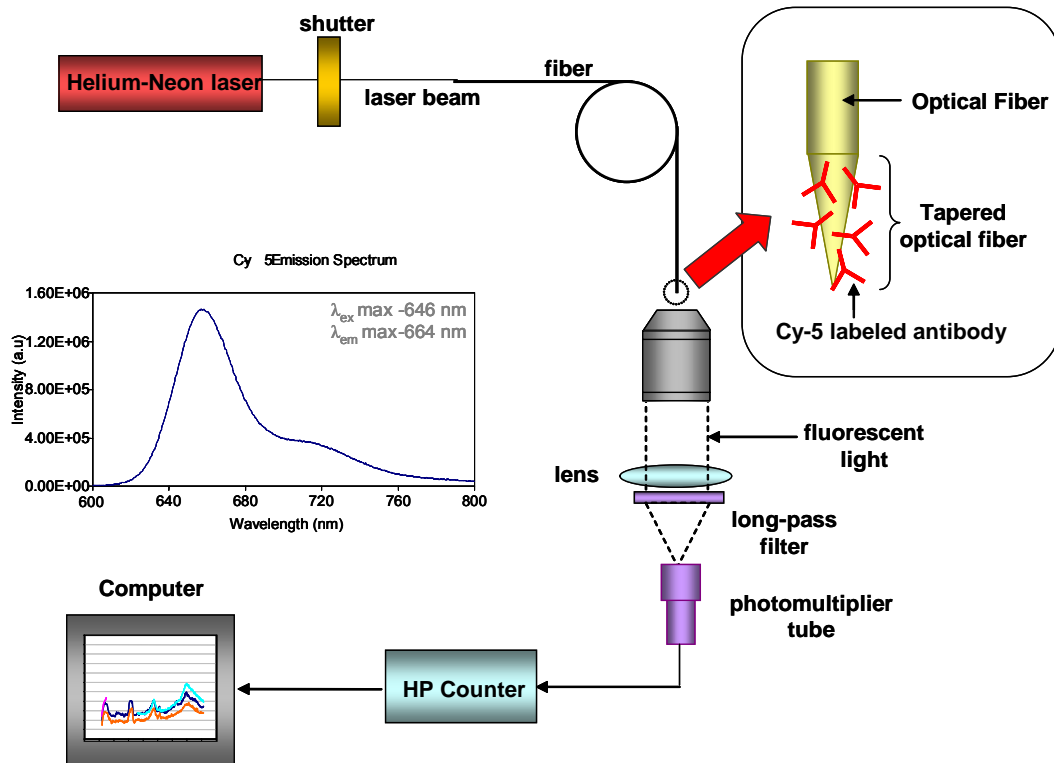
Figure 2.14 is a schematic representation of the fluorescence excitation and measurement procedure used to detect Cy5 labeled anti-cytochrome *c* in the evaluation study. Inset is the excitation and emission spectrum of Cy5.
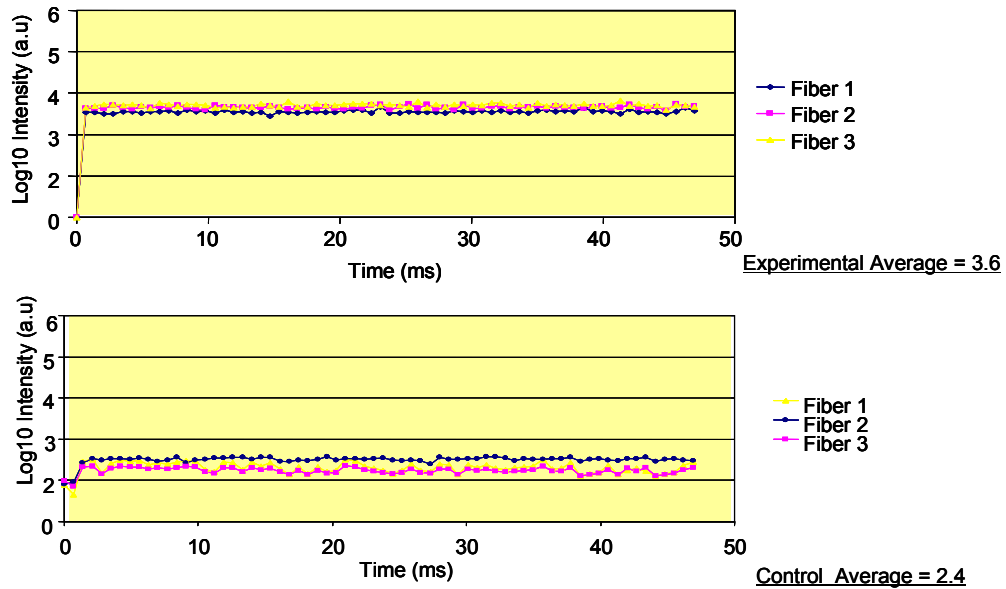
Figure 2.15: shows the results of evaluation study that involved immobilizing Cy5 labeled anti-cytochrome *c* on functionalized nanotips and monitoring their presence. The top graph represents the detection of Cy5 labeled anti-cytochrome *c* (experimental) and the graph below represents the control group.

The tip is held several nanometers above the surface using a feedback mechanism that measures surface–tip interactions on the scale of nanoNewtons. Variations in tip height are recorded while the tip is scanned repeatedly across the sample, producing a topographic image of the surface. The AFM has the ability to image at atomic resolution (sub-angstrom level) and can achieve a resolution of 10 pm, and unlike electron microscopes, can image samples in air and under liquids. The AFM'sresolution combined with its ability to image a wide variety of samples under a wide variety of conditions such as air and in fluids. Images have appeared in the literature showing DNA, single proteins, structures such as gap junctions, and living cells [46]. AFM operates by measuring attractive or repulsive forces between a tip and the sample [47]. In its repulsive "contact" mode, the instrument lightly touches a tip at the end of a leaf spring or "cantilever" to the sample. As a raster-scan drags the tip over the sample, some sort of detection apparatus measures the vertical deflection of the cantilever, which indicates the local sample height. Thus, in contact mode the AFM measures hard-sphere repulsion forces between the tip and sample. In non-contact mode, the AFM derives topographic images from measurements of attractive forces; the tip does not touch the sample [47].

2.12.1 Experimental Procedure

PCS optical fibers were pulled using the laser based fiber puller, from 600 μm diameter to 50 nm diameters. The pulled fibers were coated with 99.999 % silver metal in silver thermal deposition chamber. After coating the nanotips with silver, the

nanotips were functionalized to allow the immobilization of Cy-5 labeled cytochrome c antibody. After the construction of antibody-modified nanotips, we imaged the nanotips using contact mode to locate the distribution of the immobilized cytochrome c antibody. Contact mode is the most common method of operation of the AFM and as the name suggests the tip and sample remain in close contact as the scanning proceeds.

2.12.2 Results and Discussion

Figure 2.16 shows AFM images of optical nanosensor tips. The results obtained revealed that we were unable to achieve sub-angstrom resolution and therefore unable to determine the distribution of cytochrome c antibody immobilized on the nanotips.However, we were able to obtain, with the acquired images, the dimensions of the nanotips. Idealistically, if this worked and we were able to determine the location and distribution of cytochrome c antibody, it would essentially allow us to study the biophysics of molecular interactions and its role in important processes such as signal transduction.

2.13 Evaluation of Optical Nanosensors

Since I had already positively demonstrated the immobilization of antibody onto functionalized nanotips, the next step was to demonstrate that an immunochemical assay was possible using the optical nanosensors. Evaluation of the
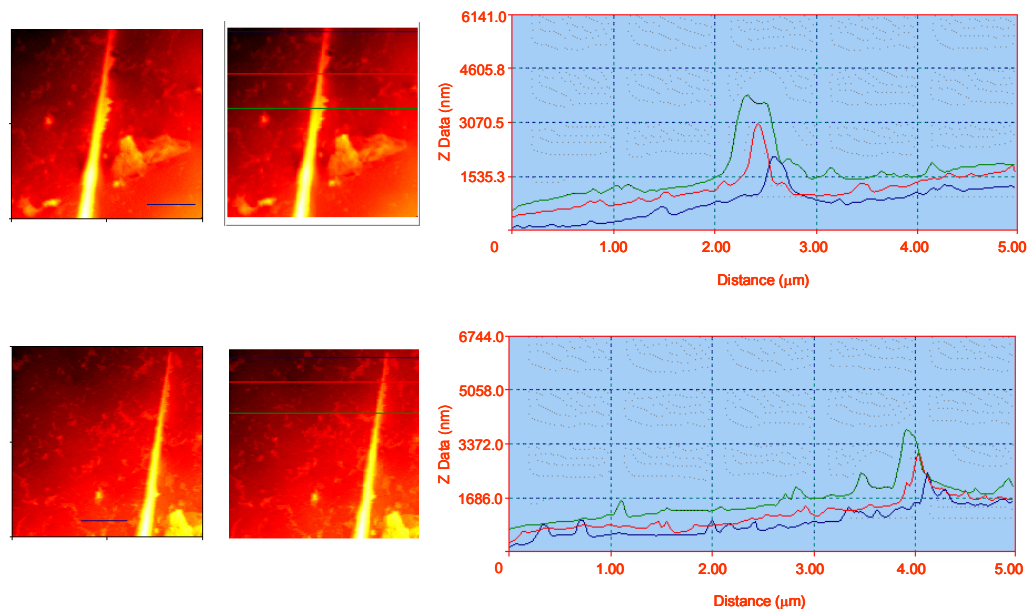
Figure 2.16 shows AFM images of optical nanosensor tips captured using an atomic force microscope in contact mode. The graphs show the dimensions of the nanotips at different locations

optical nanosensors was performed to assess the reactivity of antibody immobilized onto the functionalized nanotips. Basically it involved determining whether or not the immobilized antibody could effectively and efficiently bind target analyte and in essence demonstrate that an antibody-antigen interaction can be detected. The evaluation process was performed by immobilizing antibody to fluorescein onto functionalized nanotips and detecting fluorescein molecules in solution. Fluorescein was chosen because of the following advantages: it has a relatively high absorptivity, an excellent fluorescence quantum yield, and excitation maxima ~494 nm closely matches the 488 nm spectral line of the Argon-ion laser.

2.13.1 Experimental Procedure

PCS optical fibers were pulled using the laser based fiber puller, from 600 μm diameter to 50 nm diameter. The pulled fibers were coated with 99.999 % silver metal in silver thermal deposition chamber. After coating the nanotips with silver, the nanotips were functionalized to facilitate the immobilization of antibody to fluorescien for the experimental group, and without antibody to fluorescein for the control group. Anti-fluorescein solution is prepared by dissolving the lyophilizate in 1 ml double distilled water results in a concentration of 0.1 mg antibody/ml. The antibody is suitable for the detection of fluorescein and fluorescein-labeled compounds. The detection of bound antibody can be carried out directly in one step using an antibody to fluorescein. Both groups of optical nanosensors were incubated in fluorescein (10^{-4}M) prepared in PBS. Both were incubated for 5 minutes in

fluorescein and the evaluation of optical nanosensors study involved two groups, experimental : antibody to fluorescein was immobilized on functionalized nanotips, and, control : without antibody on functionalized nanotips. <u>Figure 2.17</u> shows fluorescence excitation and measurement process.

2.13.2 Results and Discussion

The characterization study was performed to determine the coupling and compatibility of the optical nanosensor fabrication process and protein binding chemistry procedure. This involved immobilizing anti-fluorescein onto functionalized nanotips to detect fluorescein *in situ*. <u>Figure 2.18</u> shows the results of the characterization study involving measurerements performed using anti-fluorescein-based optical nanosensors. The top fluorescence intensity plot represents optical nanosensors used to make the experimental group measurements, while the bottom fluorescence intensity plot shows results obtained using optical nanosensors used to make the control group measurements. The difference between the experimental group and the control group is approximately more than an order of magnitude. This diffrence is significant illustrating the poitive detection of fluorescein using anti-fluorescein-based optical nanosensors.
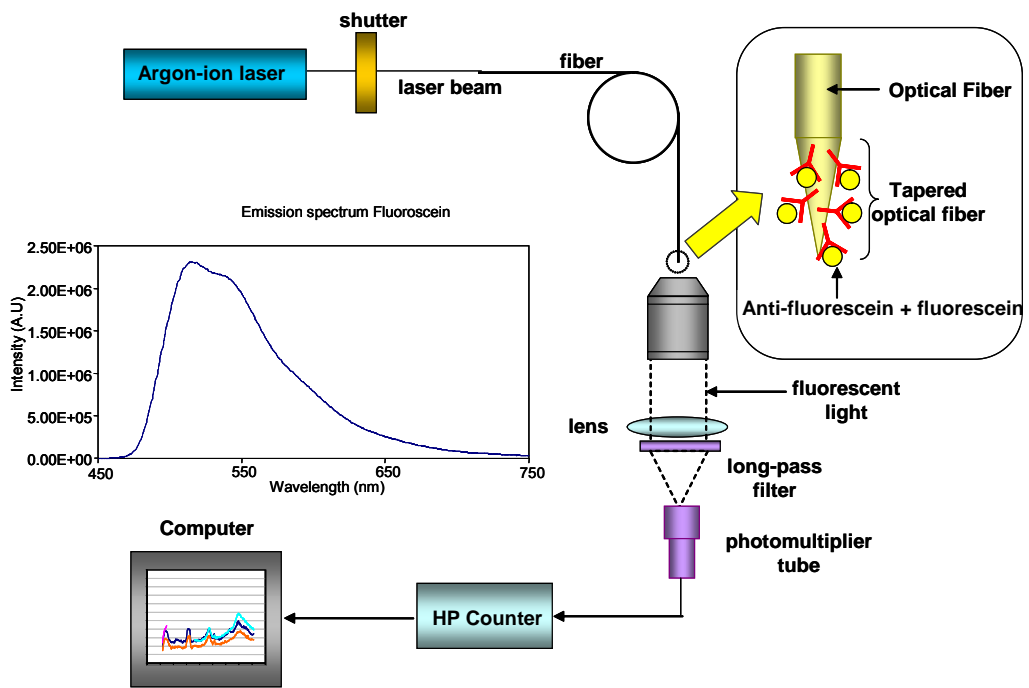
Figure 2.17 is a schematic representation of the fluorescence excitation and measurement procedure used for fluorescein detection during the characterization study of optical nanosensors employing the *direct* immunoassay format. Inset is the excitation and emission spectrum of fluorescein.

Experimental group: Average 5.1

Control group: Average 3.5
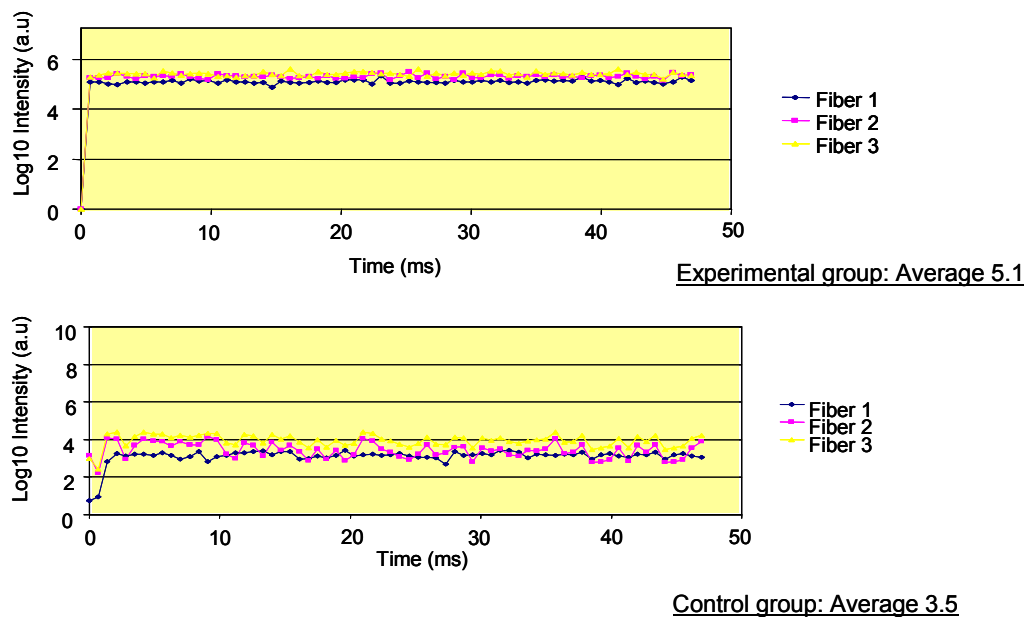
Figure 2.18 shows the results of characterization study for the detection of fluorescein using anti-fluorescein-based optical nanosensors. The top graph is the experimental group while the graph below is the control.

2.14 Summary

This work demonstrates the successful optimization process of optical nanosensor fabrication performed by fine-tuning the input parameters of Sutters Instrument P-2000. I was able to characterize the optical nanosensors by immobilizing labeled Cy-5 labeled antibody and detecting the presence (experimental) and the discerning the absence (control) on the nanotips. I was unsuccessful in using the AFM to determine the localization and distribution of Cy-5 abeled antibody on the nanotips. It is worth mentioning that AFM has been used toimage single lysozyme molecules [24] and therefore with more effort, it will be possible to demonstrate the localization and distribution of immobilized antibody. I was also successful in demonstrating the ability to immobilized antibody to fluorescein to bind fluorescein in solution thereby detecting an antibody-antigen interaction. Optical Nanosensors developed in this work were subsequently used for the following *in vitro* and *in vivo* analyses, which employ different immunochemical assay formats;

- Chemical analysis, utilizing *direct* antibody binding assay format for measuring the carcinogen benzo[a] pyrene
- Protein interaction analysis, utilizing *indirect* antibody binding assay format for monitoring cytochrome *c* and caspase-9
- Protein Analysis, utilizing tetrapeptide substrate assay format for monitoring caspase-9 and caspase-7 activity

References

1. Zandonella, C., *Cell Nanotechnology: The Tiny Toolkit.* Nature, 2003. **423**: p. 10-12.
2. Behbehani, M., *Cell Physiology Source Book*, ed. N. Sperelakis. 1995, San Diego: Academic Press. 490-494.
3. Morris, C., *Cell Physiology Source Book*, ed. N. Sperelakis. 1995, San Diego: Academic press.
4. Tsien, R., *Intracellular signal transduction in four dimensions: from molecular design to physiology.* Am J Physiol Cell Physiol, 1992. **263**: p. C723-C728.
5. Giuliano, K., Post, PL., Hahn, KM., Taylor, DL., *Fluorescent protein biosensors: measurement of molecular dynamics in living cells. .* Annu Rev Biophys Biomol Struct., 1995. **24**: p. 405-34.
6. Jankowski, J., Tratch, S., Sweedler, JV., *Assaying single cells with capillary electrophoresis.* Trends Anal. Chem., 1995. **14**: p. 170-176.
7. Luzzi, V., Lee, C.L., Allbritton, N.L., *Localized sampling of cytoplasm from Xenopus oocytes for capillary electrophoresis.* Anal Chem, 1997. **69**(23): p. 4761-4767.
8. Li, H., Sims, C.E., Wu, H., Allbritton, N.L., *Spatial Control of Cellular Measurements with the Laser-Micropipet.* Anal. Chem., 2001. **73**.
9. Tan, W., Shi, ZY., Smith, S., Birnbaum, D., and Kopelman, R., *Submicrometer Intracellular Chemical Optical Fiber Sensors.* Science, 1992. **258**(5083): p. 778-781.
10. Tan, W., Shi, ZY., Smith, S., and Kopelman, R., *Development of Submicron Chemical Optic Sensors.* Anal. Chem, 1992. **64**(23): p. 2985-2990.
11. Munkholm, C., D.R. Walt, and F.P. Milanovich, *Preparation of Co2 Fiber Optic Chemical Sensor.* Abstracts of Papers of the American Chemical Society, 1987. **193**: p. 183-ANYL.
12. Munkholm, C., D.R. Parkinson, and D.R. Walt, *Intramolecular Fluorescence Self-Quenching of Fluoresceinamine.* Journal of the American Chemical Society, 1990. **112**(7): p. 2608-2612.
13. Tan, W.H., et al., *Submicrometer Intracellular Chemical Optical Fiber Sensors.* Science, 1992. **258**(5083): p. 778-781.
14. Sumner, J., Aylott, JW., Monson, E., Kopelman, R., *A fluorescent PEBBLE nanosensor for intracellular free zinc.* Analyst, 2002. **127**(1): p. 11-16.
15. Alarie, J.P. and T. VoDinh, *Antibody-based submicron biosensor for benzo a pyrene DNA adduct.* Polycyclic Aromatic Compounds, 1996. **8**(1): p. 45-52.
16. Vo-Dinh, T., Alarie, JP., Cullum, BM., Griffin, GD., *Antibody-based nanoprobe for measurement of a fluorescent analyte in a single cell.* Nat Biotechnol, 2000. **18**(7): p. 764-767.
17. Kasili, P.M., Cullum, B.M., Griffin, G.D., and Vo-Dinh, T., *Nanosensor for In-Vivo Measurement of the Carcinogen Benzo [a] Pyrene in a Single Cell.* Journal of Nanoscience and Nanotechnology, 2003. **2**(6): p. 653-658.

18.   Cullum, B., Griffin, GD., Miller, GH., Vo-Dinh, T., *Intracellular measurements in mammary carcinoma cells using fiber-optic nanosensors.* Anal Biochem, 2000. **277**(1): p. 25-32.

19.   Vo-Dinh, T., and Cullum, BM., *CRC Handbook for Biomedical Photonics.* Nanosensors for Single Cell Analysis, ed. T. Vo-Dinh. 2003, Newyork: CRC Press. 14.

20.   Cullum, B.M., et al., *Intracellular measurements in mammary carcinoma cells using fiber-optic nanosensors.* Analytical Biochemistry, 2000. **277**(1): p. 25-32.

21.   Cullum, B.M. and T. Vo-Dinh, *The development of optical nanosensors for biological measurements.* Trends in Biotechnology, 2000. **18**(9): p. 388-393.

22.   Cullum, B.M. and T. Vo-Dinh, *Optical nanosensors and biological measurements.* Biofutur, 2000. **2000**(205): p. A1-A6.

23.   Vo-Dinh, T.G., G. D.; Alarie, J. P.; Cullum, B. M.; Sumpter, B. and Noid, D., *Development of Nanosensors and Bioprobes.* J. Nanoparticle Research, 2000. **2**: p. 17.

24.   Vo-Dinh, T., et al., *Antibody-based nanoprobe for measurement of a fluorescent analyte in a single cell.* Nature Biotechnology, 2000. **18**(7): p. 764-767.

25.   Cullum, B., Vo-Dinh, T., *The development of optical nanosensors for biological measurements.* Trends Biotechnol, 2000. **18**(9): p. 388-393.

26.   Vo-Dinh, T., et al., *Antibody-Based Fiberoptics Biosensor for the Carcinogen Benzo(a)Pyrene.* Applied Spectroscopy, 1987. **41**(5): p. 735-738.

27.   Aylott, J., *Optical nanosensors - an enabling technology for intracellular measurements.* Analytst, 2003. **128**(4): p. 309-312.

28.   S, U., *Fluorescence Assay in Biology and Medicine.* Vol. 2. 1969, New York, San Francisco, London: Academic Press. 659.

29.   http://www.pti-nj.com/, *Fluorescence: The Phenomenon.* 1997, Photon Technology International.

30.   Udenfriend, S., *Fluorescence Assay in Biology and Medicine.* Vol. 2. 1969, New York, San Francisco, London: Academic Press. 659.

31.   Harrick, N., *Internal Reflection Spectroscopy.* 1967, New York: John Wiley & Sons, Inc.

32.   Kröger, K., Jung, A., Reder, S., Gauglitz, G., *Versatile biosensor surface based on peptide nucleic acid with label free and total internal reflection fluorescence detection for quantification of endocrine disruptors.* Analytica Chimica Acta, 2002. **469**(1): p. 37-49.

33.   Axelrod, D., *Total Internal Reflection Fluorescence Microscopy in Cell Biology.* Traffic, 2001. **2**(11): p. 764-774.

34.   Potyrailo, R., Hobbs, SE., Hieftje, GM., *Optical waveguide sensors in analytical chemistry: today's instrumentation, applications and trends for future development.* FRESENIUS JOURNAL OF ANALYTICAL CHEMISTRY, 1998. **362**(4): p. 349-373.

35.   Guo, Z., Guilfoyle, RA., Thiel, AJ., Wang, R., and Smith, LM., *Direct fluorescence analysis of genetic polymorphisms by hybridization with oligonucleotide arrays on glass supports. Nucleic Acids Res., 22, 5456–5465.* Nucleic Acids Res., 1994. **22**: p. 5456–5465.

36.   Alarie, J., VoDinh, T., *Antibody-based submicron biosensor for benzo[a]pyrene DNA adduct.* Polycyclic Aromatic Compounds, 1996. **8**(1): p. 45-52.

37.   Kumar, A., Larsson, O., Parodi, D., and Liang, Z., *Silanized nucleic acids: a general platform for DNA immobilization.* Nucleic Acids Res., 2000. **28**(14): p. 71e-71.

38.   Lamture, J., Beattie, KL., Burke, BE., Eggers, MD., Ehrlich, DJ., Fowler, R., Hollis, MA., Kosicki, BB., Reich, RK., Smith, SR., *Direct detection of nucleic acid hybridization on the surface of a charge coupled device.* Nucleic Acids Res., 1994. **22**(11): p. 2121-2125.

39.   Alarie, J., Sepaniak, MJ., Vo-Dinh T., *Evaluation of Antibody Immobilization Techniques for Fiber Optic-based Fluoroimmunosensing.* Anal. Chim Acta, 1990. **229**(2): p. 169-176.

40.   Tromberg, B., Sepaniak, MJ., Alarie, JP., Vo-Dinh, T., Santella, RM., *Development of Antibody-Based Fiber-Optic Sensors for Detection of Benzo[a]Pyrene Metabolite.* Anal. Chem., 1988. **60**(18): p. 1901-1908.

41.   Dakubu, S., Ekins, R., Jackson, T., Marshall, NJ., *Chapter 4*, in *Practical Immunoassays: The State of the Art.*, W. Butt, Editor. 1984, Dekker: New York.

42.   Wessendorf, M., Brelje, T. C., *Which fluorophore is brightest? A comparison of the staining obtained using fluorescein, tetramethylrhodamine, lissamine rhodamine, texas red, and cyanine 3.18.* Histochemistry, 1992. **98**: p. 81-85.

43.   Harms, G.S., Sonnleitner, M., Schütz, GJ., and H.J. Gruber, and Schmidt, T., *Molecule Anisotropy Imaging.* Biophys. J., 1999. **77**: p. 2864-2870.

44.   Sako, Y., Minoguchi, S., and Yanagida, T., *Single molecule imaging of EGFR signalling on the surface of living cells.* Nature Cell Biol., 2000. **2**: p. 168-172.

45.   Schütz, G.J., Kada, G., Pastushenko, VP., and and H. Schindler, *Properties of lipid microdomains in a muscle cell membrane visualized by single molecule microscopy.* EMBO J., 2000a. **19**: p. 892-901.

46.   Hoh, J., and Hansma, PK., *Atomic force microscopy for high resolution imaging in cell biology.* Trends Cell Biol., 1992. **2**: p. 208-213.

47.   Binnig, G., Quate, CF., and Gerber, C., *Atomic Force microscope.* Phys. Rev. Lett., 1986. **56**: p. 930-933.

48.   Turner, A., Karube, I., Wilson, GS., ed. *Biosensors – Fundamentals and Applications.* 1987, Oxford University Press: Oxford.

49.   Schmid, R., and Karube, I., *Biotechnology*, in *Biosensors and Bioelectronics*, H. Rehm, and Reed G., Editor. 1998, VCH Verlagsgesellschaft: Weinheim-Basel-Cambridge-Newyork.

50.   Updike, S., and Hicks, GP., *The Enzyme Electrode*. Nature, 1967. **214**: p. 986-988.

51.   Guilbault, G., and Montalvo, JGJ., *A Urea specific enzyme electrode*. Journal of The American Chemical Society, 1969. **9**: p. 2164-2167.

52.   Bilitewski, U., and Schmid, RD. *Alcohol determination by modified carbon paste electrodes*. in *The GBF International Workshop on Biosensors*. 1989. Braunschweig, Germany.

53.   Kulys, J., Bilitweski, U., and Schmid, RD. *Biosensors based on chemically modified electrodes*. in *The GBF International Workshop on Biosensors*. 1989. Braunschweig, Germany.

54.   Robinson, G., *Optical Immunosensors: An Overview*, in *Advances in Biosensors*, T. APF, Editor. 1991, JAI Press Inc: London. p. 230-252.

55.   B.M. Cullum , T.V.-D., *The development of optical nanosensors for biological measurements*. Trends Biotechnol, 2000. **18**(9): p. 388-393.

56.   M. Shortreed, R.K., M. Kunh, B. Hoyland, *Fluorescent fiber-optic calcium sensor for physiological measurements*. Anal Chem., 1996. **68**(8): p. 1414-8.

57.   S.L. Barker, R.K., Anal Chem., 1998. **70**(23): p. 49062-6.

58.   M. Brasuel, R.K., T.J. Miller, R. Tjalkens, M.A. Philbert, *Fluorescent nanosensors for intracellular chemical analysis: decyl methacrylate liquid polymer matrix and ion-exchange-based potassium PEBBLE sensors with real-time application to viable rat C6 glioma cells*. Anal Chem., 2001. **73**(10): p. 2221-8.

59.   H. A. Clark, R.K., R. Tjalkens, M.A. Philbert, *Optical nanosensors for chemical analysis inside single living cells. 2. Sensors for pH and calcium and the intracellular application of PEBBLE sensors*. Anal Chem, 1999. **71**(21): p. 4837-43.

60.   H. A. Clark, M.M., M.A. Philbert, R. Kopelman, *Optical nanosensors for chemical analysis inside single living cells. 1. Fabrication, characterization, and methods for intracellular delivery of PEBBLE sensors*. Anal Chem, 1999. **71**(21): p. 4831-6.

61.   T. Vo-Dinh, J.P.A., B.M. Cullum, G.D. Griffin, *Antibody-based nanoprobe for measurement of a fluorescent analyte in a single cell*. Nat Biotechnol, 2000. **18**(7): p. 764-767.

62.   B.M. Cullum , G.D.G., G.H. Miller, T. Vo-Dinh, *Intracellular measurements in mammary carcinoma cells using fiber-optic nanosensors*. Anal Biochem, 2000. **277**(1): p. 25-32.

63.   T. Vo-Dinh, B.M.C., G.D. Griffin, Radiat. Res, 2001. **156**(4): p. 437-438.

64.   Vo-Dinh, T., *Chemical Analysis of Polycyclic Aromatic Compounds*. 1989, New York: Wiley.

65.   http://www.city.toronto.on.ca/health/pdf/cr_appendix_b_pah.pdf.

66.   A.V. Castellano, J.L.C., M.C. Hernandez, P.S. Aleman, J.C. Jimenez, *Benzo(a)pyrene levels in Jinamar Valley: preliminary results*. AFINIDAD, 1999. **56**(480): p. 113-120.

67. L. Shriver-Lake, B.D., R. Edelstein, K. Breslin, S. Bhatia, F. Ligler, *Antibody immobilization using heterobifunctional crosslinkers.* Biosen. and Bioelect., 1997. **12**(11): p. 1101-1106.
68. J.R. Sportsman, G.S.W., Anal Chem, 1980. **52**: p. 2013-2018.
69. J.H. Lin, J.H., J.D. Andrade, IEEE Trans. Biomed. Eng, 1988. **35**: p. 466-471.
70. G.D. Griffin, K.R.A., R.N. Thomason, C.M. Murchison, M. Mcmanis, P.G. Wecker, T. Vo-Dinh. *Polynuclear Aromatic Hydrocarbons.* in *Polynuclear Aromatic Hydrocarbons, Tenth International Symposium.* 1985. Columbus, OH: Battelle Press.
71. T. Kuljukka-Rabb, K.P., S. Isotalo, S. Mikkonen, L. Rantanen, K. Savela, *Time- and dose-dependent DNA binding of PAHs derived from diesel particle extracts, benzo[a]pyrene and 5-methylchrysene in a human mammary carcinoma cell line (MCF-7).* Mutagenesis, 2001. **16**(4): p. 353-358.
72. D.C. Spink, B.H.K., M.M. Hussain, B.C. Spink, S.J. Wu, N. Liu, R. Pause, L.S. Kaminsky, *Induction of CYP1A1 and CYP1B1 in T-47D human breast cancer cells by benzo[A]pyrene is diminished by arsenite.* DRUG METABOLISM AND DISPOSITION, 2002. **30**(3): p. 262-269.

Part Three

The Development and Application of Antibody-based

Optical Nanosensors for Measuring the Carcinogen Benzo[a]Pyrene

in a Single Living Cell

Part three is a version of a paper published in the *Journal of Nanoscience and Nanotechnology* in December 2002 by Paul M. Kasili, Brian M. Cullum, Guy D. Griffin and Tuan Vo-Dinh: **Kasili P.M,** Cullum B.M, Griffin G.D, and Vo-Dinh T., Nanosensor for *in vivo* measurement of the carcinogen benzo[a]pyrene in a single cell, *Journal of Nanoscience and Nanotechnology* 2 (6): 653-658 DEC 2002.

3.0 Abstract

This work describes the development and application of an antibody-based optical nanosensor for *in situ* measurements of the carcinogen, benzo[a]pyrene (BaP) in a single cell. This antibody-based optical nanosensor is miniaturized enabling the detection of fluorescent analytes in single cells. In addition to measuring fluorescent analytes in single cells, the nanosensor has the potential to be applied for both diagnostic and proteomics purposes. In this work, the human breast carcinoma cell line, MCF-7, was used as the model system to perform BaP measurements in single cells. A standard concentration curve for BaP was established and used to perform quantitative analyses of BaP in individual cells. From these analyses, it was estimated that the concentration of BaP in the individual cells investigated was $\sim 3.61 \times 10^{-10}$M. The results obtained demonstrate the application of antibody-based nanosensors for performing *in situ* measurements inside single living MCF-7 cells.

3.1 Introduction

In recent years, much research effort has been expended in trying to combine the two technologies of biosensors and immunoassay to produce sensors capable of measuring the formation of an immunochemical complex [48]. A wide range of techniques have been assessed in an attempt to match the performance of biosensors with that of conventional immunoassay techniques. Some of the techniques evaluated include, electrochemistry [49], solid-state devices [50, 51] and optical techniques [52, 53]. Even though both electrochemical and solid-state immunosensors have shown to produce dose-response curves, they lack the sensitivity to be useful devices. In an attempt to overcome problems associated with sensitivity, many researchers have opted to use optical transducers for the construction of immunosensors. Optical transducers have a number of advantages in the fabrication of optical biosensors, they are well-characterized materials from which to fabricate the device e.g., quartz or silica, sensitive methods of detecting the signal produced and have rapid signal generation, processing and recording times [54].

Optical biosensors represent the second major family of biosensors, after electrochemical biosensors. This has been made possible, mainly by progress in fiber-optic technology, and laser miniaturization. Optical biosensors can be miniaturized to different scales depending on the prescribed function and can thus be categorized depending on their relative dimensions. In this work we use miniaturized optical biosensors, at the scale of a billionth of a meter, aptly named optical nanosensors [54]. Optical nanosensors can typically be classified into one of two broad categories,

chemical or biological, depending on the probe being used to perform the measurements[55]. Kopelman and coworkers have developed and used both biological and chemical nanosensors to perform physiological measurements of calcium[56] and nitric oxide [57], among other physicochemicals. They can be fully inserted into a single living cell and have been developed and applied for minimally invasive intracellular chemical analysis in cells [58-60]. Similarly, these nanosensors have been used to monitor biological processes such as pathogenesis due to chemical pollutants thereby providing a method of monitoring chemicals in microenvironments.

Among the two categories of nanosensors, biological nanosensors have been developed and used by Vo-Dinh and coworkers to perform *in situ* measurements of the fluorescent analyte benzopyrene tetrol (BPT), a metabolite of the carcinogen benzo[*a*]pyrene (BaP) in single living cells [61, 62]. These nanosensors fall under the biological category of optical nanosensors based on the fact that they have antibodies immobilized on the optical fiber. The antibody-based nanosensors can be partially inserted into a single living cell without affecting the life cycle of the cell [19]. A cell survival study was previously performed [61] whereby an investigation was performed to determine whether penetration of the cell by the nanosensor resulted in intracellular or membrane damage of such a nature as to compromise cellular viability. The cell survival study was critical because it provided much needed insight as to whether or not penetration of the cell by the optical nanosensor affected cell viability. It was determined by microscopic observation that the process of mitosis

continued normally and that nanosensor insertion and withdrawal did not affect the life cycle of the cell. In retrospect, optical nanosensors that fall into the above-mentioned categories are beneficial because they reduce sample volume and absolute detection limit a billion-fold, and simultaneously reduce the response time by a factor of a thousand [58]. It is important for analytical purposes to perform molecular recognition with high specificity and sensitivity to be able to detect and quantify the extent of the antibody-antigen interactions. The application of an antibody-based nanosensor for *in situ* measurements of BPT in a single cell was previously reported in our group [55, 63]. Here, we report the application of anti-benzo[*a*]pyrene (BaP) based optical nanosensors for in situ measurements of the fluorescent analyte and the carcinogen benzo[*a*]pyrene. We selected the fluorescent molecule BaP as the analyte model system because it is a PAH of environmental and toxicological interest as a result of its mutagenic/carcinogenic properties and its ubiquitous presence in the environment [61, 64]. Therefore, detection of BaP transport inside single cells is of great biomedical interest since it can serve as a means for monitoring BaP exposure, which can lead to DNA damage [61].

BaP ($C_{20} H_{12}$) is one of the more potent carcinogens among the polynuclear aromatic hydrocarbons (PAH's) and is a fundamental indicator of exposure and carcinogenic activity of all PAH's. The PAH group of compounds are ubiquitous environmental contaminants that are formed by the incomplete combustion of organic materials, such as wood or fossil fuels. PAH, molecules are made up of three or more benzene rings, at least two of which are fused with two neighboring rings sharing two

adjacent carbon atoms. In addition to PAH that are composed of carbon and hydrogen atoms only, some PAH contain heteroatoms such as nitrogen and sulphur. PAH form a large and heterogeneous group, but the most toxic members of this family known to-date are PAH molecules that have four to seven rings. BaP is the most studied of this family of compounds and is a relatively large unsubstituted five-ring compound. BaP is lipophilic, sparingly soluble in water, and soluble in organic solvents [65]. Because of its relatively high environmental levels and high level of toxicity resulting in larger health impact than any other PAH identified in the environment, BaP is often selected as a surrogate for other PAH compounds and therefore it the most studied of the PAH family of compounds. Moreover, because of it relatively high environmental levels and high level of toxicity resulting in larger health impact than any other PAH identified in the environment. Since DNA adduct formation is the critical step in the process of carcinogenesis, it is important to measure BaP in order to determine exposure to PAH's before DNA damage occurs [66]. Figure 3.1 describes DNA adduct formation leading to BaP carcinogenesis.

Measurement of BaP is dependent on the scale at which the measurement is being performed and the type of environment being probed. Currently, the optical nanosensor is the only available technology capable of measuring BaP in single living cells. This is possible by the small scale of the nanosensor in comparison to the scale of the cell under investigation. In addition, the optical nanosensor allows for minimally invasive cell analysis and in the process allows for the continuation of normal cellular processes such as mitosis. In order to perform these measurements, it
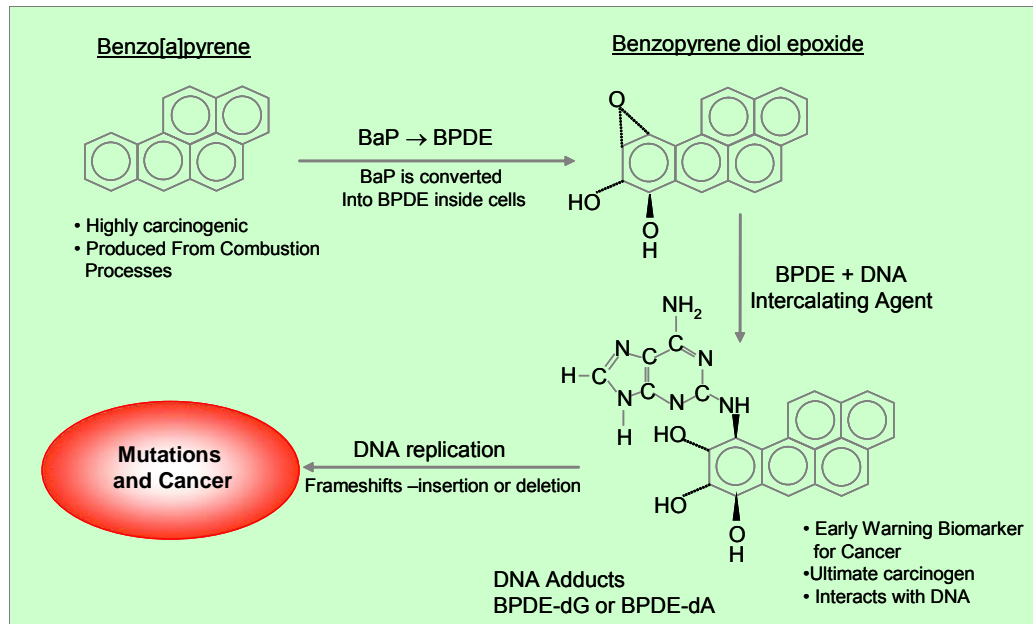
Figure 3.1 shows the pathway of DNA adduct formation that ultimately leads to BaP carcinogenesis

is necessary to use antibodies targeted to BaP. With the nanosensor with immobilized antibodies, it is possible to specifically detect BaP molecules due to the specific binding of anti-BaP to BaP. The nanosensor system was designed utilizing molecular covalent methods where a receptor unit, the antibody, was covalently linked to the sensor unit, the optical fiber. The fluorescent BaP molecules are bound by interaction with the immobilized antibody receptor, forming a receptor-ligand complex. Following laser excitation of this complex, a fluorescence response from BaP provides a basis for the quantification of BaP concentration in the cell being monitored. The fluorescence signal generated allows for a high sensitivity of detection. By utilizing the interaction between the anti-BaP and BaP, it is possible to determine fluorescence differences that can determine the presence of anti-body-BaP complexes.

The intracellular measurements of BaP depend on the reaction times involved. In a previous study, the reaction time established for antibody-BPT complexing was 5 minutes [61]. Similarly, the reaction time established in thus study for antibody-BaP complexing was 5 minutes. This was used as a standard time to enable calibration from fiber to fiber. Additionally, the nanosensors were calibrated using standard analytical procedures using measurements of known concentration of BaP reference solutions.

3.2 Experimental Procedure

3.2.1 Cell Lines

Human breast cancer cell line, MCF-7, were obtained from American Type Culture Collection (Rockville, MD, USA, Cat-no. HTB22). MCF-7 cells were grown in Dulbecco's Modified Eagle's Medium ((DMEM) (Mediatech, Inc., Herndon, VA)) supplemented with 1 mM L-Glutamine (Gibco, Grand Island, NY) and 10% fetal bovine serum (Gibco, Grand Island, NY). Baseline static culture productivity for each cell line was established in growth medium (described above) in standard T25 flasks (Corning, Corning, NY). The flasks were incubated at 37°C, 5% CO_2 and 86% humidity. Cell growth was monitored daily by microscopic observation until a 60–70% state of confluence was achieved. The growth conditions were chosen so that the cells would be in log phase growth during BaP treatment, but would not be so close to confluence that a confluent monolayer would form by the termination of the chemical exposure [7]. In preparation for experiments, cells were harvested from the T25 flasks and 0.25ml (4.0×10^5 cells/ ml) seeded into 60mm tissue culture dishes (Corning Costar Corp., Corning, NY) for overnight attachment. From a 4.464×10^{-3}M stock solution of BaP in ethanol, a range of 0.0001-1% solutions were prepared by adding the BaP solution in DMEM. The resultant solutions were added to multiple culture dishes and left in contact with the cells for a 4-hour incubation period. The amount of BaP in ethanol used was in small enough quantities such that normal cell growth did not seem affected by microscopic observation. BaP was prepared as a 1mM stock solution in reagent grade ethanol and further diluted before addition to the cells.

Following incubation of the MCF-7 cells with BaP, the medium containing BaP was aspirated, the dishes were rinsed once with sterile PBS, and the PBS was replaced with fresh growth medium before performing intracellular measurements using the nanosensor.

3.2.2 Preparation of Antibody-based Nanosensors

Preparation of antibody-based optical nanosensors has been previously described [61]. Briefly, this process involved cutting and polishing plastic clad silica (PCS) fibers with a 600-μm-size core (Fiberguide Industries, Stirling, New Jersey). Briefly, the fibers were pulled to a final tip diameter of 50 nm and then coated with 200 nm of silver metal (99.999% pure) using a thermal evaporation deposition system (Cooke Vacuum Products, South Norwalk, CT) achieving a final diameter of 250nm (Figure 3.2). The fused silica optical fibers were acid-cleaned followed by several rinses with distilled water. Finally, the substrates were allowed to air dry at room temperature in a dust free environment. The fiber tips were then silanized and treated with an organic cross-linking reagent. The silanization agent covalently binds to the silica surface of the optical nanosensor tips modifying the hydroxyl group to a terminus of choice that is compatible with the organic cross-linking reagent. Silanes were determined to be the reagents most preferred for the attachment of antibodies since these silanes produced highly uniform and reproducible films and have a terminus amendable for use with a variety of hetero-bifunctional cross-linkers [67].
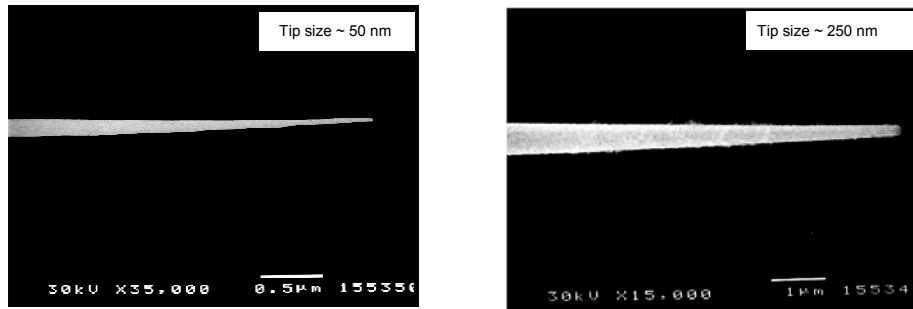
Figure 3.2 shows scanning electron micrographs of optical nanotips diameter of 50 nm (LEFT) and then coated with 200 nm of silver metal using a thermal evaporation deposition system achieving a final diameter of 250nm (RIGHT)

The choice of imidazole-terminal film is particularly attractive since the protein to be immobilized can be used without chemical modification. Antibodies bound using this procedure remained securely immobilized during washing and subsequent manipulations in immunoassay procedures, as opposed to procedures that use adsorption to attach proteins [68, 69]. Antibody to BaP was produced by co-author, Dr. G.D. Griffin. The tapered tips of the optical nanotips with silane groups and cross-linkers were immersed in a solution of anti-BaP in PBS and allowed to incubate for 3 days after which the nanosensors were inserted into single cells and used to detect and measure BaP.

3.2.3 Measurement System and Procedure

Figure 3.3 shows a schematic representation of the fluorescence measurement system. The 325 nm laser line of a HeCd laser (Omnichrome, <5mW laser power) was focused onto a 600-µm-delivery fiber that is terminated with a subminiature A (SMA) connector. The antibody-immobilized tapered fiber was coupled to the delivery fiber through the SMA connector and secured to the microscope with micromanipulators. The fluorescence emitted from the cells was collected by the microscope objective and passed through a 330-380 nm bandpass filter and then focused onto a photon-counting photomultiplier tube (PMT) for detection. The output from the PMT was recorded using a universal counter and a personal computer (PC) with custom-designed software for data treatment and processing. The experimental

HeCd Laser

Incubator
Nanosensor
Cell

197319792003

HP universal
counter

Data acquisition PC

HP power supply

PMT

Nikon inverted
fluorescence microscope
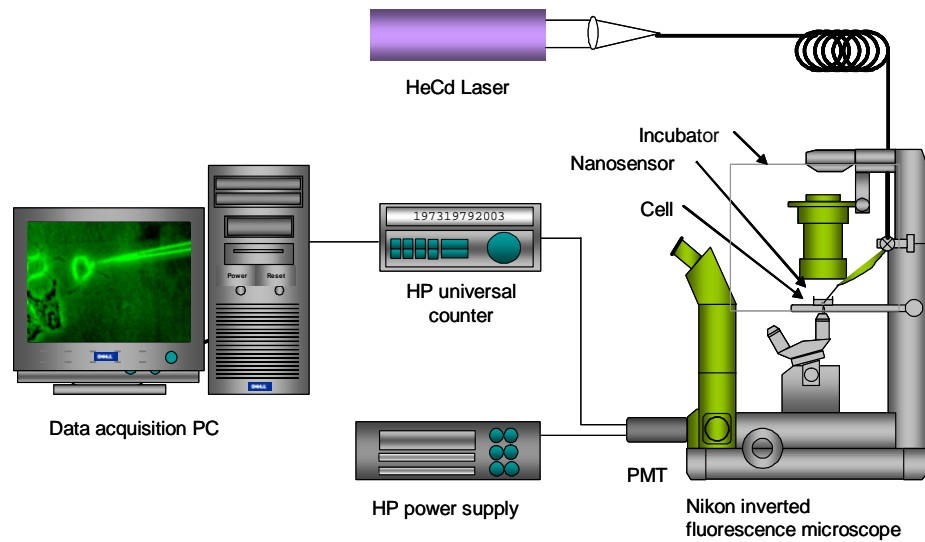
Figure 3.3 shows the components of the laser-induced fluorescence measurement system consists of HeCd laser (325nm), optical fiber, Nikon inverted fluorescence microscope equipped with UV fluorescence filters (330-380nm) to reject the laser-line and collect the fluorescence emission, a highly sensitive photomultiplier tube (PMT), a universal counter and a data acquisition PC

setup used to probe single cells was adapted to this purpose from a standard micromanipulation/microinjection apparatus. Figure 3.4 shows the Nikon Diaphot 300 inverted microscope (Nikon, Inc., Melville, NY) having a Diaphot 300/Diaphot 200 Incubator, to maintain the cell cultures at 37°C on the microscope stage, was used for these experiments. The micromanipulation equipment used consisted of MN-2 (Narishige Co. Ltd., Tokyo, Japan) Narishige three-dimensional manipulators for coarse adjustment, and Narishige MMW-23 three-dimensional hydraulic micromanipulators for final movements. The optical fiber nanosensor was mounted on a micropipette holder (World Precision Instruments, Inc., Sarasota, FL). To record the fluorescence of BaP molecules bound to antibodies at the fiber tip, a Hamamatsu PMT detector assembly (HC125-2) was mounted in the front port of the Diaphot 300 microscope. The fluorescence emitted by the bound BaP molecules was collected by the PMT and the data transmitted via a laboratory interface to a PC for data acquisition and processing.

3.3 Results and Discussion

Before making measurements, the cells were harvested from culture flasks and transferred to culture dishes. After attachment to the bases of the petri dishes, the MCF-7 cells were treated with a specified percentage of BaP/ ethanol in DMEM. The solution of BaP in DMEM was then aspirated and replaced with fresh DMEM. The nanosensors were gently inserted into individual living cells and incubated for about 5
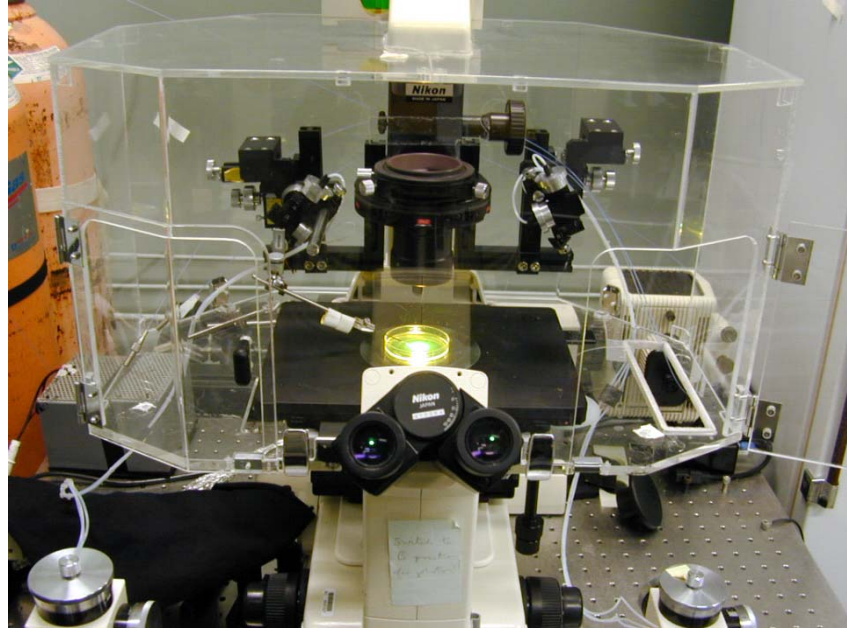
Figure 3.4 shows an image of Nikon Diaphot inverted fluorescence microscope the main component of the laser-induced fluorescence measurement system

minutes to allow antibody-BaP interaction, and the fluorescence signal was recorded.

Calibration measurements and five separate trials (each trial repeated five times) were conducted to determine the limit of detection and the reproducibility of the nanosensors. In each trial, MCF-7 cells plated in tissue culture petri dishes were incubated 4 hours prior to experimentation with DMEM solutions ranging from 0.0001-1% BaP/ethanol (concentration range of $10^{-10} - 10^{-6}$ M BaP). In addition, for each trial, one petri dish (control) was incubated under normal growth conditions, with DMEM and without the addition of BaP.

Detection and measurements of BaP in single cells using the nanosensor were carried out using the following procedure. A culture dish of cells was placed on the pre-warmed microscope stage set at 37°C. The nanosensor, mounted on a micropipette holder of a micromanipulation system, was moved into position (i.e., in the same plane as the cells), using bright-field phase contrast microscopic illumination, so that the tip was just outside of the cell to be probed. The total magnification used was 600×. The nanosensor was gently micromanipulated into the cell, past the cell membrane and extending a short way into the cytoplasm. Room light and microscope illumination light were switched-off; the laser shutter opened, and laser light allowed to illuminate the optical fiber and excitation light was transmitted into the fiber tip. First, a signal reading was taken with the nanosensor inside the cell with the laser shutter closed in order to record the dark signal. During these micromanipulations, great care was taken not to penetrate the nuclear envelope. After 5 minutes, the laser shutter was opened and fluorescence readings were

recorded. Figure 3.5 shows an image of an optical nanosensor prior to insertion and after insertion into a single MCF-7 cell illustrating how the intracellularmeasurements were executed and Figure 3.6 shows a schematic of the fluorescence excitation and detection process.

Figure 3.7 shows the results of test-tube studies of % BaP/ethanol in DMEM using five nanosensors for each measurement performed in growth medium outside the cell. The graph consists of the logarithmic scale of the concentration of BaP in DMEM obtained when measured doses of BaP in ethanol were placed in DMEM, and the intensity counts acquired upon antibody-BaP complexing. The results showed that the average fluorescence intensity values increased with increasing concentration and reached a plateau phase as a result of saturation. Shown in the calibration curve are error bars that represent a 95% confidence interval (CI). As can be seen on the curve, error bars of the concentrations 10^{-8}, 10^{-7}, 10^{-6} M overlap implying that the difference between the means is not statistically significant (P>0.05). The readings are higher in test-tube studies as compared to intracellular studies because there is a difference in diffusional kinetics as a result of the different levels of viscosity of DMEM and the aqueous cytoplasm. Granted that the inside of a cell is more like a scaffold, with a complex structure and machinery to transport proteins and other cellular components to specific sites, hence there is an increased diffusional limitation and this has the effect of decreasing the levels of BaP close to the silica surface and the rate of attachment of the BaP to the antibody on the surface. In comparison to the cell, the

94
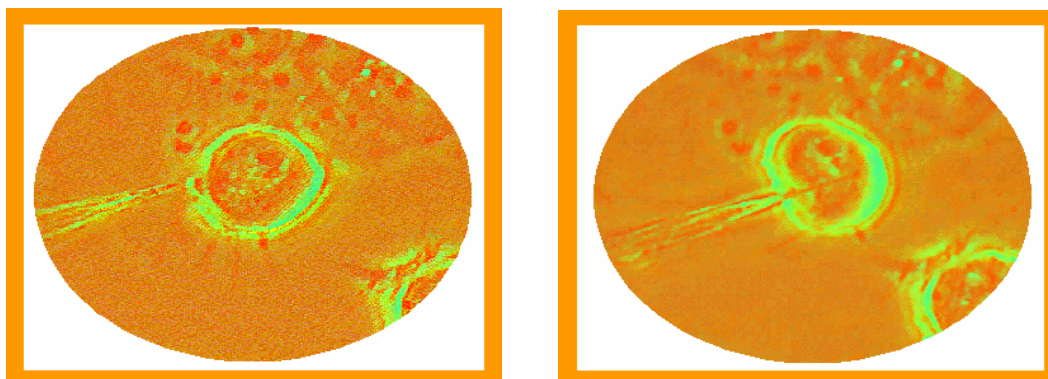
Figure 3.5 shows an image of an optical nanosensor prior to insertion (LEFT) and after insertion (RIGHT) into a single MCF-7 cell illustrating how the single cell measurements were performed
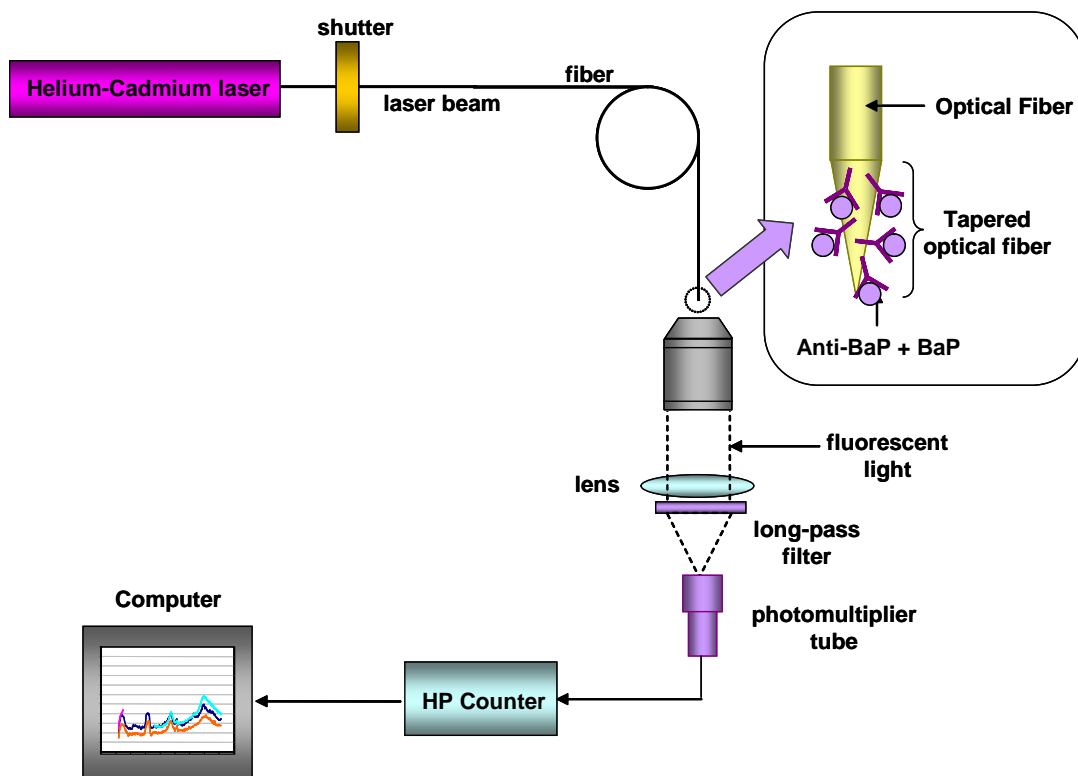
Figure 3.6 shows schematic of the fluorescence excitation and detection process. A fluorescence signal is detected and measured once the anti-benzo [a] pyrene (BaP) immobilized on the nanotips bind BaP
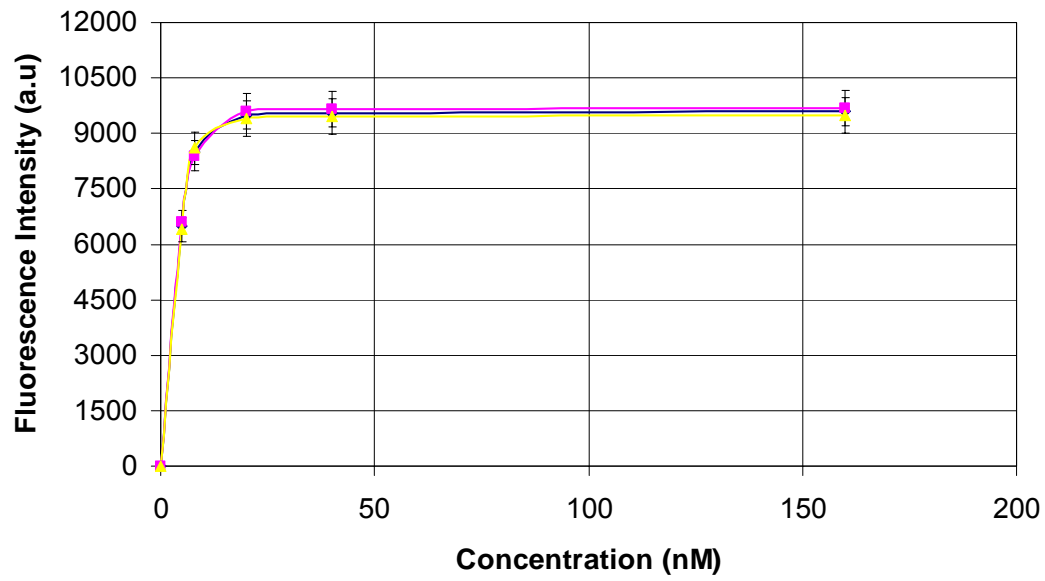
Figure 3.7 shows the results of test-tube studies of % BaP/ethanol in DMEM using five nanosensors for each measurement performed in growth medium outside the cell. Each colored line represents an average of five *in situ* BaP measurements.

BaP/ ethanol in DMEM in the test-tube is an environment without diffusional limitations. Figure 3.8 shows the results of intracellular measurements of BaP performed with nanosensors using both the control and experimental groups of MCF-7 cells. MCF-7 cells were incubated with 0.0001-1% BaP (% BaP/ethanol in DMEM). The graph consists of the final concentration of BaP in DMEM obtained when measured doses of BaP in ethanol were placed in DMEM (the final mixture was used for cell culture), and the intensity counts acquired upon antibody-BaP complexing within a single cell. Each point consists of average intensity value derived from five measurements performed for each concentration (10^{-10} – 10^{-6} M) of BaP/ ethanol in DMEM using a set of five nanosensors. The results showed that for the control group of cells, the fluorescence signal detected relative to the level of background signal was not significant.

Although a background signal was generated, it was not significant enough to confound the determination of BaP. Moreover, there are no other molecules that appear to interfere with the fluorescence measurements that would confound the determination of BaP. The explanation for this is the high specificity of antibody, the time required for the metabolism of BaP to BPT, and the use of near field excitation. The application of monoclonal antibodies renders the nanosensors selective for measurement of BaP. These antibodies are specific against a single structural determinant and thus capable of discriminating between similar epitopes. They
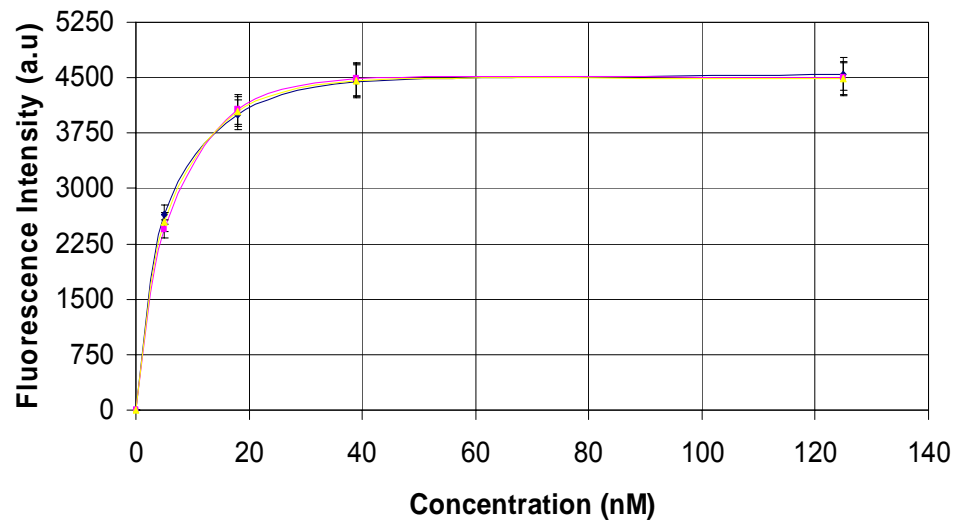
Figure 3.8 shows the results of intracellular measurements of BaP performed using anti-BaP-based optical nanosensors in MCF-7 cells. Each colored line represents an average of five *in situ* BaP measurements.

exhibit very selective binding capabilities for specific structures [70]. As a result, BaP specific monoclonal antibodies immobilized on a nanosensor tip are useful for monitoring small quantities of BaP in complex matrices because of their high specificity for the molecular structure of BaP. These antibodies also exhibit high affinity.

BaP is metabolized to 7,8-dihydrodiol-benzopyrene, which is metabolized into the epoxide metabolite of benzopyrene, BPDE, its carcinogenic form. The epoxide then binds with macromolecules such as protein and DNA (BPDE-DNA) to cause cytotoxicity. DNA adduct formation of 2.5 µM BaP occurs at 12 hr exposure, after which BPDE adducts decrease [71]. Metabolism of 3 µM BaP peaks at 9 to 16 hrs after exposure [72]. By exposing MCF-7 cells to varying concentrations of BaP $(4.464 \times 10^{10} - 4.464 \times 10^{-6}M)$ for a 4 hr incubation period, we do not provide sufficient time for either BaP metabolism or DNA adduct formation. Therefore, BPT is an unlikely to confound the determination of BaP.

The application of near field excitation contributes to the specificity of the nanosensor and virtually nullifies any effects that may confound the determination of BaP. Excitation of BaP lies in the strong evanescent-wave component of near-field excitation. The near field of the fiber (on the distal end) is where the antibody is immobilized and antibody-antigen complexing occurs and thus only BaP molecules that lie on the near-field are excited [61]. Consequently, the nanosensor used to monitor the cells incubated with % BaP/ ethanol in DMEM transduced a relatively

higher fluorescent signal as a result of BaP molecules sequestered at the tapered tip of the antibody-based nanosensor.

Figure 3.9 shows the excellent degree of reproducibility achieved using the nanosensors to perform the intracellular detection of BaP. This figure shows the results obtained using five antibody-based nanosensors to probe MCF-7 cells incubated in 0.01% BaP in DMEM. Similarly, five antibody-based nanosensors were used to probe MCF-7 cells incubated without BaP/ ethanol in DMEM. The relative variations from nanosensor to nanosensor with or without bound BaP were approximately 7-10%. The fluorescence signal obtained using the nanosensors used to probe cells incubated with BaP/ ethanol in DMEM is relatively higher than the signal obtained by nanosensors used to probe cells incubated without BaP/ ethanol in DMEM. Despite reproducibility being a challenging aspect of this project, we managed to produce highly reproducible nanosensors. Excellent reproducibility was achieved as a result of improvements and refinements of the input parameters of the laser based micropipette-pulling device. Optimization of input parameters involved varying the user input parameters: heat, delay and pull strength. By varying the heating temperature as well as the tension applied to the fiber, we successfully produced reproducible tip diameters from fiber to fiber. This was confirmed by acquiring SEM images of the pulled fibers. The optimization of the input parameters of the micropipette pulling device enables very good batch reproducibility which is
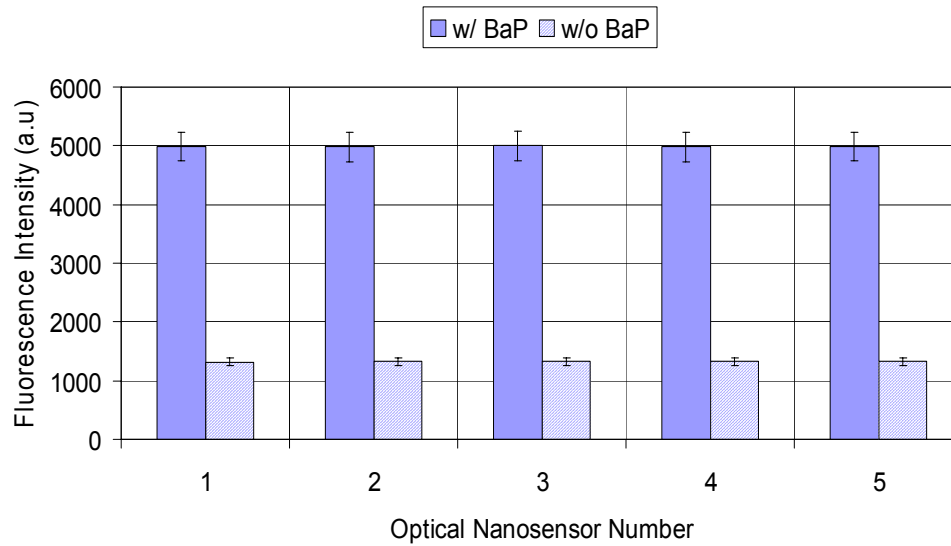
Figure 3.9 shows the excellent degree of reproducibility achieved using the nanosensors to perform the intracellular detection of BaP. This figure shows the results obtained using five antibody-based nanosensors to probe MCF-7 cells incubated in 0.01% BaP in DMEM.

especially essential for a technology aimed to single-use nanosensors allowing calibration to be done by measurement of the performance of one nanosensor. This study demonstrated the excellent reproducibility of antibody-based nanosensors.

3.4 Shelf life and Stability of Immobilized Protein

The stability of the immobilized antibody was determined in terms of the retention of activity after 21 days of storage at 4oC. No significant loss of activity was observed at the end of this period. In contrast, it was found that after drying, solid support with immobilized antibody rapidly lost activity within a few days. Therefore an aqueous environment is recommended for the long-term storage of these immobilized antibodies. Figure 3.10 shows the side-by-side comparison of nanosensors that have been utilized immediately after the immobilization of antibody and another set that have been used 21 days after preparation. The results show that here is no significant loss of activity by the end of the 21-day period.

3.5 Conclusion

In this work, we demonstrated the development and application of a rapid, selective and sensitive method for the determination of the carcinogen BaP in single cells using antibody-based nanosensors targeted to the fluorescent analyte, BaP. The results obtained in this work demonstrate in situ measurements performed inside single living cells using an antibody-based nanosensor and the potential application of antibody-based nanosensors in proteomics. The results obtained also support the
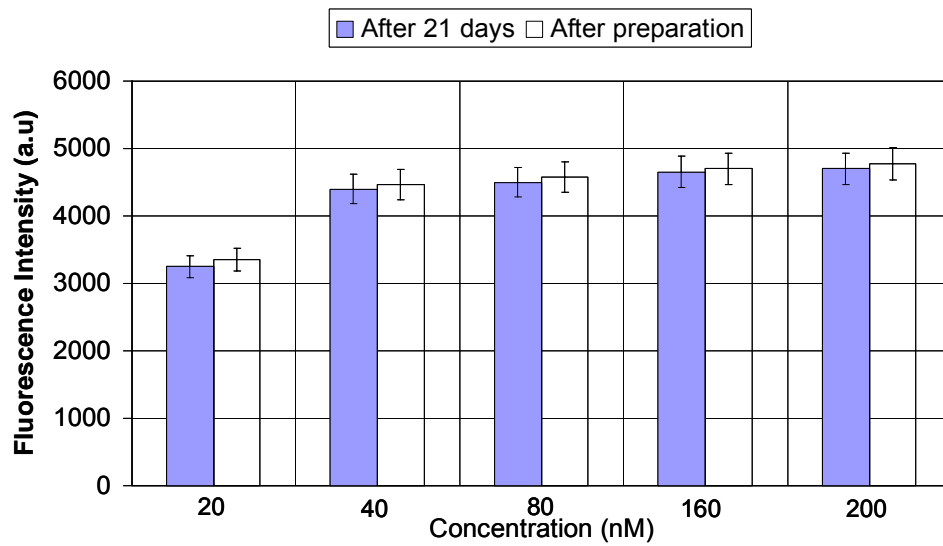
Figure 3.10 shows the side-by-side comparison of nanosensors that have been utilized immediately after the immobilization of antibody and another set that have been used 21 days after preparation. It can be seen from these results that there is no significant loss of activity by the end of the 21-day period.

previously reported [7] study involving the development and application of optical nanosensors for the detection of BPT. The quantification limits were extrapolated using linear regression and calculated to be ~3.61 x 10-10M. This is the lowest concentration of BaP estimated in a single MCF-7 cell. This result indicates that BaP can be monitored and measured using antibody-based optical nanosensors within single living cells.

3.6 Summary

Optical nanosensors were successfully nanofabricated and applied to measure BaP both *in vitro* and *in vivo*. They have a steep linear response with saturation point developing fast and a very narrow dynamic range (~5 – 20 nM). They have a low detection limit ~36.1 nM and excellent reproducibility that was determined from the percent 10% variability from nanosensor-to-nanosensor in measurements performed using the. Antibody stability after immobilization was observed when the optical nanosensors were stored at $4^{o}C$ in an aqueous environment. Optical nanosensors have the potential to analyze at the single cell level the activities of specific proteins participating in cell signaling networks/ pathways. By monitoring these proteins we can understand how they are regulated at the lowest possible levels.

References

1. Turner, A., Karube, I., Wilson, GS., ed. *Biosensors – Fundamentals and Applications*. 1987, Oxford University Press: Oxford.

2. Schmid, R., and Karube, I., *Biotechnology*, in *Biosensors and Bioelectronics*, H. Rehm, and Reed G., Editor. 1998, VCH Verlagsgesellschaft: Weinheim-Basel-Cambridge-Newyork.

3. Updike, S., and Hicks, GP., *The Enzyme Electrode.* Nature, 1967. **214**: p. 986-988.

4. Guilbault, G., and Montalvo, JGJ., *A Urea specific enzyme electrode.* Journal of The American Chemical Society, 1969. **9**: p. 2164-2167.

5. Bilitewski, U., and Schmid, RD. *Alcohol determination by modified carbon paste electrodes*. in *The GBF International Workshop on Biosensors*. 1989. Braunschweig, Germany.

6. Kulys, J., Bilitweski, U., and Schmid, RD. *Biosensors based on chemically modified electrodes*. in *The GBF International Workshop on Biosensors*. 1989. Braunschweig, Germany.

7. Robinson, G., *Optical Immunosensors: An Overview*, in *Advances in Biosensors*, T. APF, Editor. 1991, JAI Press Inc: London. p. 230-252.

8. B.M. Cullum , T.V.-D., *The development of optical nanosensors for biological measurements.* Trends Biotechnol, 2000. **18**(9): p. 388-393.

9. M. Shortreed, R.K., M. Kunh, B. Hoyland, *Fluorescent fiber-optic calcium sensor for physiological measurements.* Anal Chem., 1996. **68**(8): p. 1414-8.

10. S.L. Barker, R.K., Anal Chem., 1998. **70**(23): p. 49062-6.

11. M. Brasuel, R.K., T.J. Miller, R. Tjalkens, M.A. Philbert, *Fluorescent nanosensors for intracellular chemical analysis: decyl methacrylate liquid polymer matrix and ion-exchange-based potassium PEBBLE sensors with real-time application to viable rat C6 glioma cells.* Anal Chem., 2001. **73**(10): p. 2221-8.

12. H. A. Clark, R.K., R. Tjalkens, M.A. Philbert, *Optical nanosensors for chemical analysis inside single living cells. 2. Sensors for pH and calcium and the intracellular application of PEBBLE sensors.* Anal Chem, 1999. **71**(21): p. 4837-43.

13. H. A. Clark, M.M., M.A. Philbert, R. Kopelman, *Optical nanosensors for chemical analysis inside single living cells. 1. Fabrication, characterization, and methods for intracellular delivery of PEBBLE sensors.* Anal Chem, 1999. **71**(21): p. 4831-6.

14. T. Vo-Dinh, J.P.A., B.M. Cullum, G.D. Griffin, *Antibody-based nanoprobe for measurement of a fluorescent analyte in a single cell.* Nat Biotechnol, 2000. **18**(7): p. 764-767.

15. B.M. Cullum , G.D.G., G.H. Miller, T. Vo-Dinh, *Intracellular measurements in mammary carcinoma cells using fiber-optic nanosensors.* Anal Biochem, 2000. **277**(1): p. 25-32.

16. Vo-Dinh, T., and Cullum, BM., *CRC Handbook for Biomedical Photonics*. Nanosensors for Single Cell Analysis, ed. T. Vo-Dinh. 2003, Newyork: CRC Press. 14.

17. T. Vo-Dinh, B.M.C., G.D. Griffin, Radiat. Res, 2001. **156**(4): p. 437-438.

18. Vo-Dinh, T., *Chemical Analysis of Polycyclic Aromatic Compounds*. 1989, New York: Wiley.

19. http://www.city.toronto.on.ca/health/pdf/cr_appendix_b_pah.pdf.

20. A.V. Castellano, J.L.C., M.C. Hernandez, P.S. Aleman, J.C. Jimenez, *Benzo(a)pyrene levels in Jinamar Valley: preliminary results*. AFINIDAD, 1999. **56**(480): p. 113-120.

21. L. Shriver-Lake, B.D., R. Edelstein, K. Breslin, S. Bhatia, F. Ligler, *Antibody immobilization using heterobifunctional crosslinkers*. Biosen. and Bioelect., 1997. **12**(11): p. 1101-1106.

22. J.R. Sportsman, G.S.W., Anal Chem, 1980. **52**: p. 2013-2018.

23. J.H. Lin, J.H., J.D. Andrade, IEEE Trans. Biomed. Eng, 1988. **35**: p. 466-471.

24. G.D. Griffin, K.R.A., R.N. Thomason, C.M. Murchison, M. Mcmanis, P.G. Wecker, T. Vo-Dinh. *Polynuclear Aromatic Hydrocarbons*. in *Polynuclear Aromatic Hydrocarbons, Tenth International Symposium*. 1985. Columbus, OH: Battelle Press.

25. T. Kuljukka-Rabb, K.P., S. Isotalo, S. Mikkonen, L. Rantanen, K. Savela, *Time- and dose-dependent DNA binding of PAHs derived from diesel particle extracts, benzo[a]pyrene and 5-methylchrysene in a human mammary carcinoma cell line (MCF-7)*. Mutagenesis, 2001. **16**(4): p. 353-358.

26. D.C. Spink, B.H.K., M.M. Hussain, B.C. Spink, S.J. Wu, N. Liu, R. Pause, L.S. Kaminsky, *Induction of CYP1A1 and CYP1B1 in T-47D human breast cancer cells by benzo[A]pyrene is diminished by arsenite*. DRUG METABOLISM AND DISPOSITION, 2002. **30**(3): p. 262-269.

Part Four

Antibody-based Optical Nanosensor for the Measurement of Apoptosis

4.0 Abstract

This work describes the application of optical nanosensor technology to measure apoptosis whereby the feasibility of antibody-based optical nanosensors for monitoring apoptosis by detecting protein-protein interaction and identifying protein activity were demonstrated. It describes the application of these nanosensors for the *in vitro* and pseudo *in vivo* measurement of two key apoptosis proteins cytochrome c and caspase-9, which are involved in the mitochondrial pathway of apoptosis. The *in vitro* and pseudo *in vivo* measurement involve the application of the antibody-based optical nanosensor employing the indirect detection scheme or sandwich type immunoassay whereby one of the partners in the immune interaction is labeled with a fluorescent molecule. The capture and reporter antibodies bind different epitopes of the same target biomolecule, and the interactions detected in the evanescent field of the optical nanosensor. This is a highly sensitive technique especially suitable for monitoring antibody-antigen interaction [73]. For both the *in vitro* and pseudo *in vivo* measurements, apoptosis was induced using a photodynamic therapy (PDT) agent δ-aminolevulinic acid (ALA) that initiates the mitochondrial pathway of apoptosis. This pathway involves cytochrome c release from mitochondria followed by the activation of caspase-9.

4.1 Introduction

Optical nanosensors are in general small devices, which incorporates a biological component onto a transducer as a key functional element. They are based

on a direct spatial coupling between a biologically active compound and a signal transducer. The biological component is usually an antibody or enzyme immobilized onto the transducer, the electronic or optic sensing system that detects the environmental changes brought about by the biological reaction. The colorimetric, fluorometric or chemiluminescent product of the reaction is often detected by the transducer [48, 74].

Optical nanosensors based on the antigen–antibody interaction are generally known as immunosensors. The high specificity and high sensitivity that defines an antigen–antibody reaction has been used in a vast range of laboratory-based tests incorporating antibody components. The analytes detected and measured have included many medical diagnostic molecules, clinical disease markers, bacteria, and such environmental pollutants as polynuclear aromatic hydrocarbons (PAH's). There are two different types of immunosensors, *direct* and *indirect* immunosensors. *Direct* immunosensors are based on the immobilization of antibodies on a transducer surface which serve to capture target moleculecules with either colorimetric or fluorescent properties. Accordingly, they register immunochemical complex formation at the transducer surface via optical changes for direct detection of target molecules. The advantage of a direct immunosensor is that measurement of the antigen–antibody interaction can be accomplished immediately without any need for additional antibodies or markers such as enzymes or fluorescent labels. On the other hand, *Indirect* immunosensors involves the use of antibodies involved in an immune interaction which includes a capture and reporter antibody. As the naming suggests,

the capture antibody functions to bind and immobilize the target molecule, while the labeled reporter antibody binds to another epitope of the target molecule to "report" the binding event. These combine the high selectivity of immunoreactions with the high sensitivity characteristic of the fluorescence effect [73, 75].

In this work, the *indirect* immunosensing method was used to perform the *in vitro* and pseudo *in vivo* measure two important apoptosis proteins, cytochrome c and caspase-9. This involved measuring cytochrome *c* and caspase-9 in cytosolic cell extract (*in vitro*) obtained from two cell groups; one in which apoptosis had been induced and the other in which apoptosis had not been induced. Optical nanosensor with capture antibody was incubated in cytosolic extract to initially form a primary immunocomplex. Following primary immunocomplex formation, the optical nanosensors incubated with Cy5 labeled reporter antibody forming a secondary immunocomplex. Similarly, pseudo *in vivo* measurement involved inserting and incubating an optical nanosensor with capture antibody into a single living cell. The optical nanosensor was gently withdrawn from within the living cell and incubated in a phosphate buffered saline (PBS) containing Cy5 labeled reporter antibody resulting in the formation of a secondary immunocomplex. In both cases, Cy5 label was excited using evanescent optical waves at the near-field of the optical nanosensors generated from the 632.8 nm of HeNe and the fluorescence intensity is recorded as a function of time.

4.2 Antibody-based Optical Nanosensors

Optical nanosensors used in this work exploit antibodies to monitor apoptosis proteins. One of the key factors in determining the usefulness of any biosensor is its specificity, which can be defined as its ability to specifically measure the analyte of interest, without having other biochemical species interfere with the measurement. Specificity is an important characteristic because it allows measurements to be made in complex environments. Since their first use in antibody-based optical biosensors for the measurement of the carcinogen benzo[a]pyrene[26], antibodies have gained increasing importance as bioreceptor molecules for optical biosensing applications [76-83]. Antibodies are immunoglobulins capable of specific combinations with antigenic molecules that caused their production. They exhibit very selective binding capabilities for specific structures and can posses both high specificity and binding affinity for a given antigen or hapten [84]. Two classes of antibodies exist, both of which have been used in constructing optical biosensors, (i) monoclonal antibodies, and (ii) polyclonal antibodies. Monoclonal antibodies are often used when the measurement of a very specific analyte is desired, while polyclonal antibodies exhibit less specificity. Specificity of monoclonal antibodies makes them extremely efficient for binding within complex matrices. On the other hand, polyclonal antibodies often recognize multiple epitopes, making them more tolerant to small changes in the nature of the antigen. Due to the complex nature of biological systems, the specific binding abilities of antibodies make them one of the most powerful biorecognition molecules to be used for constructing nanosensors [19].

The use of antibodies as biorecognition molecules on optical nanosensors for measuring apoptosis proteins was performed using the *direct* and *indirect* immunoassay formats respectively. The simpler of the two assay formats is the direct immunoassay format, which is most compatible when working with molecules that have intrinsic fluorescent properties. The main advantage of this format is that there is no need to label the interactants. The working principle of the direct immunoassay format, involves binding the target biomolecule to immobilized primary antibody, at which time an optical property e.g., fluorescence intensity, of the target molecule is measured. The *direct* immunoassay format is not applicable in cases where an optical property of a target molecule cannot be measured or is not intrinsically fluorescent [26], presenting a challenge and limitation. In such cases, this limitation can be overcome by using the *indirect* immunoassay format. This immunoassay format is straightforward and involves a capture antibody and a labeled reporter antibody, which bind to the non-fluorescent target molecule forming a sandwich type structure assay. After the sandwich type structure or secondary immunocomplex is formed, the fluorophore on the reporter antibody can be excited and detected. Typically, the fluorescent signal produced is representative of the binding event. Therefore, the *indirect* immunoassay format enables the measurement of biomolecules that are not intrinsically fluorescent and in a way makes it possible to study biomolecules in significant biochemical pathways such as apoptosis [19].

4.3 Apoptosis

Apoptosis or programmed cell death (PCD) is a highly ordered, genetically controlled process that plays a fundamental role in both normal biological processes and disease states. Apoptosis is a combination of the Greek words *apo*, off, and *ptosis*, falling) or programmed cell death, is an orderly and genetically controlled form of cell death defined distinct morphological and biochemical features. It usually affects single cells or small groups of cells in an asynchronous fashion. Apoptosis consist of four key phases [85];

- *The Initiation Phase*
- *Decision Phase*
- *The Committed or Effector phase*
- *The Cellular Degradation Phase*

4.3.1 The Initiation Phase

The molecular pathway includes an initiation phase**,** which starts after signaling by internal triggers**,** (a) increases in intracellular Ca^{2+} (b) activation of protein kinases A and C (c) increases in protein synthesis C, changes in gene regulation (d). external triggers such as (a) ligation to distinct receptors or (b). endogenous mechanisms related to aging or to exogenous irreversible cellular or nuclear damage.

4.3.2 The Decision Phase

During the decision phase transduction occurs of the apoptotic signal to nuclear and cytoplasmic target enzymes, which includes activation of endonucleases and enzymatic alterations of the cytoskeleton. There are numerous proteins and lipid-derived moieties that modulate the apoptotic mechanism in positive or negative direction.

4.3.3 The Committed or Effector Phase

The committed or effector phase is started when the cell has arrived at a stage of no return. The nuclear DNA is cleaved in multiples of 180-200 base pairs, the plasma membrane, integrity and the mitochondria remain initially intact, the cell splits up into apoptotic bodies, small vesicles which enclose the nuclear and cellular remnants.

4.3.4 The Cellular Degradation Phase

The cellular degradation phase is arrived, when the apoptotic bodies are phagocytosed by adjacent cells and macrophages. It is thought that the pharmacodynamics of anticancer drugs consists of two distinct steps. The first step includes the interaction with its cellular target; which is not lethal per se. The commitment of the cell to undergo apoptosis forms the second step. The efficacy of anticancer drugs is determined by the ability to selectively sensitize tumor cells to apoptosis.

4.4 The Importance of Measuring Apoptosis

Specific morphological and biochemical features characterize apoptosis. It is a normal and abnormal component of the development and health of multi-cellular organisms. Cells die in response to a variety of stimuli and during apoptosis, they do so in a controlled, regulated fashion. This makes apoptosis distinct from another form of cell death called necrosis in which uncontrolled cell death leads to lysis of cells, inflammatory responses and, potentially, to serious health problems. Apoptosis, by contrast, is a process in which cells play an active role in their own death, which is why apoptosis is often referred to as cell suicide.

Over the past decade, the importance of apoptosis has been appreciated, and it is now thought to be the main mode of cell death in liver diseases, neuronal cell death in neurodegenerative disease (e.g., Alzheimer's disease). Apoptosis has been found to have a role in one mechanism leading neuronal cell death associated with Alzheimer's disease and in liver disease. On the other hand, the loss of ability of cells to undergo apoptosis is one of the causes of uncontrollable cell growth leading to cancer. Tumor growth is determined not only by increased cell division, but also by decreased tumor-cell attrition. Therefore most, if not all, cancer cells acquire resistance to the various mechanisms that lead to apoptosis [86, 87].

4.5 Apoptosis Pathways

There are three major apoptosis pathways:

- *Mitochondrial Pathway*

- *Death Receptor Pathway*

- *Endoplasmic Reticulum Pathway*

The first, *Mitochondria Pathway* is triggered when mitochondria are irreversibly damaged. It is mediated by mitochondria, which release apoptogenic proteins, mainly cytochrome *c*. Cytochrome *c* once released into the cytosol binds to a cytosolic protein apoptotic protease-activating factor (Apaf-1) and this complex in the presence of dATP or ATP facilitates activation of caspase-9, which in turn activates downstream caspases [88, 89]

The *Death Receptor Pathway* triggered by the binding of extracellular ligand, tumor necrosis factor alpha (TNF-α), Lymphotoxin, Fas ligand (FasL) to their cell surface receptors leading to caspase-8 activation [90].

The third pathway is initiated by *Endoplasmic Reticulum* (ER) stress (due to depletion of ER calcium or accumulation of unfolded proteins) and causes activation of caspase-12 [91], which recently has been shown to activate caspase-9 [92]. It is unclear whether this pathway may operate in human cells because a human homologue of murine caspase-12 has not been found.

4.5.1 Mitochondrial Pathway of Apoptosis

This work is focuses on the mitochondrial pathway of apoptosis (Figure 4.1) because it is through this apoptosis pathway that the effects of chemotherapeutic and
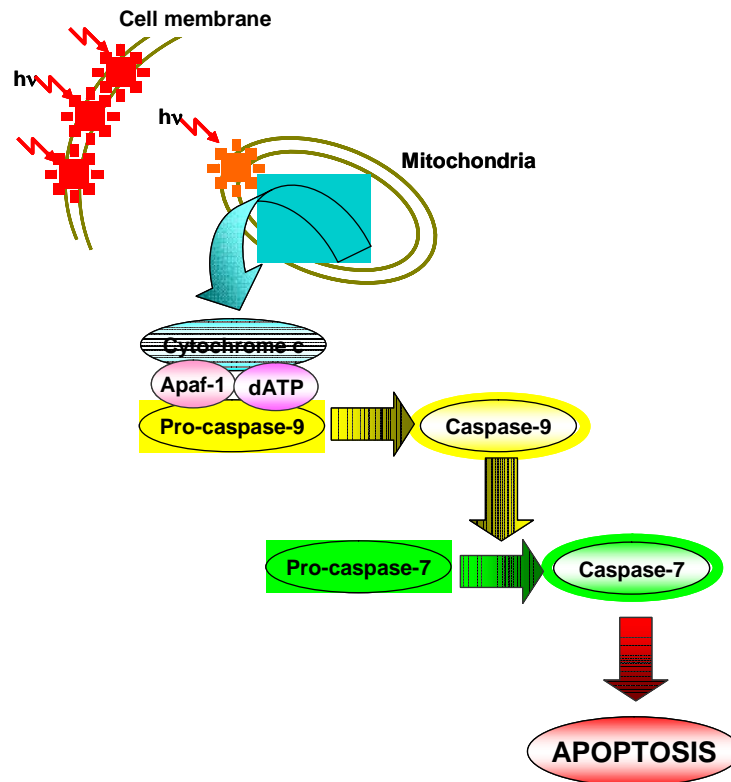
Figure 4.1 shows the Mitochondria Pathway of Apoptosis which is triggered when mitochondria are irreversibly damaged. It is mediated by mitochondria, which release apoptosis proteins, cytochrome c into the cytosol. Once released into the cytosol, cytochrome c binds to a cytosolic protein apoptotic protease-activating factor (Apaf-1) and this complex in the presence of dATP or ATP facilitates activation of caspase-9, which in turn activates downstream caspases such as caspase-7

photodynamic therapy (PDT) drugs are realized. The mitochondrial pathway of apoptosis can be activated by a variety of agents including PDT drugs or photosensitizers e.g., ALA, reactive oxygen species e.g., H_2O_2, and certainchemotherapy drugs e.g., Tamoxifen. These therapeutic agents cause mitochondrial damage, which results in lowering of mitochondrial membrane potential and subsequently altered membrane permeability leading to the release of cytochrome-c form intermembrane space of mitochondria. Cytochrome c binds to apoptosis protease activating factor –1 (Apaf-1) and caspase-9, in the process activating capse-9. Activated caspase-9 cleaves either caspase-3 or caspase-7 resulting in downstream events involved in cell death [93]. Caspase-9, caspase-7 and caspase-3 are **C**ysteine **asp**artate-specific prote**ases** (**Caspases**) involved in highly specific proteolytic cleavage events in dying cells. Caspases are specialized cysteine-dependent proteases that cleave major structural proteins of the cytoplasm and nucleus [93] and activation of caspases is often considered a key biochemical hallmark of apoptosis.

In normal healthy cells caspases exist as poorly active or inactive zymogens that can be activated by autocleavage or processing by other proteases. Mitochondria contain both the pro-caspase-9 and comparatively little of the processed, mature form of caspase-9 and cytochrome c. Upon the induction of apoptosis, cytochrome c is exported from the mitochondria to the cytoplasm and mitochondrial pro-caspase-9 translocates to the cytosol and to the nucleus. Mitochondria also release mature

caspase-9 upon induction of permeability transition *in vitro*. Cytochrome c and caspase-9 appear to be equally and functionally important initiators of the apoptosis.

4.5.2 Cytochrome c

Cytochrome c is a protein that is important to the process of creating cellular energy, the main function of mitochondria. Cytochrome *c* is an essential component of the mitochondrial respiratory chain. It is a 15KDa soluble protein, localized in the intermembrane space and loosely attached to the surface of the inner mitochondrial membrane. In response to a variety of apoptosis-inducing agents, cytochrome *c* is released from mitochondria to the cytosol [94]. When mitochondria are damaged, cytochrome *c* is released into the main body of the cell, and if the cell itself is damaged, into the surrounding tissue. The release of cytochrome *c* is part of the cascade of cellular events that lead to apoptosis, or programmed cell death. Apoptosis is triggered by the genes a cell carries, and differs from necrosis, cell death from catastrophic outside forces. When some trigger sets off the cycle that leads to apoptosis, cytochrome *c* appears outside the mitochondria within one hour. Cytochrome *c* is not a factor in necrosis. Cytochrome *c* release from mitochondrion is indicative of apoptosis and can be used as evidence that apoptosis is occurring [95].

4.5.3 Caspase-9

Caspase-9 is one of the most important cysteinyl aspartate specific protease (caspase) among the caspase family members. Caspase-9 is synthesized as inactive

pro-enzyme that is processed in cells undergoing apoptosis. The processed form consists of large (35Kda) and small (11Kda) subunits. Antibody can detect the 35Kda protein corresponding to the large subunit. Caspase-9 is thought to trigger a caspase-cascade leading to apoptosis [96]. As a result of mitochondrial membrane permeabilization, which may set the point-of-no-return of the death process [97, 98] caspase activators including cytochrome c and caspase-9, are released from the mitochondria intermembrane space into the cytosol. Cytochrome c release triggers the assembly of the cytochrome c/ Apaf-A/ pro-caspase-9 activation complex, the apoptosome [99, 100], moreover, caspases-9 is processed in response to cytochrome c.

4.6 Photodynamic Therapy (PDT)

Because the focus of this work is the mitochondrial pathway of apoptosis, the PDT agent or photosensitizer ALA was used to induce apoptosis. PDT is a treatment modality for various cancers and other diseases associated with selective accumulation or production of photosensitizers in diseased tissue and cells [101]. PDT induces apoptosis in human carcinoma cells (MCF-7 cells) when the combined administration of a photosensitizer followed by its activation by light of the appropriate wavelength is used [102]. Photodamage to mitochondria caused by the production of reactive oxygen species from the reaction of PDT agents and light results in immediate loss of mitochondrial membrane potential together with the release of cytochrome c into the cytosol. This is followed by a rapid activation of

caspases [103]. <u>Figure 4.2</u> shows a diagrammatic representation outlining the PDT process while the photophysics PDT sensitization. The photosensitizer possesses an absorption maximum at a wavelength corresponding with that of the incident laser light, and shining light on the photosensitizer causes excitation to the singlet excited state (^{1}P*). The singlet excited photosensitizer can decay back to the ground state with release of energy in the form of fluorescence - enabling identification of tumor tissue. If the singlet state lifetime is suitable (and this is true for many photosensitizers) it is possible for the singlet to be converted into the triplet excited state (^{3}P*) which is able to transfer energy to another triplet. One of the very few molecules with a triplet ground state is oxygen, which is found in most cells. Energy transfer therefore takes place to afford highly toxic singlet oxygen (^{1}O$_2$) from ground state oxygen (^{3}O$_2$), provided the energy of the ^{3}P* molecule is higher than that of the product ^{1}O$_2$. As a result, the reactive oxygen species produced destroys cancer cells.

4.6.1 Photodynamic Therapy Agents or Photosensitizers: δ-Aminolevulinic Acid

Photodynamic therapy agents or photosensitizers are chemical substances or medications that increase the sensitivity of cells, tissues or organs to irradiation by optical radiation. Photosensitizers used for PDT are capable of inducing cancer cell death through apoptosis. Cancer cells are injured by the photosensitizing action of the PDT agent and cell death results from activation of the internal constituents of the

122
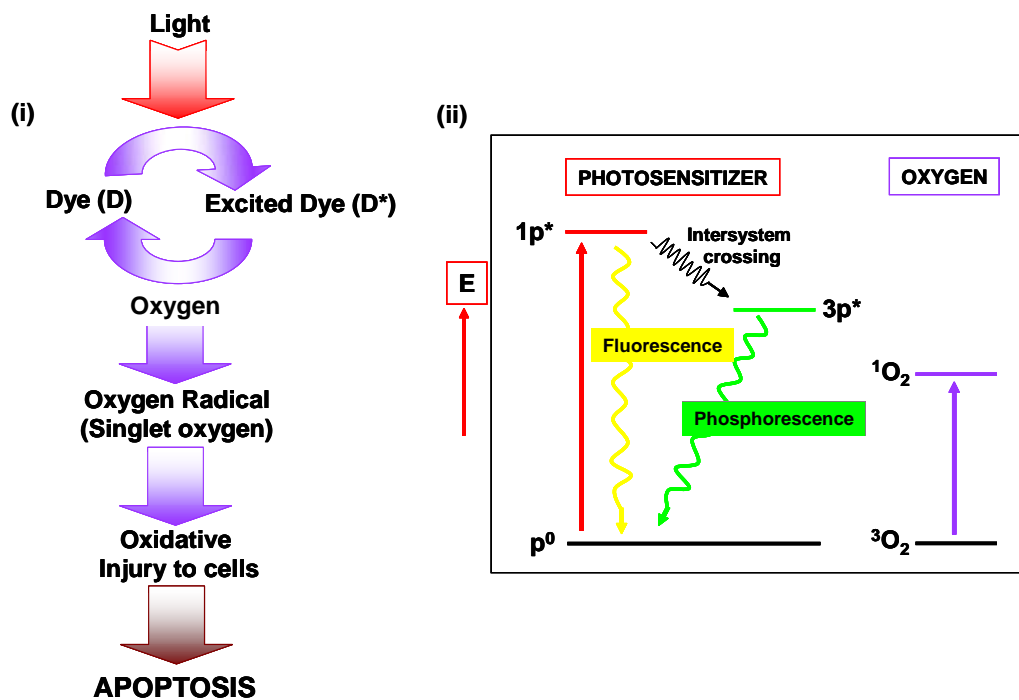
Figure 4.2 (i) shows the photodynamic therapy process leading up to apoptosis. A photosensitizing agent or dye (D) is exposed to light of a particular wavelength for activation. The excited form of the dye (D*) transfers the energy acquired from excitation light to molecular oxygen forming oxygen radicals that causes oxidative damage to cancer cells ultimately destroying them. (ii) shows a simplified Jablonski diagram of the photophysics of photosensitization (vibrational levels omitted).

apoptosis machinery [104]. The photosensitizer used to induce the mitochondrial pathway of apoptosis is δ-Aminolevulinic (ALA). The photosensitizer ALA is a precursor of protoporphyrin IX (PpIX) [105]. ALA is converted into PpIX by cells, which can then be activated by blue or red light [102]. Following light activation, PpIX is excited to a high-energy triplet state that can transfer its energy to molecular oxygen to form highly reactive oxygen species [106]. Reactive oxygen species can induce a number of biological processes including apoptosis [107, 108]. ALA induced PpIX causes mitochondrial damage and induce apoptosis through release of cytochrome c and caspase-9 though, some cells, may survive PDT [109]. The consequence of cytochrome *c* release is the activation of a series of proteases known as caspases. The caspase cascade commences with the cleavage of procaspase-9.

Apoptosis has been shown to occur following ALA administration and photoactivation in pancreatic carcinoma cells [110], V79 Chinese hamster fibroblast cells, [111], colonic adenocarcinoma cells [111] and MCF-7 cells[112]. ALA generates signals to the mitochondria that induce the release of cytochrome c [113]. Following its release from the mitochondria, cytochrome c activates the initiator procaspase-9 producing the activated form, caspase-9, which in turn activates other effector caspases such as caspae-7 and caspase-3. ALA-PDT induces rapid apoptosis as early as 2-3 hours after light exposure. This observation and the known localization of PpIX to the mitochondria following incubation with ALA suggests that ALA-PDT induces apoptosis by disrupting the mitochondrial transmembrane potential followed by cytochrome C and subsequent induction of caspases [114].

4.7 Human Mammary Adenocarcinoma Cells: MCF-7 cells

For this work, the human mammary adenocarcinoma cell line, MCF-7 was used. MCF-7 is a tumorigenic cell line (American Type Culture Collection (ATCC), Rockford, MD), derived from human breast tumor. These cell are self-adherent and amendable to manipulation. These cells are maintained as monolayers and are commonly used to study apoptosis in breast cancer cells. MCF7 cells are significant because they are known to cause breast cancer in 8-10 percent of the female population in the US. Breast cancer is the most common malignancy and the most frequent cause of cancer related death among women (Cancer Facts & Figures- 2001, American Cancer Society (ACS). The MCF7 cells are also one of the most commonly used cells for breast cancer research, are well characterized, and have been found to be tumorigenic in nude mice. In addition, the initiation of apoptosis in MCF-7 cells has been reported using photosensitizers in combination with laser irradiation doses [115]. Another reason for opting to work with MCF-7 cells is that some have been found to lose their ability to bind chemotherapeutic agents such as tamoxifen [116]. It is also important to look for alternative forms of inducing apoptosis tat can lead to the discovery and development of new therapies to treat cancer cells that have developed resistance to chemotherapy drugs.

Induction of apoptosis by photosensitizers has been previously examined using MCF-7 cells, which have been reported to extensively release large amounts of cytochrome *c* and subsequently activate caspase-9 2-3h after exposure to ALA and

photoactivation. It has been shown the response to photosensitizer-induced apoptosis in MCF-7 cells is due to activation of the caspase cascade downstream of cytochrome *c* release [117].

MCF-7 cells are self-adherent and usually for adherent cells, mechanical stresses applied to cells, such as scraping them from the surface or using trypsin-EDTA, can trigger a variety of cellular responses. Additionally, most cells express abundant adhesion proteins that provide a structural link between the cytoskeleton and extracellular surfaces (extra cellular matrix). Forces applied to remove cells can trigger immediate and long-term changes in cellular physiology. For adherent cells, mechanical manipulation prior to the time of sampling can interfere with measurements of cellular biochemistry. If perturbations occur before sampling, substantial changes in the physiology of the cell can occur for instance changes in ion concentration or enzyme activation, especially enzymes that are normally confined to cellular sub-compartments. For example proteases often escape from damaged lysosomes and once in the cytosol, the proteases cleave inappropriate targets, i.e., proteins or peptides to which they normally do not have access. In addition compartmentalized enzymes that released into the cytoplasm may have sufficient time to encounter and modify inappropriate substrates [118]. Spatial localization of proteins particularly enzymes has been identified as a mechanism to regulate the flow of information through signaling cascades in cells [119]. The absence of manipulation prior to performing cell measurements results in minimal effects on the cell [8]. For this reason, the ability to perform minimally invasive measurements within intact

single living cells with temporal and spatial resolution is important for the analysis of a cell as a system. Optical nanosensors can perform such measurements and reveal the intricacies of biochemical pathways in intact living cells.

4.7.1 Cell Culture: Maintaining and Propagating MCF-7 Cells

MCF-7 cells obtained from American Type Culture Collection (Rockville, MD, USA, Cat-no. HTB22) were cultured as monolayers in T-25 plastic tissue culture flask. Cells were maintained in Dulbecco's minimally essential media (DMEM) with phenol red, supplemented with 10% fetal calf serum, 1% L-glutamine, 3.5 g/l glucose, and 1% penicillin and streptomycin, and incubated at 37 $^{\circ}$C in humidified air with 5% CO_2. MCF-7 cells were routinely monitored under a phase contrast microscope until they achieved confluency (80-90%) to warrant propagation.

MCF-7 cells were split and propagated every 3-5 days. The process involves emptying the culture medium from the respective T-25 tissue culture flasks, rinsing with 5ml PBS and then gently resuspending the cells in the T-25 flask surface using trypsin (sterile process). The proteolytic enzyme trypsin was brought to room temperature and a 1ml was pipetted into each of the T-25 culture flasks. The trypsin was left to sit in flasks for about 3-5 minutes at 37°C giving sufficient time for the trypsin to detach the adherent MCF-7 cells from the base of the tissue culture flask. After the 3-5 minute period expired, the cells are briefly visualized under the inverted phase contrast microscope to ensure the cells are fully detached. At this point the cells appear circular in shape. Into each of the flasks, 5ml of DMEM is pipetted to

neutralize the action of trypsin. From the total 6 ml of each tissue culture flask, 0.25ml is transferred into two T-25 tissue culture flasks, each containing 5 ml. The cells are then incubated at $37^{\circ}C$, 5% CO_2 and 86% humidity. The cells were examined daily using the inverted phase contrast microscope to determine the degree of confluency. The DMEM medium should appear red as a result of phenol red. In cases where DMEM turns yellow before achieving at least 75% confluency, the acidic medium is replaced with fresh DMEM. After 3-5 days the cells are split and propagated. Some of the cells are harvested and preserved at $-70^{\circ}C$ for future use. Freezing can be lethal to the cells due to the effects of damage by ice crystals, dehydration, alterations in concentration of analytes and changes in pH. To minimize the effects of freezing, the cryoprotective agent DMSO is used. The freezing medium consists of 90% DMEM and 10% DMSO.

4.8 Experimental Protocol

As stated previously, the objective of this project is to use optical nanosensor based on evanescent fluorescence to measure apoptosis in single living cells by monitoring cytochrome c and caspase-9. Prior to measuring cytochrome c and caspase-9, preliminary experiments were performed to determine the photocytoxicity of ALA and to confirm if ALA induced the mitochondrial pathway of apoptosis. After completing the preliminary studies, experiments were performed whereby apoptosis was induced using ALA and both cytochrome c and caspase-9 were detected and identified using the antibody-based optical nanosensor. These

experiments were first performed *in vitro* and second, pseudo *in vivo* using the sandwich immunoassay format. The *in vitro* measurement were performed in cytosolic cell extract while the pseudo *in vivo* measurements were performed in the following way; the optical nanosensors with capture antibody were incubated in single cells, withdrawn and then incubated in a solution containing labeled reporter antibody. For both measurement formats, evanescent optical waves generated in the near field of the optical nanosensor were used to excite the fluorophore labeled reporter antibody after secondary immunocomplex formation. The fluorescent signal generated was recorded and is representative of the binding events.

4.8.1 Photocytotoxicity Study

The cellular events occurring after mitochondria receive the apoptotic signal, involve the mitochondrial outer membrane becoming permeable (lowering of mitochondrial membrane potential) to cytochrome c, which is translocated from mitochondria to the cytosol. Once released into the cytosol, cytochrome c activates downstream caspases, leading to the rapid disintegration of the cell [88]. The objective of this study was to explore the *in vitro* photosensitizing potential of ALA generated PpIX and its capacity to induce apoptosis in human mammary carcinoma cells, MCF-7. The photosensitizing process involves the combination of light and light sensitive ALA, in an oxygen-rich environment. ALA absorbs energy from photons and transfers this energy to surrounding oxygen molecules. This leads to the formation of toxic oxygen species such as singlet oxygen and free radicals. These are

very reactive and can damage proteins, lipids, nucleic acids and other cellular components leading to cell death. MCF-7 cells were incubated with ALA for two hours followed by exposure to 11 J cm^{-2} of visible light from a HeNe laser. Photocytotoxicity was assessed at 24 hours, 48 hours, 72 hours, and 96 hours using a coulter counter to perform dead cell count assay.

4.8.2 Experimental Procedure: Photocytotoxicity Study of ALA

MCF-7 cells were grown in Dulbecco's Modified Eagle's Medium ((DMEM) (Mediatech, Inc., Herndon, VA)) supplemented with 1 mM L-Glutamine (Gibco, Grand Island, NY) and 10% fetal bovine serum (Gibco, Grand Island, NY). Baseline static culture productivity for each cell line was established in growth medium (described above) in standard T25 flasks (Corning, Corning, NY). The flasks were incubated at 37°C, 5% CO$_2$ and 86% humidity. Cell growth was monitored daily by microscopic observation until a 75% state of confluence was achieved. The growth conditions were chosen so that the cells would be in log phase growth during photosensitizer treatment. The cells were harvested from the T25 flasks and 0.25ml (4.0 x 10^5 cells/ ml) seeded into T-75 flasks. From a 1mM stock solution of δ-aminolevulinic acid, 0.5mM [120] solutions was prepared by adding the δ-aminolevulinic acid, solution in DMEM. The prepared solutions were added to multiple T-25 culture flasks of the experimental group and treated control group left in contact with the cells for a 2-3-hour incubation period. Following incubation of the MCF-7 cells with δ-aminolevulinic acid; the medium containing δ-aminolevulinic

acid was replaced with fresh DMEM. The ALA taken up by the MCF-7 cells was activated using 632.8 nm HeNe laser. Photocytotoxicity was assessed 24 hours, 48 hours, 72 hours, 96 hours and 120 hours using dead cell count assay.

4.8.3 Experimental Section

The photocytotoxicity test was performed to determine the effect of the photosensitizer ALA on cell growth. This was accomplished by performing a series of tests were performed whereby MCF-7 cells were exposed to the following experimental conditions; Group I MCF-7 cells were incubated in the dark at 37°C with 0.5 mM ALA in DMEM for 2-3 hours followed by exposure to 632.8 nm red light from a HeNe laser at (2.22 J/cm^2) in DMEM with 10% FCS. To determine the influence of light on MCF-7 cells, Group II were incubated with 0.5 mM ALA in DMEM for 2-3 hours, exposed to red light from a HeNe laser at (2.22 J/cm^2). To determine the influence of ALA on MCF-7 cells, Group III MCF-7 cells were incubated in the dark at 37°C with 0.5 mM ALA in DMEM for 2-3 hours. Group IV, MCF-7 cells were incubated in the dark at 37°C without ALA and were not exposed to 632.8 nm red light from a HeNe laser. All procedures after addition of ALA were performed in the dark. For statistical significance, five T-25 flasks were used for each treatment group The dead cell count data obtained using the coulter counter were compared for Groups I – IV. Typically, dead MCF-7 cells detach from the base of tissue culture flasks and remain suspended in growth medium because, when they die, they lose their self-adherence capability. Therefore, after administering the various

cell treatments, cells in the experimental groups die and lose their capability for self-adherence. The media containing un-bound MCF-7 cells are passed through a G20 syringe to generate a single cell suspension. Fresh growth media is introduced into the tissue culture flasks after aspirating un-bound cells to be counted. Cell mortality was compared for Groups I - IV and expressed as the effect of the different forms of treatment they received. To statistically validate the dead cell count results obtained from the replicate experiments performed, a student t-test was performed.

4.9 Student's t-test

As mentioned above, the dead cell count was obtained routinely at set time points on successive days from the flasks with the treatment Groups I - IV. Each treatment was performed in replicate to statistically validate the outcome. As mentioned previously, in order to validate the results obtained from Groups I – IV, of the photocytotoxicity study a student's t-test was performed. The t-test was used to determine if the results of Groups I -IV differ on a single variable, photodynamic treatment. This study was used to determine whether cell death differs among cells exposed to different experimental treatment regiments of ALA-PDT. Here, it was particularly useful in analyzing scores of Groups I – IV on the particular variable, ALA-PDT. The null hypothesis (H_0) was stated based on the assumption that there is no difference in parameters (mean, variance) for Groups I – IV. According to the null hypothesis, any observed difference in samples is due to chance or sampling error and not the variable ALA-PDT.

The software application program, MS Excel was used to calculate the p-values of the t-tests and determine the significance of the results. Data points obtained from Groups I – IV acquired using LabView data acquisition program were converted using MS Excel Text Wizard to obtain a data format compatible with the MS Excel interface. The type of t-test used was two sample unequal variance and a 2-tailed distribution with a threshold of 0.05 (5%). This means that if the p-value is less than 0.05, then the null hypothesis is rejected and it can be stated with a 95% level of confidence that the two parameters are not the same. The calculated p-value is compared with the desired significance level set for the t-test and, if it is smaller, the result is significant. That is, if the null hypothesis will be rejected at the 5% significance level, and this is reported as "$p < 0.05$".

4.10 Results and Discussion: Photocytotoxicity Study

The aim of the photocytoxicity study of ALA was to determine the effect of ALA on MCF-7 cells. The outcome of the treatments administered, Groups I – IV were determined by dead cell count using a coulter counter. These results were plotted and are shown in Figure 4.3. The outcome of the photocytotoxicity study revealed that in the first five days following treatment, cell death was observed only in the experimental treatment Group I, ALA(+) PDT(+). Increasing cell death is evident from the graph peaking on day three. However, from the dead cell count results obtained for Group II -ALA(+) PDT(-), Group III -ALA(-) PDT(+) and Group

133
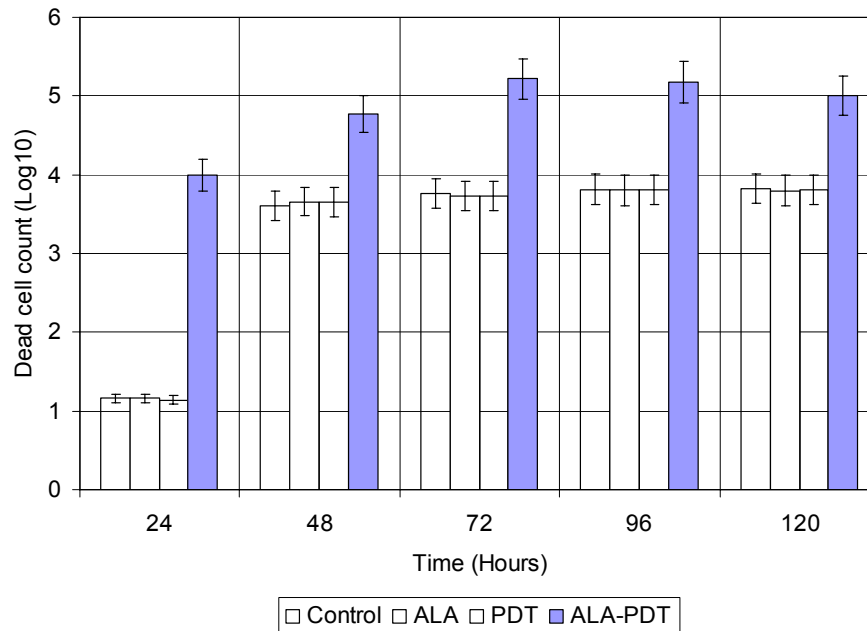
Figure 4.3 shows the results of the dead cell count assay. On five successive days, three T-25 flasks were obtained from the incubator and the unbound (dead) MCF-7 cells counted. Each bar shows the average MCF-7 cells obtained and counted from three T-25 flasks. The calculated p-values for the students t-test are 0.039972, 0.039906, 0.039914 (ALL $p<0.05$). These p-value results obtained from the student-t test indicate that (+)ALA(+)PDT treatment significantly affects MCF-7 cell proliferation compared to (+)ALA(-)PDT, (-)ALA(+)PDT and (-)ALA(-)PDT. The error bars represent 95% confidence interval (CI).

<u>IV</u> -ALA(-) PDT(-), there was no significant increase cell mortality. Using the *t*-test, it was confirmed that the results of <u>Groups I</u> -<u>IV</u> differ on the single variable, photodynamic treatment. The calculated *p*-values determine the null hypothesis is unlikely to be true. It indicates the strength of evidence for rejecting the null hypothesis rather than simple concluding that apoptosis is a concerted effect of ALA and photoactivation. The finding that apoptosis is a concerted effect of ALA and photoactivation achieved statistical significance as shown by the results obtained using the *t*-test. The calculated *p*-values of students *t*-test were 0.039972, 0.039906, 0.039914 ($p<0.05$). These *p*-value results obtained from the student-t test indicate that (+)ALA(+)PDT significantly affect MCF-7 cell proliferation compared to (+)ALA(-)PDT, (-)ALA(+)PDT and (-)ALA(-)PDT. In summary, no photocytotoxicity was observed for either laser irradiation without ALA, or ALA without laser radiation, but cell death was observed and determined for the combination of ALA and laser radiation. Additionally, <u>Groups II</u> and <u>III</u>, ALA(+) PDT(-) and ALA(-) PDT(+) reveal the absence of dark and light toxicity. Therefore, it can be concluded that incubation of MCF-7 cells with 0.5 mM ALA for 3 h and subsequent photoactivation with light from a HeNe laser results in a significant increase in cell death compared with Groups II – IV.

4.11 In Vitro and Pseudo In Vivo Measurement of Apoptosis

Optical nanosensors based on evanescent fluorescence sandwich type immunoassay were developed and used for the *in vitro* and pseudo *in-vivo* analysis of

cytochrome c and caspase-9. *In vitro* analysis of cytochrome *c* and caspase-9 was performed using cytosolic cell extract. However, pseudo-*in vivo* analysis involves probing a single cell with antibody-based optical nanosensor and then withdrawing the optical nanosensor from within the cell and incubating it with Cy5 labeled reporter antibody. The two measurement schemes employ the *indirect* immunoassay technique that involves using primary (capture) and dye conjugated secondary (reporter) antibody. The distinction of the two techniques lies in the first step of binding the target molecule with capture antibody. The pseudo *in vivo* technique involves incubating optical nanosensor in single living cells and then incubating the optical nanosensors with Cy5 labeled reporter antibody solution in a microfuge tubes. Based on the previous photocytotoxicity study, two groups were used for *in vitro* and pseudo *in vivo* studies: Group I, control group of cells PDT(-) ALA(-), and Group II, experimental group of cells PDT(+) ALA(+). For these studies, cytochrome c and caspase-9 antibody were immobilized on optical nanosensors to bind cytochrome c and caspase-9 respectively. Optical nanosensors were then incubated in the cytosolic cell extract obtained from Group I, (+)ALA (+)PDT, and Group II, (-)ALA (-)PDT. This was be followed by binding Cy5 labeled reporter antibody which facilitates the fluorescence detection of the secondary immunocomplex formed after excitation using a 632.8 nm HeNe laser. The fluorescence signals generated are detected using a PMT, and acquired and processed using LabView.

4.11.1Materials and Methods

Plastic clad silica (PCS) fibers with a 600-µm-size core (Fiberguide Industries, Stirling, New Jersey). *Indirect* immunoassay capture and reporter antibody for cytochrome c and caspase-9 measurement, cytochrome c (Ab-3): capture Ab, cytochrome c (Ab-4): reporter Ab, caspase-9 (Ab-1): capture Ab, caspase-9 (Ab-2): reporter Ab were purchased from purchased from Santa Cruz Biotechnology, Santa Cruz, CA.

4.11.2 Cytosolic Cell Extraction (Cell Fractionation Protocol)

MCF-7 cells were grown to 70–80% confluency and exposed to 0.5mM ALA to induce apoptosis. Concurrently control groups of MCF-7 cells were cultured without induction. Cytosolic protein was extracted as described Tikkanen *et al.* [121]. Briefly, cells were rinsed in calcium- and magnesium-free Hanks' balanced salt solution and lifted with 3mM EDTA. Detached cells were rinsed and collected by centrifugation at 3000 RPM for 5 minutes at 4°C and washed in ice cold PBS. The cells were centrifuged again at 3000 RPM for 5 minutes at 4°C and the supernatant removed. The cells were then lysed in hypotonic buffer containing 10 mM Tris-Cl, pH 7.5, 1 mM EDTA, 1 mM DTT, 0.5 mM 4-(2-aminoethyl) benzenesulfonyl fluoride, 10 mM leupeptin, 2 µg/ml aprotinin, and 4 µM pepstatin and incubated on ice for 10 minutes. The cells were immediately centrifuged at 3000 rpm for 10 min at 4 °C and the supernatant was collected as cytosol.

4.11.3 Fluorescent Measurement System and Procedure

Figure 4.4 shows a schematic representation of the fluorescence measurement system. The 632.8 nm laser line of a HeNe laser (Melles Griot, <15mW laser power) was focused onto a 600-μm-delivery fiber that is terminated with a subminiature A (SMA) connector. The antibody-immobilized nanosensor was coupled to the delivery fiber through the SMA connector and secured to the microscope with micromanipulators. The fluorescence emitted from the tip of the nanosensor was collected by the microscope objective and passed through a Cy5 long pass filter (Chroma, Brattleboro, VT) and then focused onto a PMT for detection. The output from the PMT was recorded using a universal counter, and a personal computer (PC) with custom-designed software (LabView platform) for data treatment and processing. The experimental setup used to probe single cells was adapted to this purpose from a standard micromanipulation/microinjection apparatus. The micromanipulation equipment used consisted of MN-2 (Narishige Co. Ltd., Tokyo, Japan) Narishige three-dimensional manipulators for coarse adjustment, and Narishige MMW-23 three-dimensional hydraulic micromanipulators for final movements. The optical fiber nanosensor was mounted on a micropipette holder (World Precision Instruments, Inc., Sarasota, FL). To record the fluorescence of Cy5 labeled secondary immunocomplex, a Hamamatsu PMT detector assembly (HC125-2) was mounted in the front port of the Diaphot 300 microscope.

HeCd Laser

Incubator

Nanosensor

Cell

197319792003

Power   Reset

HP universal counter

Data acquisition PC

PMT

HP power supply

Nikon inverted fluorescence microscope
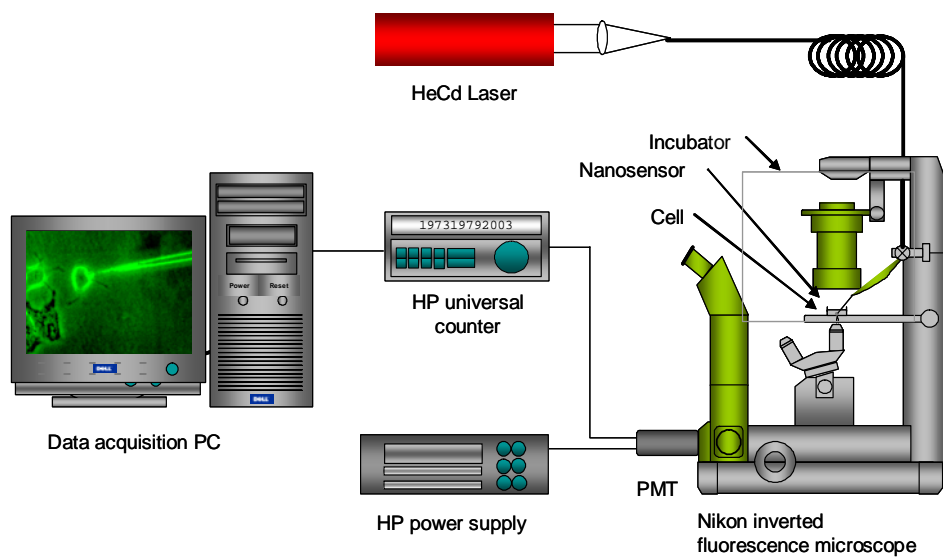
Figure 4.4 shows a diagrammatic representation of the Laser-induced fluorescence measurement system

The fluorescence emitted when Cy5 fluoresced was collected using the optical configuration in the inverted fluorescent microscope and delivered to a PMT mounted on the frontal port. The fluorescent signal detected was converted to a measurable electrical signal and transmitted to a PC for data acquisition and processing.

4.11.4 In Vitro Measurement of Apoptosis using Cytosolic Cell Extract

The functionalized tips of the nanosensor were divided into Group I, (+)ALA (+)PDT, and Group II, (-)ALA (-)PDT, corresponding to the treatment groups and the measurements performed in replicate. The nanotips were immersed in solutions of capture antibody, cytochrome c (*Ab-3*) and caspase-9 (*Ab-1*) respectively, and allowed to incubate for 12 hours at 4°C. The nanosensors were then inserted into microfuge tubes containing cytosolic cell extract in PBS and incubated for 5-10 minutes. The microfuge tubes contained cell lysates from both Group I, (+)ALA (+)PDT, and Group II, (-)ALA (-)PDT. Finally, the nanosensors were incubated in microfuge tubes containing either Cy5 labeled cytochrome c (*Ab-4*) reporter antibody or Cy5 labeled caspase-9 (*Ab-2*) reporter antibody 30 minutes. The nanosensors were sequentially secured onto an x-y-z micromanipulator mounted on an inverted fluorescence microscope (Figure 4.5). Using the microscope eyepiece for observation the nanosensor was positioned using an x-y-z micromanipulator to within the field of view and the excitation source tuned on. The Cy5 labeled reporter antibody is excited using evanescent optical waves and the fluorescence signal generated is collected
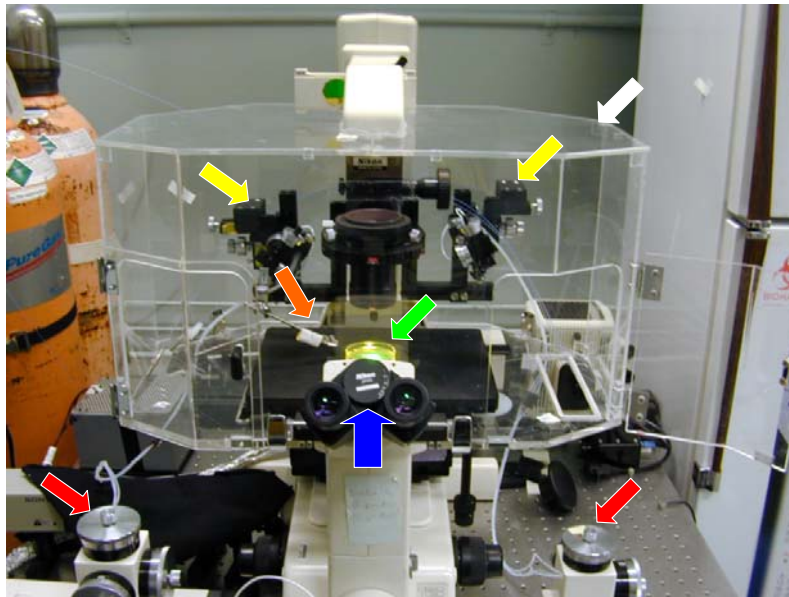
Figure 4.5 shows an image of Nikon Inverted fluorescence microscope, the main component of the laser-induced fluorescence measurement system. Red (LEFT and RIGHT) arrows point to the fine x-y-z micromanipulator mounted on the inverted fluorescence microscope. Yellow (LEFT and RIGHT) arrows point to the coarse x-y-z micromanipulator. The white arrow points to the plexiglass incubator. Orange (LEFT) arrow points to the optical nanosensor. Green (RIGHT) arrow points to the petri dish with cells

using the fluorescence microscope optics, and detected with a PMT and recorded. Figure 4.6 shows a diagrammatic representation of the fluorescence excitation and detection process.

4.11.5 Results of In Vitro Studies using Cytosolic Cell Extract

Figure 4.7 shows the results. The first bar represents the averaged results of Group II while the second bar represents the averaged results of Group I. In the case of Group II, it is evident that secondary immunocomplex formation did not occur because Cy5 fluorescence was not detected and thus it can be said that apoptosis was not induced. For Group I, secondary immunocomplex formation was evident by the detection of Cy5 fluorescence. These results (Figure 4.11) indicate that positive detection and identification of cytochrome c and caspase-9.

4.11.6 Pseudo In Vivo Measurement of Apoptosis

The functionalized nanotips were used for experimental and control measurements, which were performed in replicates. The nanotips were incubated in solutions of capture antibody, cytochrome c (Ab-3) and caspase-9 (Ab-1) respectively, and allowed to incubate for 12 hours at 4oC. The nanosensors were inserted into single live MCF-7 cells (Figure 4.8) and incubated for 5-10 minutes. The
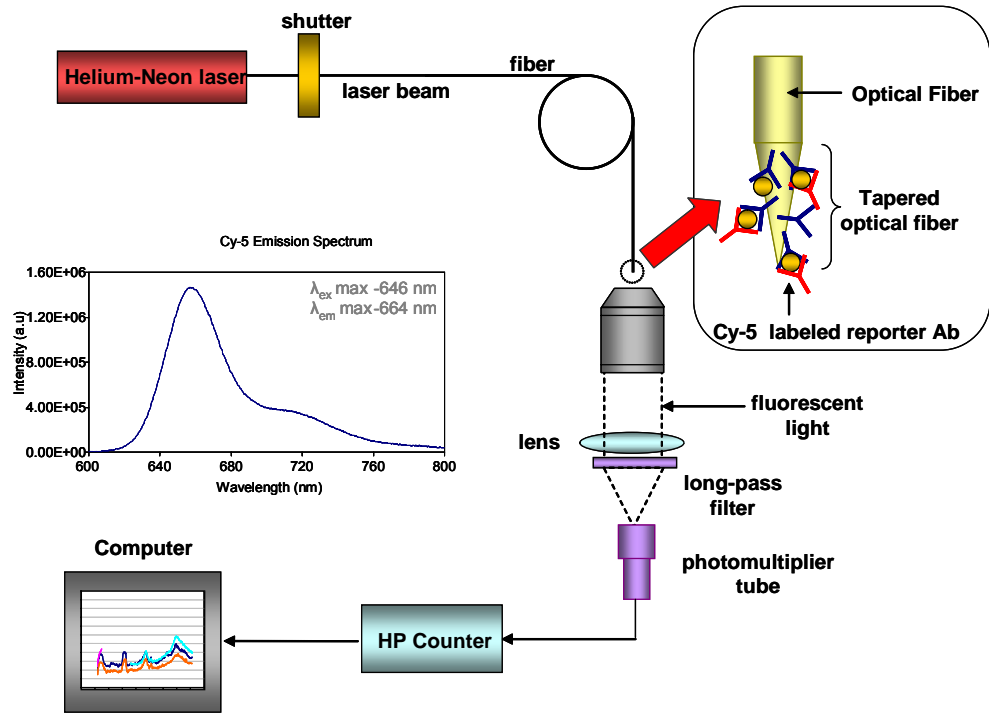
Figure 4.6 shows a schematic representation of the components of the laser-induced fluorescence measurement system and outlining the fluorescence excitation and detection process
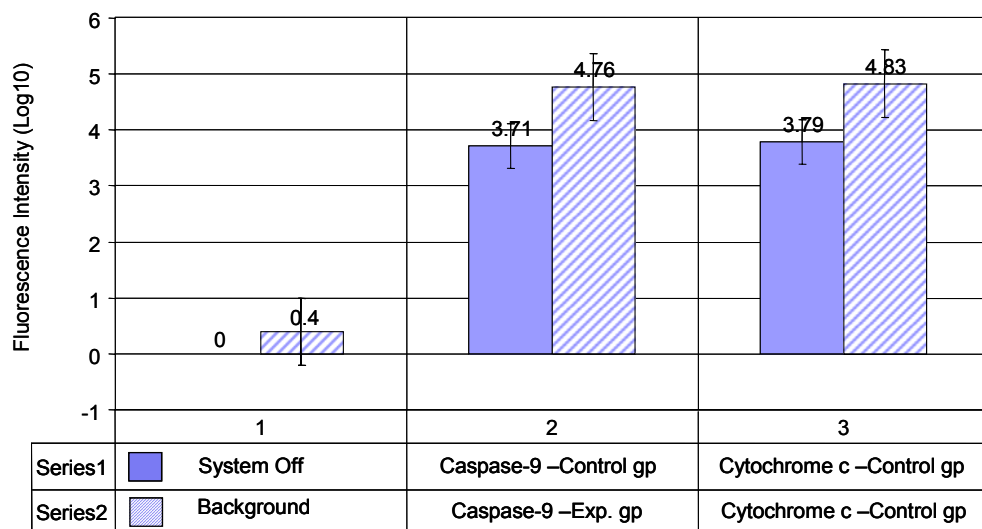
Figure 4.7 shows the collective mean results of the *in vitro* measurement of cytochrome *c* and caspase-9, including the background signal (scattered room light) and with the detector off. Each bar represents the mean of replicate measurements with the error bars represent 95% confidence interval (CI).

Figure 4.8 shows the intracellular measurement of apoptosis in a single MCF-7 cell. The top image (i) shows an optical nanosensor prior to insertion and a single MCF-7 cell while the BOTTOM image (ii) shows the optical nanosensor inserted into the MCF-7 cell.

MCF-7 cells used were from both the experimental (apoptosis induced) and control (without apoptosis induction) study groups. Finally, the nanosensors were incubated in microfuge tubes containing either Cy5 labeled cytochrome c (Ab-4) reporter antibody or Cy5 labeled caspase-9 (Ab-2) reporter antibody 30 minutes. The nanosensors were sequentially secured onto an x-y-z micromanipulator mounted on an inverted fluorescence microscope. Using the microscope eyepiece for observation, the nanosensor was positioned using an x-y-z micromanipulator to within the field of view and the excitation source tuned on. The Cy5 labeled reporter antibody is excited using evanescent optical waves and the fluorescence signal generated is collected using the optical configuration of the fluorescence microscope and detected with a PMT.

4.11.7 Results for Pseudo In Vivo Measurement of Apoptosis

Figure 4.9 shows the comprehensive results of the measurement of cytochrome *c* and caspase-9 obtained using the pseudo *in vivo* measurement technique. The results are represent averages obtained from a series of replicate measurements performed. As can be seen from the results obtained from the control cells (-)ALA (-)PDT and experimental cells, (+)ALA (+)PDT, there is no significant increase in the fluorescence signal obtained for the experimental cells therefore confounding the *in vivo* detection and identification of cytochrome *c* and caspase-9.

146
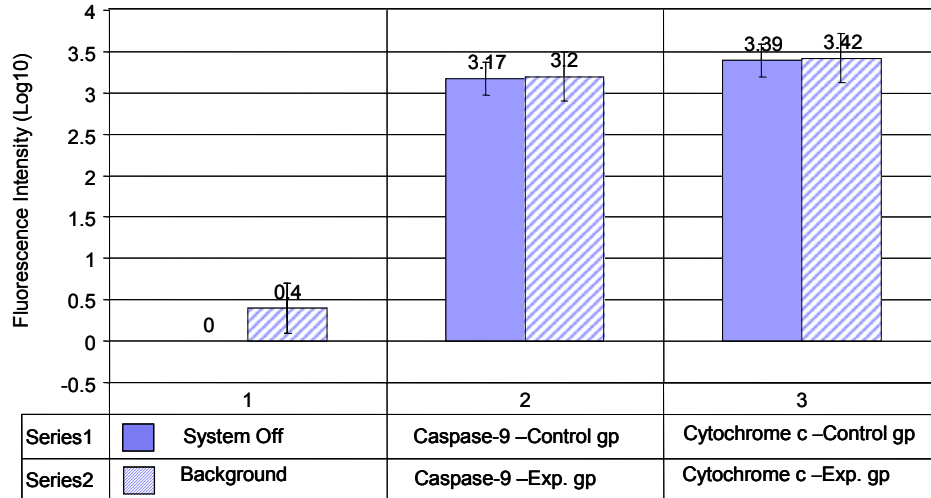
Figure 4.9 shows the results obtained for pseudo *in vivo* measurement of apoptosis. Each bar represents the mean of replicate measurements with the error bars represent 95% confidence interval (CI).

In this case, the pseudo *in vivo* immunoassay technique did not facilitate the detection of secondary immunocomplex formation of either cytochrome *c* or caspse-9, suggesting that secondary antibody binding was unsuccessful. The results revealed that secondary immunocomplex formation did not occur and therefore the inability to detect Cy5 fluorescence that would have been emitted if the reporter antibody was bound. This suggests one of two possible scenarios. One, the physical action of withdrawing the optical nanosensors from within the cells after incubation could have disrupted the structural stability of the bound target molecule (cytochrome *c* or caspase-9) and as a consequence, direct spatial coupling could not be achieved. On the other hand, it could have been the effect of insufficient cytochrome *c* or caspase-9 bound to the capture antibody during primary immunocomplex formation and this could have limited the sensitivity of detection after secondary immunocomplex formation.

4.12 Summary

This work described the application of optical nanosensors for the sensitive and selective recognition of cytochrome c and caspase-9 in situ in cytosolic cell extracts. Apoptosis was induced using a photodynamic therapy (PDT) agent δ-aminolevulinic acid (ALA) that initiates the mitochondrial pathway of apoptosis. This pathway involves cytochrome c release from mitochondrial followed by the activation of caspase-9. To measure cytochrome c and caspase-9, capture antibody targeted towards cytochrome c or capase-9, is immobilized onto functionalized nanotips to

bind these respective proteins. Once these proteins are bound, the nanotips containing the primary immunocomplex are complexed with Cy5 labeled reporter antibody forming a secondary immunocomplex. The Cy5 labeled reporter antibody facilitates the detection and identification of secondary immunocomplex formation when Cy5 is excited using 632.8 nm light from helium/neon (HeNe) laser and fluorescence emission occurs in the far-red at about 667 nm. Fluorescence signals were detected for *in vitro* studies providing for sensitive and selective recognition of both cytochrome c and caspase-9 while the same did not occur for the pseudo *in vivo* studies. Unfortunately, I was unable to detect cytochrome c and caspase-9 within single living cells using the pseudo *in vivo* technique. The experimental data obtained from *in vitro* measurement of apoptosis indicated that optical nanosensor coupled with the *indirect* fluorescent immunoassay can be used to detect and identify specific antibodies directed against cytochrome c and caspase-9. However, the experimental data obtained from pseudo *in vivo* studies reveal that the pseudo *in vivo* immunoassay technique is not capable of measuring of apoptosis. This was demonstrated by the inability of the technique to detect and identify cytochrome *c* and caspase-9 and therefore, I could not implicate these proteins involved in the regulation of mitochondrial cell death using antibody-based optical nanosensors.

References

1.   Zandonella, C., *Cell Nanotechnology: The Tiny Toolkit.* Nature, 2003. **423**: p. 10-12.

2.   Behbehani, M., *Cell Physiology Source Book*, ed. N. Sperelakis. 1995, San Diego: Academic Press. 490-494.

3.   Morris, C., *Cell Physiology Source Book*, ed. N. Sperelakis. 1995, San Diego: Academic press.

4.   Tsien, R., *Intracellular signal transduction in four dimensions: from molecular design to physiology.* Am J Physiol Cell Physiol, 1992. **263**: p. C723-C728.

5.   Giuliano, K., Post, PL., Hahn, KM., Taylor, DL., *Fluorescent protein biosensors: measurement of molecular dynamics in living cells. .* Annu Rev Biophys Biomol Struct., 1995. **24**: p. 405-34.

6.   Jankowski, J., Tratch, S., Sweedler, JV., *Assaying single cells with capillary electrophoresis.* Trends Anal. Chem., 1995. **14**: p. 170-176.

7.   Luzzi, V., Lee, C.L., Allbritton, N.L., *Localized sampling of cytoplasm from Xenopus oocytes for capillary electrophoresis.* Anal Chem, 1997. **69**(23): p. 4761-4767.

8.   Li, H., Sims, C.E., Wu, H., Allbritton, N.L., *Spatial Control of Cellular Measurements with the Laser-Micropipet.* Anal. Chem., 2001. **73**.

9.   Tan, W., Shi, ZY., Smith, S., Birnbaum, D., and Kopelman, R., *Submicrometer Intracellular Chemical Optical Fiber Sensors.* Science, 1992. **258**(5083): p. 778-781.

10. Tan, W., Shi, ZY., Smith, S., and Kopelman, R., *Development of Submicron Chemical Optic Sensors.* Anal. Chem, 1992. **64**(23): p. 2985-2990.

11. Munkholm, C., D.R. Walt, and F.P. Milanovich, *Preparation of Co2 Fiber Optic Chemical Sensor.* Abstracts of Papers of the American Chemical Society, 1987. **193**: p. 183-ANYL.

12. Munkholm, C., D.R. Parkinson, and D.R. Walt, *Intramolecular Fluorescence Self-Quenching of Fluoresceinamine.* Journal of the American Chemical Society, 1990. **112**(7): p. 2608-2612.

13. Tan, W.H., et al., *Submicrometer Intracellular Chemical Optical Fiber Sensors.* Science, 1992. **258**(5083): p. 778-781.

14. Sumner, J., Aylott, JW., Monson, E., Kopelman, R., *A fluorescent PEBBLE nanosensor for intracellular free zinc.* Analyst, 2002. **127**(1): p. 11-16.

15. Alarie, J.P. and T. VoDinh, *Antibody-based submicron biosensor for benzo a pyrene DNA adduct.* Polycyclic Aromatic Compounds, 1996. **8**(1): p. 45-52.

16. Vo-Dinh, T., Alarie, JP., Cullum, BM., Griffin, GD., *Antibody-based nanoprobe for measurement of a fluorescent analyte in a single cell.* Nat Biotechnol, 2000. **18**(7): p. 764-767.

17. Kasili, P.M., Cullum, B.M., Griffin, G.D., and Vo-Dinh, T., *Nanosensor for In-Vivo Measurement of the Carcinogen Benzo [a] Pyrene in a Single Cell.* Journal of Nanoscience and Nanotechnology, 2003. **2**(6): p. 653-658.

18.   Cullum, B., Griffin, GD., Miller, GH., Vo-Dinh, T., *Intracellular measurements in mammary carcinoma cells using fiber-optic nanosensors.* Anal Biochem, 2000. **277**(1): p. 25-32.

19.   Vo-Dinh, T., and Cullum, BM., *CRC Handbook for Biomedical Photonics.* Nanosensors for Single Cell Analysis, ed. T. Vo-Dinh. 2003, Newyork: CRC Press. 14.

20.   Cullum, B.M., et al., *Intracellular measurements in mammary carcinoma cells using fiber-optic nanosensors.* Analytical Biochemistry, 2000. **277**(1): p. 25-32.

21.   Cullum, B.M. and T. Vo-Dinh, *The development of optical nanosensors for biological measurements.* Trends in Biotechnology, 2000. **18**(9): p. 388-393.

22.   Cullum, B.M. and T. Vo-Dinh, *Optical nanosensors and biological measurements.* Biofutur, 2000. **2000**(205): p. A1-A6.

23.   Vo-Dinh, T.G., G. D.; Alarie, J. P.; Cullum, B. M.; Sumpter, B. and Noid, D., *Development of Nanosensors and Bioprobes.* J. Nanoparticle Research, 2000. **2**: p. 17.

24.   Vo-Dinh, T., et al., *Antibody-based nanoprobe for measurement of a fluorescent analyte in a single cell.* Nature Biotechnology, 2000. **18**(7): p. 764-767.

25.   Cullum, B., Vo-Dinh, T., *The development of optical nanosensors for biological measurements.* Trends Biotechnol, 2000. **18**(9): p. 388-393.

26.   Vo-Dinh, T., et al., *Antibody-Based Fiberoptics Biosensor for the Carcinogen Benzo(a)Pyrene.* Applied Spectroscopy, 1987. **41**(5): p. 735-738.

27.   Aylott, J., *Optical nanosensors - an enabling technology for intracellular measurements.* Analytst, 2003. **128**(4): p. 309-312.

28.   S, U., *Fluorescence Assay in Biology and Medicine.* Vol. 2. 1969, New York, San Francisco, London: Academic Press. 659.

29.   http://www.pti-nj.com/, *Fluorescence: The Phenomenon*. 1997, Photon Technology International.

30.   Udenfriend, S., *Fluorescence Assay in Biology and Medicine*. Vol. 2. 1969, New York, San Francisco, London: Academic Press. 659.

31.   Harrick, N., *Internal Reflection Spectroscopy*. 1967, New York: John Wiley & Sons, Inc.

32.   Kröger, K., Jung, A., Reder, S., Gauglitz, G., *Versatile biosensor surface based on peptide nucleic acid with label free and total internal reflection fluorescence detection for quantification of endocrine disruptors.* Analytica Chimica Acta, 2002. **469**(1): p. 37-49.

33.   Axelrod, D., *Total Internal Reflection Fluorescence Microscopy in Cell Biology.* Traffic, 2001. **2**(11): p. 764-774.

34.   Potyrailo, R., Hobbs, SE., Hieftje, GM., *Optical waveguide sensors in analytical chemistry: today's instrumentation, applications and trends for future development.* FRESENIUS JOURNAL OF ANALYTICAL CHEMISTRY, 1998. **362**(4): p. 349-373.

35. Guo, Z., Guilfoyle, RA., Thiel, AJ., Wang, R., and Smith, LM., *Direct fluorescence analysis of genetic polymorphisms by hybridization with oligonucleotide arrays on glass supports. Nucleic Acids Res., 22, 5456–5465.* Nucleic Acids Res., 1994. **22**: p. 5456–5465.

36. Alarie, J., VoDinh, T., *Antibody-based submicron biosensor for benzo[a]pyrene DNA adduct.* Polycyclic Aromatic Compounds, 1996. **8**(1): p. 45-52.

37. Kumar, A., Larsson, O., Parodi, D., and Liang, Z., *Silanized nucleic acids: a general platform for DNA immobilization.* Nucleic Acids Res., 2000. **28**(14): p. 71e-71.

38. Lamture, J., Beattie, KL., Burke, BE., Eggers, MD., Ehrlich, DJ., Fowler, R., Hollis, MA., Kosicki, BB., Reich, RK., Smith, SR., *Direct detection of nucleic acid hybridization on the surface of a charge coupled device.* Nucleic Acids Res., 1994. **22**(11): p. 2121-2125.

39. Alarie, J., Sepaniak, MJ., Vo-Dinh T., *Evaluation of Antibody Immobilization Techniques for Fiber Optic-based Fluoroimmunosensing.* Anal. Chim Acta, 1990. **229**(2): p. 169-176.

40. Tromberg, B., Sepaniak, MJ., Alarie, JP., Vo-Dinh, T., Santella, RM., *Development of Antibody-Based Fiber-Optic Sensors for Detection of Benzo[a]Pyrene Metabolite.* Anal. Chem., 1988. **60**(18): p. 1901-1908.

41. Dakubu, S., Ekins, R., Jackson, T., Marshall, NJ., *Chapter 4*, in *Practical Immunoassays: The State of the Art.*, W. Butt, Editor. 1984, Dekker: New York.

42. Wessendorf, M., Brelje, T. C., *Which fluorophore is brightest? A comparison of the staining obtained using fluorescein, tetramethylrhodamine, lissamine rhodamine, texas red, and cyanine 3.18.* Histochemistry, 1992. **98**: p. 81-85.

43. Harms, G.S., Sonnleitner, M., Schütz, GJ., and H.J. Gruber, and Schmidt, T., *Molecule Anisotropy Imaging.* Biophys. J., 1999. **77**: p. 2864-2870.

44. Sako, Y., Minoguchi, S., and Yanagida, T., *Single molecule imaging of EGFR signalling on the surface of living cells.* Nature Cell Biol., 2000. **2**: p. 168-172.

45. Schütz, G.J., Kada, G., Pastushenko, VP., and and H. Schindler, *Properties of lipid microdomains in a muscle cell membrane visualized by single molecule microscopy.* EMBO J., 2000a. **19**: p. 892-901.

46. Hoh, J., and Hansma, PK., *Atomic force microscopy for high resolution imaging in cell biology.* Trends Cell Biol., 1992. **2**: p. 208-213.

47. Binnig, G., Quate, CF., and Gerber, C., *Atomic Force microscope.* Phys. Rev. Lett., 1986. **56**: p. 930-933.

48. Turner, A., Karube, I., Wilson, GS., ed. *Biosensors – Fundamentals and Applications.* 1987, Oxford University Press: Oxford.

49. Schmid, R., and Karube, I., *Biotechnology*, in *Biosensors and Bioelectronics*, H. Rehm, and Reed G., Editor. 1998, VCH Verlagsgesellschaft: Weinheim-Basel-Cambridge-Newyork.

50.   Updike, S., and Hicks, GP., *The Enzyme Electrode*. Nature, 1967. **214**: p. 986-988.

51.   Guilbault, G., and Montalvo, JGJ., *A Urea specific enzyme electrode*. Journal of The American Chemical Society, 1969. **9**: p. 2164-2167.

52.   Bilitewski, U., and Schmid, RD. *Alcohol determination by modified carbon paste electrodes*. in *The GBF International Workshop on Biosensors*. 1989. Braunschweig, Germany.

53.   Kulys, J., Bilitweski, U., and Schmid, RD. *Biosensors based on chemically modified electrodes*. in *The GBF International Workshop on Biosensors*. 1989. Braunschweig, Germany.

54.   Robinson, G., *Optical Immunosensors: An Overview*, in *Advances in Biosensors*, T. APF, Editor. 1991, JAI Press Inc: London. p. 230-252.

55.   B.M. Cullum , T.V.-D., *The development of optical nanosensors for biological measurements*. Trends Biotechnol, 2000. **18**(9): p. 388-393.

56.   M. Shortreed, R.K., M. Kunh, B. Hoyland, *Fluorescent fiber-optic calcium sensor for physiological measurements*. Anal Chem., 1996. **68**(8): p. 1414-8.

57.   S.L. Barker, R.K., Anal Chem., 1998. **70**(23): p. 49062-6.

58.   M. Brasuel, R.K., T.J. Miller, R. Tjalkens, M.A. Philbert, *Fluorescent nanosensors for intracellular chemical analysis: decyl methacrylate liquid polymer matrix and ion-exchange-based potassium PEBBLE sensors with real-time application to viable rat C6 glioma cells*. Anal Chem., 2001. **73**(10): p. 2221-8.

59.   H. A. Clark, R.K., R. Tjalkens, M.A. Philbert, *Optical nanosensors for chemical analysis inside single living cells. 2. Sensors for pH and calcium and the intracellular application of PEBBLE sensors*. Anal Chem, 1999. **71**(21): p. 4837-43.

60.   H. A. Clark, M.M., M.A. Philbert, R. Kopelman, *Optical nanosensors for chemical analysis inside single living cells. 1. Fabrication, characterization, and methods for intracellular delivery of PEBBLE sensors*. Anal Chem, 1999. **71**(21): p. 4831-6.

61.   T. Vo-Dinh, J.P.A., B.M. Cullum, G.D. Griffin, *Antibody-based nanoprobe for measurement of a fluorescent analyte in a single cell*. Nat Biotechnol, 2000. **18**(7): p. 764-767.

62.   B.M. Cullum , G.D.G., G.H. Miller, T. Vo-Dinh, *Intracellular measurements in mammary carcinoma cells using fiber-optic nanosensors*. Anal Biochem, 2000. **277**(1): p. 25-32.

63.   T. Vo-Dinh, B.M.C., G.D. Griffin, Radiat. Res, 2001. **156**(4): p. 437-438.

64.   Vo-Dinh, T., *Chemical Analysis of Polycyclic Aromatic Compounds*. 1989, New York: Wiley.

65.   http://www.city.toronto.on.ca/health/pdf/cr_appendix_b_pah.pdf.

66.   A.V. Castellano, J.L.C., M.C. Hernandez, P.S. Aleman, J.C. Jimenez, *Benzo(a)pyrene levels in Jinamar Valley: preliminary results*. AFINIDAD, 1999. **56**(480): p. 113-120.

67. L. Shriver-Lake, B.D., R. Edelstein, K. Breslin, S. Bhatia, F. Ligler, *Antibody immobilization using heterobifunctional crosslinkers.* Biosen. and Bioelect., 1997. **12**(11): p. 1101-1106.
68. J.R. Sportsman, G.S.W., Anal Chem, 1980. **52**: p. 2013-2018.
69. J.H. Lin, J.H., J.D. Andrade, IEEE Trans. Biomed. Eng, 1988. **35**: p. 466-471.
70. G.D. Griffin, K.R.A., R.N. Thomason, C.M. Murchison, M. Mcmanis, P.G. Wecker, T. Vo-Dinh. *Polynuclear Aromatic Hydrocarbons.* in *Polynuclear Aromatic Hydrocarbons, Tenth International Symposium.* 1985. Columbus, OH: Battelle Press.
71. T. Kuljukka-Rabb, K.P., S. Isotalo, S. Mikkonen, L. Rantanen, K. Savela, *Time- and dose-dependent DNA binding of PAHs derived from diesel particle extracts, benzo[a]pyrene and 5-methylchrysene in a human mammary carcinoma cell line (MCF-7).* Mutagenesis, 2001. **16**(4): p. 353-358.
72. D.C. Spink, B.H.K., M.M. Hussain, B.C. Spink, S.J. Wu, N. Liu, R. Pause, L.S. Kaminsky, *Induction of CYP1A1 and CYP1B1 in T-47D human breast cancer cells by benzo[A]pyrene is diminished by arsenite.* DRUG METABOLISM AND DISPOSITION, 2002. **30**(3): p. 262-269.
73. Sethi, R., *Transducer Aspasects of Biosensors.* Biosensors & Bioelectronics, 1994. **9**: p. 243-264.
74. Hall, E., *Biosensors.* 1990, Buckingham: Open University Press.
75. Byfield, M., Abuknesha, RA., *Biochemical Aspects of Biosensors.* GEC J. Res., 1991. **9**: p. 97 – 117.
76. Vo-Dinh, T., et al., *Evaluation of the Fiberoptic Antibody-Based Fluoroimmunosensor for DNA Adducts in Human Placenta Samples.* Clinical Chemistry, 1991. **37**(4): p. 532-535.
77. Vo-Dinh, T.G., G. D. and Sepaniak, M. J., in *Fiber Optic Chemical Sensors and Biosensors*, O.S. Wolfbeis, Editor. 1991, CRC Press: Boca Raton. p. 217 - 257.
78. Kienle, S., et al., *Electropolymerization of a phenol-modified peptide for use in receptor-ligand interactions studied by surface plasmon resonance.* Biosensors & Bioelectronics, 1997. **12**(8): p. 779-786.
79. Pathak, S.S. and H.F.J. Savelkoul, *Biosensors in immunology: the story so far.* Immunology Today, 1997. **18**(10): p. 464-467.
80. Regnault, V., et al., *Both kinetic data and epitope mapping provide clues for understanding the anti-coagulant effect of five murine monoclonal antibodies to human beta(2)-glycoprotein I.* Immunology, 1999. **97**(3): p. 400-407.
81. Huber, A., S. Demartis, and D. Neri, *The use of biosensor technology for the engineering of antibodies and enzymes.* Journal of Molecular Recognition, 1999. **12**(3): p. 198-216.
82. Van Regenmortel, M.H.V., et al., *Measurement of antigen-antibody interactions with biosensors.* Journal of Molecular Recognition, 1998. **11**(1-6): p. 163-167.
83. Tromberg, B.J., et al., *Fiberoptic Chemical Sensors for Competitive-Binding Fluoroimmunoassay.* Analytical Chemistry, 1987. **59**(8): p. 1226-1230.

84. Velander, W., Subramanian, A., Madurawe, RD., Orthner, C., *The use of Fab masking antigens to enhance the activity of immobilized antibody.* Biotechnology and Bioengineering, 1992. **39**: p. 1013-1023.

85. Su, J., Anderson, AJ., Cummings, BJ., Cotman, CW., *Immunohistochemical evidence for apoptosis in Alzheimer's disease.* Neuroreport., 1994. **5**(18): p. 2529-2533.

86. Casey, C., Nanji, A., Cederbaum, AI., Adachi, M., Takahashi, T., *Alcoholic liver disease and apoptosis.* Alcohol Clin Exp Res., 2001. **25**(5 Suppl ISBRA): p. 49S-53S.

87. Yang, J., Liu, XS., Bhalla, K., Kim, CN., Ibrado, AM., Cai, JY., Peng, TI., Jones, DP., Wang, XD., *Prevention of apoptosis by Bcl-2: Release of cytochrome c from mitochondria blocked.* Science, 1997. **275**(5303): p. 1129-1132.

88. Kluck, R., Bossy-Wetzel, E., Green, DR., Newmeyer, DD., *The release of cytochrome c from mitochondria: a primary site for Bcl-2 regulation of apoptosis.* Science, 1997. **275**(5303): p. 1132-1136.

89. Nagata, S., *Apoptosis by Death Factor.* Cell, 1997. **88**: p. 355-365.

90. Nakagawa, T., Zhu, H., Morishima, N., Li, E., Xue, J., Yanker, BA., Yuan, J., *Caspase-12 mediates endoplasmic-reticulum-specific apoptosis and cytotoxicity by amyloid-beta.* Nature, 2000. **403**: p. 98-103.

91. Morishima, N., Nakanishi, K., Takenouchi, H., Shibata, T., Yasuhiko, Y., *An ER stress-specific caspase cascade in apoptosis: cytochrome c- independent activation of caspase-9 by caspase-12.* J. Biol. Chem., 2002. **277**: p. 34287-34294.

92. Nicholson, D., and Thornberry, NA., *Caspases: killer proteases.* Trends Biochem Sci., 1997. **8**: p. 299-306.

93. Kluck RM, B.-W.E., Green DR, Newmeyer DD,, *The release of cytochrome c from mitochondria: a primary site for Bcl-2 regulation of apoptosis.* Science, 1997. **275**(5303): p. 1132-6.

94. Wang G.Q, G.B.R., Wieckowski E, Goldstein L.A, Gambotto A, Kim T.H, Fang B, Rabinovitz A, Yin X, Rabinowich H,, *A Role for Mitochondrial Bak in Apoptotic Response to Anticancer Drugs.* J. Biol. Chem., 2001. **276**: p. 34307-34317.

95. Li P, N.D., Budihardjo I, Srinivasula S.M, Ahmad M, Alnemri E.S, Wang X,, *Cytochrome c and dATP-Dependent Formation of Apaf-1/Caspase-9 Complex Initiates an Apoptotic Protease Cascade.* Cell, 1997. **91**(4): p. 479-489.

96. Zamzami N, M.P., Castedo M, Zanin C, Vayssiere JL, Petit PX, Kroemer G., *Reduction in mitochondrial potential constitutes an early irreversible step of programmed lymphocyte death in vivo.* J Exp Med, 1995. **181**(5): p. 1661-72.

97. Fletcher GC, X.L., Passingham SK, Tolkovsky AM., *Death commitment point is advanced by axotomy in sympathetic neurons.* J Cell Biol, 2000. **150**(4): p. 741-754.

98.   Liu X, K.C., Yang J, Jemmerson R, Wang X., *Induction of apoptotic program in cell-free extracts: requirement for dATP and cytochrome c.* Cell, 1996. **86**(1): p. 147-57.

99.   Budihardjo I, O.H., Lutter M, Luo X, Wang X,, *Biochemical pathways of caspase activation during apoptosis.* Annu Rev Cell Dev Biol, 1999. **15**: p. 269-90.

100.   Dougherty, T., Gomer, CJ., Henderson, BW., Jori, G., Kessel, D., Korbelik, M., Moan, J., and Peng, Q., *Photodynamic therapy.* J. Natl. Cancer Inst., 1998. **90**: p. 889-905.

101.   Bissonnette, R., and Lui, H., *Current status of photodynamic therapy in dermatology.* Dermatol. Clin., 1997. **15**: p. 507-519.

102.   Kessel, D., Luo, Y., *Photodynamic therapy: a mitochondrial inducer of apoptosis.* Cell Death Differ., 1999. **6**: p. 28-35.

103.   Inoue S, S.-E.A.E., Omoteyama,, Human Cell, 2001. **14**(3): p. 211-221.

104.   Hinnen, P., de Rooij, FWM., van Velthuysen, MLF., Edixhoven, A., van Hillegersberg, R., Tilanus, HW . *Biochemical basis of 5-aminolaevulinic acid-induced protoporphyrin IX accumulation: a study in patients with (pre) malignant lesions of the oesophagus.* Br. J. Cancer, 1998. **78**: p. 679-682.

105.   Henderson, B., and Dougherty, TJ., *How does photodynamic therapy work?* Photochem Photobiol., 1992. **55**(1): p. 145-157.

106.   Vaux, D., Haecker, G., Strasser, A., *An evolutionary perspective on apoptosis.* Cell, 1994. **76**(5): p. 777-779.

107.   Kerr, J., Wyllie, AH., and Currie, AR., *Apoptosis: a basic biological phenomenon with wide-ranging implications in tissue kinetics.* Br. J. Cancer, 1972. **26**(4): p. 239-257.

108.   Hornung R, W.H., Crompton NE, Keefe KA, Jentsch B, Perewusnyk G, Haller U, Kochli OR,, *m-THPC-mediated photodynamic therapy (PDT) does not induce resistance to chemotherapy, radiotherapy or PDT on human breast cancer cells in vitro.* Photochemistry and Photobiology, 1998. **68**(4): p. 569-574.

109.   Hajri, A., Coffy, S., and Vallat, F., *Human pancreatic carcinoma cells are sensitive to photodynamic therapy in vitro and in vivo.* Br. J. Surg., 1999. **86**(7): p. 899-906.

110.   Noodt, B., Berg K., and Stokke T., *Apoptosis and necrosis induced with light and 5-aminolaevulinic acid-derived protoporphyrin IX.* Br. J. Cancer, 1996. **74**(1): p. 22-29.

111.   Teiten, M.-H., Marchal, S., D'Hallewin, MA., Guillemin, F., and Bezdetnaya, L., *Primary Photodamage Sites and Mitochondrial Events after Foscan® Photosensitization of MCF-7 Human Breast Cancer Cells.* Photochemistry and Photobiology, 2003. **78**(1): p. 9.

112.   Schmitt, E., *Activation and role of caspases in chemotherapy-induced apoptosis.* Drug Resistance Updates, 1999. **2**: p. 21-29.

113.   Li, P., Nijhawan, D., Budihardjo, I., Srinivasula, SM., Ahmad, M., Alnemri, ES., Wang, X., *Cytochrome c and dATP-Dependent Formation of Apaf-*

l/Caspase-9 Complex Initiates an Apoptotic Protease Cascade. Cell, 1997. **91**: p. 479-489.

114. Kolárová, H., Kubínek, R., Lenobel, R., Bancírová, M., Strnad, M., Jírová, D., Lasovský, J., *In vitro photodynamic therapy with phthalocyanines on the MCF7 cancer cells.* Internet Journal of Photochemistry and Photobiology., 1999: p. http://www.photobiology.com/photo99/contrib/kolarova/index.htm.

115. Bachmann-Moisson, N., Vandoeuvre-les, N., Barberi-Heyob, M., Gramain, MP., Bour, C., Marchal, S., Parache, RM., Guillemin, FH., Merlin, JL. *Evaluation of interacellular tamoxifen-induced fluorescence in tamoxifen-resistant human breast adenocarcinoma cells, pp.308-312.* in *SPIE: Optical Biopsies and Microscopic Techniques II.* 1997. San Remo, Italy: SPIE--The International Society for Optical Engineering.

116. Sasai K, Y.H., Suzuki F,, Jpn. J. Cancer Res, 2002. **93**: p. 275-283.

117. McNeil, P., *Cellular and molecular adaptations to injurious mechanical stress.* Trends Cell Biol., 1993. **3**(9): p. 302-307.

118. Ghosh, A., Greenberg, ME., *Calcium Signaling in Neurons: Molecular Mechanisms and Cellular Consequences.* Science, 1995. **268**(5208): p. 239-247.

119. Hilf, R., Havens, JJ., Gibson, SL., *Effect of Aminolevulinic Acid on Protoporphyrin IX Accumulation in Tumor Cells Transfected with Plasmids Containing Porphobilinogen Deaminase DNA.* Photochemistry and Photobiology, 1999. **70**(3): p. 334-340.

120. Tikkanen, M., Carter, DJ., Harris, AM., Le, HM., Azorsa, DO., Meltzer, PS., and Murdoch, FE., *Endogenously expressed estrogen receptor and coactivator AIB1 interact in MCF-7 human breast cancer cells.* PNAS, 2000. **97**(23): p. 12536-12540.

121. Brasuel, M., Kopelman, R., Miller, TJ., Tjalkens, R., Philbert MA.,, *Fluorescent nanosensors for intracellular chemical analysis: decyl methacrylate liquid polymer matrix and ion-exchange-based potassium PEBBLE sensors with real-time application to viable rat C6 glioma cells.* Anal Chem., 2001. **73**(10): p. 2221-8.

122. Vo-Dinh, T., and, Allain, L, *CRC Handbook for Biomedical Photonics.* Biosensors for Medical Applications, ed. T. Vo-Dinh. 2003, New York: CRC Press. 31.

123. Vo-Dinh, T., *Nanobiosensors: Probing the Sanctuary of Individual Living cells.* J Cellular Biochemistry, Supp 161, 2002. **39**: p. 154.

124. Mehmet, H., *Apoptosis: Caspases find a new place to hide.* Nature, 2000. **403**(6765): p. 29-30.

125. Liu, X., Kim, CN., Yang, J., Jemmerson, R., and Wang, X., *Induction of apoptotic program in cell-free extracts: Requirement for dATP and Cytochrome c.* Cell, 1996. **86**(1): p. 147-157.

126. Deveraux, Q.L., Roy, N., Stennicke, H.R., Van Arsdale T, Zhou Q, Srinivasula, S.M., Alnemri, E.S., Salvesen, G.S., Reed, J.C., *IAPs block*

apoptotic events induced by caspase-8 and cytochrome c by direct inhibition of distinct caspases. EMBO J, 1998. **17**(8): p. 2215-23.

127. Sun, X., MacFarlane, M., Zhuang, J., Wolf, BB., Green, DR., Cohen, GM., *Distinct caspase cascades are initiated in receptor-mediated and chemical-induced apoptosis.* J Cell Biol, 1999. **274**(8): p. 5053-5060.

128. MacFarlane, M., Cain, K., Sun, XM., Alnemri, ES., Cohen, GM., *Processing/activation of at least four interleukin-1beta converting enzyme-like proteases occurs during the execution phase of apoptosis in human monocytic tumor cells.* J Cell Biol, 1997. **137**(2): p. 469-79.

129. Hengartner, M.O., *Apoptosis. DNA destroyers.* Nature, 2001. **412**(6842): p. 27.

130. Sportsman, J., Wilson, GS., *Chromatographic properties of silica-immobilized antibodies.* Anal Chem, 1980. **52**(13): p. 2013-2018.

131. Lin, J., Herron, J., Andrade, JD., IEEE Trans. Biomed. Eng, 1988. **35**: p. 466-471.

132. Dragovich T, R.C., Thompson CB., *Signal transduction pathways that regulate cell survival and cell death.* Oncogene, 1998. **17**(25): p. 3207-3213.

133. Mantzaris, N., Daoutidis, P., Srienc, F., and Fredrickson, AG. *Growth Processes in a Cascade of Bioreactors: Comparison of Modeling Approaches.* in *AIChE J.* 1999.

134. Thornberry, N., Lazebnik, Y., *Caspases: Enemies within.* Science, 1998. **281**: p. 1312-1316.

135. Budihardjo, I., Oliver, H., Lutter, M., Luo, X., and Wang, X., *Biochemical Pathways of caspase activation during apoptosis.* Annu. Rev. Cell. Dev. Biol., 1999. **15**: p. 269-290.

136. Mattson, M., Guo, Q., Furukawa, K., Pedersen, WA., *Presenilins, the endoplasmic reticulum, and neuronal apoptosis in Alzheimer's disease.* J Neurochem., 1998. **70**(1): p. 1-14.

Part Five

Optical Nanosensor for Measurement Caspase-9 Activity

in a Single Living Cell

Part five is a version of a manuscript submitted for publication to *Journal of the American Chemical Society* in July 2003 and accepted for publication in December 2003 by **Paul M. Kasili**, Joon Myong Song, and Tuan Vo-Dinh: **Paul M. Kasili**, Joon Myong Song, and Tuan Vo-Dinh, **Optical Sensor for the Detection of Caspase-9 Activity in a Single Living Cell.** Manuscript accepted in *Journal of the American Chemical Society*

5.0 Abstract

We demonstrate for the first time, the application and utility of a unique optical nanosensor for monitoring the onset of the mitochondrial pathway of apoptosis in a single living cell by detecting enzymatic activities of caspase-9. Minimally invasive analysis of single live MCF-7 cells for caspase-9 activity is demonstrated using the optical nanosensor which employs a modification of an immunochemical assay format for the immobilization of non-fluorescent enzyme substrate, Leucine-GlutamicAcid-Histidine-AsparticAcid-7-amino-4-methyl coumarin (LEHD-AMC). LEHD-AMC covalently attached on the tip of an optical nanosensor is cleaved during apoptosis by caspase-9 generating free AMC. An evanescent field is used to excite cleaved AMC and the resulting fluorescence signal is detected. By quantitatively monitoring the changes in fluorescence signals, caspase-9 activity within a single living MCF-7 cell was detected. By comparing of the fluorescence signals from apoptotic cells induced by photodynamic treatment, and

160

non-apoptotic cells, we successfully detected caspase-9 activity, which indicates the onset of apoptosis in the cells.

5.1 Introduction

In this work, we describe the optical nanosensor for the *in vivo* measurement of apoptosis. The basic optical technique used by optical nanosensors, is total internal reflection excitation through the transmission of fluorophore excitation along optical nanosensor followed by filtering the signal in order to separate out the higher wavelengths of interest. TIR excitation is typically used to study the interaction of materials on optically transparent surfaces as well as serving the purpose of being the basis of optical nanosensors. The principle of TIR excitation occurs at the interface of two optically transparent media of different refractive indices. Light is typically introduced into the medium of greater refractive index (n_1). At the interface of the two media, all energy associated with the light beam is not confined to the nanotips, some energy, evanescent optical waves, is lost from this beam into the less dense medium (n_2) which could be the cytoplasm of a cell under investigation, with the intensity of the energy decaying rapidly with the penetration depth of the energy into the less dense medium. Evanescent optical waves are used to excite surface bound fluorophores which subsequently emit radiation at a different wavelength. This technique is very well suited for the investigation of surface association or dissociation events that occur at the distal ends of the optical nanosensors as the material in the cytoplasm or bulk solution at distances of greater than several hundred of nanometers away from the surface are not interrogated by the evanescent wave

[54]. This means that good discrimination between species bound to the nanotips over unbound material is achieved.

Minimally invasive analysis of cellular signaling pathways inside single live cells is becoming increasingly important fundamentally because cells in a population respond asynchronously to external stimuli [122]. There is a need to further our understanding of basic cellular signaling processes in order to yield new information that is not available from population-averaged cellular measurements. In addition, many cellular signaling pathways act on timescales of a few seconds and there is critical need for single-cell measurement techniques with similar time resolution. Not only is there a need to temporally resolve such measurements, there is also a need to spatially resolve them. For these reasons, continued progress in cellular physiology requires new measurement strategies, which can be applied to individual cells [7] with great temporal and spatial resolution. For this purpose, the optical nanosensor is a suitable technology with great potential for obtaining intracellular measurements of biological entities as will be demonstrated in this work.

Biosensors have played a key role in the development of minimally invasive, highly sensitive, and selective technologies for biochemical analysis [19]. One of the most recent advances in the field of biosensors has been the development of optical nanosensors capable of detecting and responding to the interaction between analytes of biomedical interest and their corresponding antibody within single live cells [16-18]. Minimally invasive analysis of living cells involves penetrating individual live cells without causing physiological or biological damage with resultant biochemical

consequences. Intracellular measurements are made possible by the small scale of the nanosensor in comparison to the dimensions of the cell, typically one to two orders of magnitude. Optical nanosensors are thus crucial for minimally invasive analysis because they allow the penetration and sampling of individual live cells in their physiological state without disrupting their normal functions, hence allowing the continuation of vital cellular processes such as mitosis [123]. These antibody-based optical nanosensors rely on excitation using the evanescent field generated by total internal reflection at the tip of the nanosensor, thus exciting only molecules in close proximity to the boundary interface of the optical nanosensor tip. The evanescent field generated at the tip of the nanosensor is a result of the nanosensor tip being smaller than the wavelength of the laser beam, leading to a diffraction-limited condition that does not allow photons from the laser beam to be transmitted through the tip of the nanosensor, but rather allows energy to be transmitted in the form of an interfacial leaky surface mode, which is propagated as the evanescent field exciting only molecules on the periphery of the tip.

We have developed a unique enzyme optical nanosensor based on an enzyme-substrate probe to detect and identify surface dependent cleavage events of caspase-9 in a single live MCF-7 cell. The modified assay format consists of a solid phase for the immobilization of caspase-9 substrate, Leucine-GlutamicAcid-Histidine-AsparticAcid-7-amino-4-methyl coumarin (LEHD-AMC), which consists of a tetrapeptide, LEHD, coupled to a fluorescent molecule, AMC. LEHD-AMC exists as a non-fluorescent substrate prior to cleavage by caspase-9, and after cleavage, free

AMC fluoresces when excited at 325nm. Figure 5.1 shows the excitation and emission spectrum of AMC and cleavage process of LEHD-AMC to produce free fluorescent AMC.

The excitation and emission spectra of AMC were acquired using a Fluoromax-3 spectrofluorimeter (Jobin Yvon Inc, Edison, NJ). The excitation spectrum represents the relative ability of various wavelengths to stimulate AMC fluorescence emission, while the emission spectrum represents the relative fluorescence intensity when AMC is excited. In contrast to traditional, discontinuous, non-equilibrium ELISA-type cleavage assays that cannot accurately model dynamic binding mechanisms, the optical nanosensor permits investigation of surface cleavage phenomena, in addition to providing a simple way to detect caspase-9 in single cells. Caspase-9 is a prominent member of a family of death-specific enzymes known as cysteine-dependent aspartate-specific proteases, the caspases [124]. Caspase-9 is activated via mitochondrial involvement in the apoptotic pathway. Cells exposed to apoptotic stimuli release cytochrome c from mitochondria into the cytosol. In the cytosol, cytochrome c interacts with apoptotic protease activating factor-1 (Apaf-1) [125]. The cytochrome c/Apaf-1 complex cleaves the inactive caspase-9 proenzyme to generate active caspase-9 enzyme [114]. Activated caspase-9 exhibits distinct substrate recognition properties and initiates the proteolytic activities of other downstream caspases, which degrade a variety of substrates, resulting in the systematic disintegration of the cell [126-128] and ultimately, cell death.
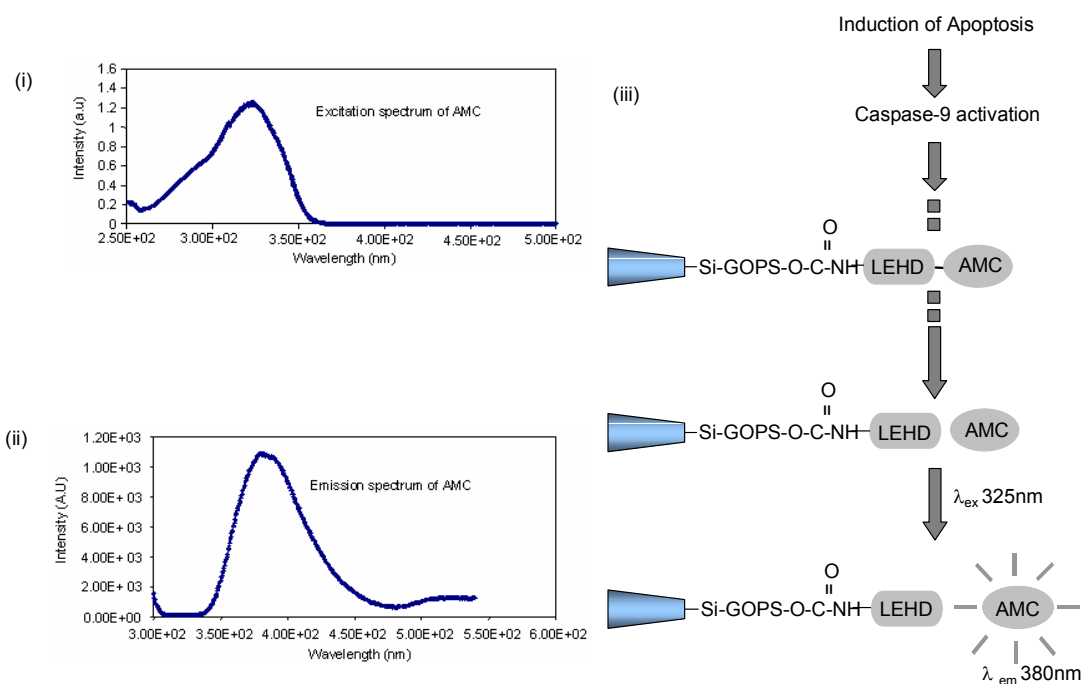
Figure 5.1 (i) shows the absorption spectrum of AMC (10^{-3} M), while (ii) shows the emission spectrum of AMC (10^{-3} M). Excitation and emission spectra were acquired to determine where to excite and detect AMC. (iii) shows a diagrammatic representation of ALA induced apoptosis, involving the activation of caspase-9 followed by the cleavage of Leucine-Glutamate-Histidine-Aspartate-7-amino-4-methyl coumarin (LEHD-AMC) and subsequent detection of free AMC.

The enzyme substrate-based optical nanosensor works on the same principle of evanescent field excitation by means of an exponentially decaying surface energy wave with a penetration depth that allows only AMC molecules in close proximity to the boundary interface of the optical nanosensor tip to be excited and detected. This feature is important because it underlines the operating principle of the nanosensor in the sense that only the cleaved AMC will be excited in the near field of the optical nanosensor. An additional feature of the nanosensor is its selectivity. Selectivity is dependent upon the selective cleavage capabilities for specific sequences by caspase-9. Another advantage of the optical nanosensors' feature of excitation and detection in the evanescent field is the reduction of sources of background, particularly specular scattering, Rayleigh scattering, and Raman scattering from regions outside the nearfield. The optical nanosensors' mode of excitation and detection unlike other techniques for molecular detection does not compromise throughput and signal-to-noise ratio. Furthermore, due to its nanoscale size, the optical nanosensor does not compromise the integrity of the cell when performing intracellular analysis. This has been illustrated in a previous study whereby a single cell was microscopically monitored after probing the cytoplasm of the cell with an optical nanosensor. The cell was observed and it was found that the cell carried out normal cellular activities, specifically mitosis [123].

In this work, we demonstrate for the first time, the application and utility of optical nanosensors for the detection and identification the onset of the mitochondrial

pathway of apoptosis in a single live MCF-7 cell by detecting the enzymatic activity of caspase-9. To perform these measurements, we covalently immobilized caspase-9 substrate, LEHD-AMC onto the tip of the nanofiber. Photodynamic therapy (PDT) protocols (Figure 5.2) employing δ-aminolevulinic acid (ALA) were used to induce apoptosis [129] in MCF-7 cells. Briefly, caspase-9 is present in the cell after apoptosis has been induced. It typically exists in a proenzyme form procaspase-9, prior to apoptosis induction. MCF-7 cells exposed to apoptotic stimuli release cytochrome c from mitochondria into the cytosol. In the cytosol, cytochrome c interacts with apoptotic protease activating factor-1 (Apaf-1) [125]. The cytochrome c/Apaf-1 complex cleaves the inactive procaspase-9, a proenzyme to generate the active enzyme, caspase-9 [114]. Activated caspase-9 then initiates the proteolytic activities of other downstream caspases. These caspases degrade a variety of substrates, resulting in the systematic disintegration of the cell. Caspase-9 is capable of cleaving multiple LEHD-AMC substrates. This is a typical mechanism of action characteristic of enzymes, the ability to hydrolyze multiple substrates because they do not undergo change when they are involved in the cleavage reactions and they can therefore be applied to multiple substrates. Our measurement system consists of the tetrapeptide substrate Leucine-Glutamic Acid-Histidine-Aspartic Acid-7-amino-4-methoxy coumarin (LEHD-AMC), which is selectively cleaved by activated caspase-9. The principle of this system is the selective detection of caspase-9 activity by detecting the fluorescent cleavage product of LEHD-AMC, AMC. When LEHD-

MCF-7 cell

δ-Aminolevulinic Acid
λ_{Ex} = 632.8nm

Apoptosis Induction

Apoptotic MCF-7 cell

Bcl-2

Nucleus

Apaf-1

Mitochondria

Inactive procaspase-9

Nucleus

Permeable mitochondria

Cytochrome c

Active caspase-9
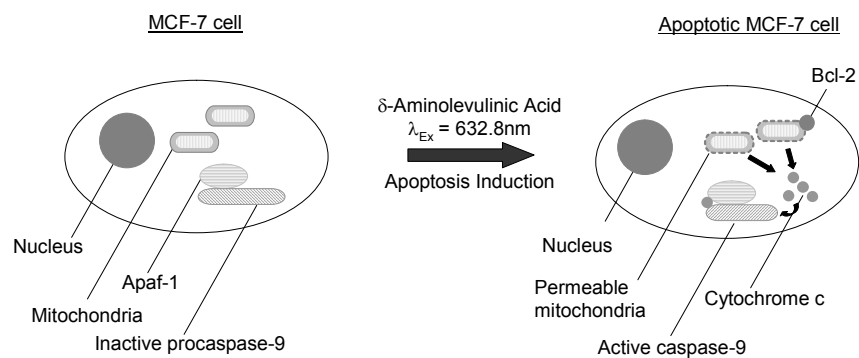
Figure 5.2 shows a diagrammatic representation of the aminolevulinic acid (ALA) photoactivation process in a MCF-7 cell. On the left is representation of a MCF-7 cell prior to the induction of apoptosis and similarly on the right is a representation of a MCF-7 cell shortly after the induction of apoptosis showing the activation of caspase-9 which ultimately leading to apoptosis.

168

AMC is cleaved by activated caspase-9, AMC is no longer tethered to the tetrapeptide LEHD that effectively quenches the fluorescence of AMC. Free AMC can therefore be excited in the near-field of the optical nanosensors and the fluorescence signal generated can be detected and measured. By comparing the fluorescence from an apoptotic MCF-7 cell and uninduced control MCF-7 cell, caspase activity can be detected. In this context, caspases-9 recognizes the specific tetrapeptide sequence LEHD and cleaves the substrate LEHD-AMC. The substrate LEHD-AMC is cleaved by caspase-9 and the released AMC molecules are excited and emitted a fluorescence signal. By comparing the fluorescence from an apoptotic cell and an uninduced control, we detected and identified caspase-9 activity.

5.2 Materials and Methods

5.2.1 Chemicals and Reagents

δ-aminolevulinic acid (ALA), phosphate buffered saline (PBS), hydrochloric acid (HCl), nitric acid (HNO_3), glycidoxypropyltrimethoxysilane (GOPS), 1,1'-carbonyldiimidazole (CDI), and anhydrous acetonitrile were purchased from Sigma-Aldrich, St. Louis, MO. Caspase-9 substrate, LEHD-7-amino-4-methyl coumarin (AMC), 2x reaction buffer, dithiothreitol (DTT), and dimethylsulfoxide (DMSO) were purchased from BD Biosciences, Palo Alto. CA.

5.2.2 Cell Lines

Human breast cancer cell line, MCF-7, was obtained from American Type Culture Collection (Rockville, MD, USA, Cat-no. HTB22). MCF-7 cells were grown in Dulbecco's Modified Eagle's Medium ((DMEM) (Mediatech, Inc., Herndon, VA)) supplemented with 1 mM L-glutamine (Gibco, Grand Island, NY) and 10% fetal bovine serum (Gibco, Grand Island, NY). Baseline static culture productivity for each cell line was established in growth medium (described above) in standard T25 tissue culture flasks (Corning, Corning, NY). The flasks were incubated in a humidified incubator at 37°C, 5% CO_2 and 86% humidity. Cell growth was monitored daily by microscopic observation until a 60–70% state of confluence was achieved. The growth conditions were chosen so that the cells would be in log phase growth during photosensitizer treatment with ALA, but would not be so close to confluence that a confluent monolayer would form by the termination of the chemical exposure [25]. In preparation for experiments, cells were harvested from the T25 flasks and 0.1ml (10^5 cells/ ml) aliquots were seeded into 60 mm tissue culture dishes (Corning Costar Corp., Corning, NY) for overnight attachment. The MCF-7 cells were studied as three separate groups with the first group being the experimental, exposed to 0.5 mM ALA for 3 h followed by photoactivation [120]. This involved incubating the cells at 37° C in 5% CO_2 for 3 h with 0.5mM ALA. Following incubation the MCF-7 cells were exposed to red light from a HeNe laser (λ 632.8 nm, <15mW, Melles Griot, Carlsbad, CA) positioned about 5.0 cm above the cells for five minutes at a fluence of 5.0 mJ/cm^2 to photoactivate ALA and subsequently induce apoptosis. The second group

was the "treated control" and was exposed to 0.5 mM ALA for 3 hours without photoactivation. The third group was the "untreated control," which received neither ALA nor photoactivation.

5.2.3 Preparation of Enzyme Substrate-based Nanosensors

Preparation of enzyme substrate-based optical nanosensors involves cutting and polishing plastic clad silica (PCS) fibers with a 600-µm-diameter core (Fiberguide Industries, Stirling, New Jersey). The optical fibers were pulled to a final tip diameter of 50 nm using the current state-of-the-art in micropipette pulling technology, the P-2000 system (Sutter Instruments, Novato, CA), and then coated with 100 nm of silver metal (99.999% pure) using a thermal evaporation deposition system (Cooke Vacuum Products, South Norwalk, CT) achieving a final diameter of 150nm. Figure 5.3 (ii) shows an image of silver-coated optical nanofiber. The nanotips were derivatized to allow the immobilization of enzyme substrate. Derivatization involved a multistep procedure. The fused silica optical fibers were acid-cleaned followed by several rinses with distilled water and then allowed to air dry at room temperature in a dust free environment. The nanotips were silanized by treatment with an organic cross-linking reagent, 10% GOPS in H_2O (v/v) at $90^{o}C$ for 3 h. The silanized fibers were washed with anhydrous acetonitrile and dried overnight in a vacuum oven at $105^{o}C$. Soon after overnight incubation, the nanotips were activated by being suspended in saturated CDI in acetonitrile for 30 min followed by
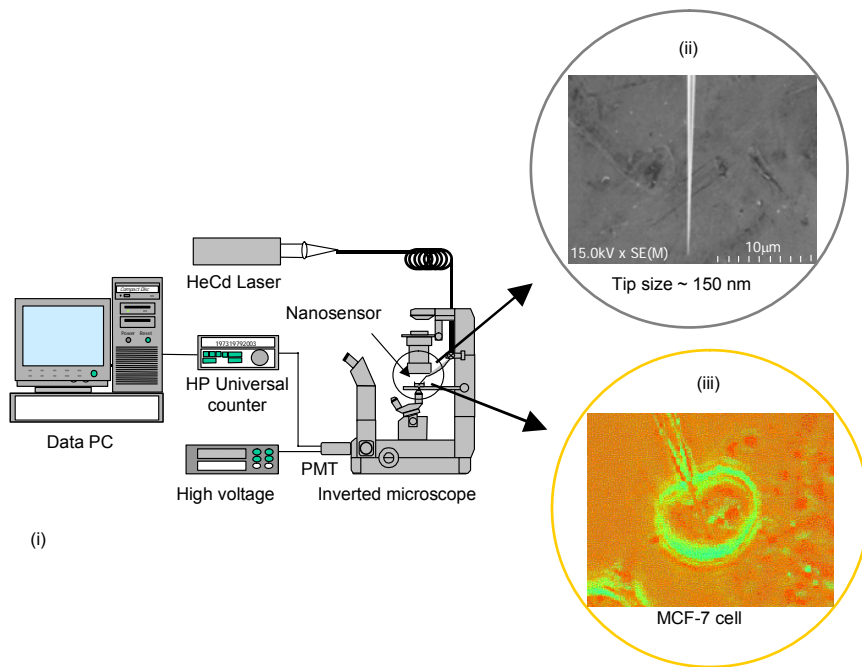
Figure 5.3: (i) Schematic diagram of fluorescence measurement system used for data acquisition and processing (ii) Scanning electron micrograph of a nanotip after coating with 100nm of silver metal, achieving a final tip diameter of 150 nm (iii) Image of optical nanosensor inserted into a single live MCF-7 cell. This image shows how we performed the intracellular measurements of MCF-7 cells.

rinsing with acetonitrile. The silanized and activated nanotips were immersed in a solution containing DMSO, 2X reaction buffer, PBS, and LEHD-AMC, and allowed to incubate for 3 h at 37$^{\text{o}}$C. The LEHD-AMC bound using this procedure remained securely immobilized during washing and subsequent manipulations in immunoassay procedures, in contrast to procedures that would use adsorption to attach proteins [130, 131]. The optical nanosensors prepared were subdivided into groups to perform parallel experimental and control measurements using MCF-7 cells.

5.2.4 Measurement System and Procedure

Figure 5.3(i) shows (above) a schematic representation of the fluorescence measurement system. The major components of this system include a HeCd laser (Omnichrome, <5mW laser power), a Nikon Diaphot 300 inverted microscope (Nikon, Inc., Melville, NY), Hamamatsu PMT detector assembly (HC125-2), and a personal computer (PC). To perform the intracellular fluorescence measurements, the 325 nm laser line of a HeCd laser was focused onto a 600-μm-delivery fiber that was terminated with a subminiature A (SMA) connector. The optical nanosensor was coupled to the delivery fiber through the SMA connector and secured to the microscope with micromanipulators. The fluorescence emitted from the cells was collected by the microscope objective and passed through a 330nm barrier filter and then focused using the internal optics of the microscope onto the PMT for detection. The output from the PMT was recorded using a universal counter and a PC with custom-designed software for data acquisition and processing.

The experimental setup used to probe single cells was adapted to this purpose from a standard micromanipulation/microinjection apparatus. The Nikon Diaphot 300 inverted microscope, having a Diaphot 300/Diaphot 200 Incubator to maintain the cell cultures at 37°C on the microscope stage, was used for these experiments. The micromanipulation equipment consisted of MN-2 (Narishige Co. Ltd., Tokyo, Japan) Narishige three-dimensional manipulators for coarse adjustment, and Narishige MMW-23 three-dimensional hydraulic micromanipulators for fine movements. The optical nanosensor was mounted on a micropipette holder (World Precision Instruments, Inc., Sarasota, FL). To record the fluorescence of AMC in the evanescent field of the optical nanosensor, a Hamamatsu PMT detector assembly (HC125-2) was mounted in the front port of the Diaphot 300 microscope.

Before making measurements, the cells were harvested from culture flasks and transferred to culture dishes. After attachment to the bases of the petri dishes, the experimental group of MCF-7 cells was treated with 0.5 mM ALA with subsequent photoactivation, the treated control received 0.5 mM ALA without photoactivation while the untreated control group did not receive any treatment. For the experimental and treated control group, the solution of ALA was aspirated after a 3-hour incubation period and replaced with fresh cell culture media. The experimental group of cells was then irradiated with HeNe laser to photoactivate ALA for a period of five minutes.

Using the experimental group of cells, three separate trials were conducted to determine the presence of caspase-9 activity. In addition, three separate trials were

performed for the treated control and untreated control respectively. Determination of the presence or absence of caspase-9 activity using the nanosensor was carried out using the following procedure. A culture dish of cells was placed on the pre-warmed microscope stage set at 37°C. The enzyme optical nanosensor shown in figure 5.3(ii) (above) is mounted on a micropipette holder of a micromanipulation system, was moved into position (i.e., in the same plane as the cells), using bright-field phase contrast microscopic illumination, so that the tip was just outside of the cell to be probed. The total magnification was 600×. The nanosensor was gently micromanipulated into the cell, past the cell membrane and extending a short way into the cytoplasm. During these micromanipulations, great care was taken not to penetrate the nuclear envelope and compromise the integrity of the nucleus. Room light and microscope illumination light were switched-off; the laser shutter opened, and laser light allowed to illuminate the optical fiber and excitation light was transmitted into the fiber tip. First, a signal reading was taken with the nanosensor inside the cell with the laser shutter closed in order to record the dark signal. After five min, the laser shutter was opened allowing the excitation light to be transmitted to the nanosensor tip and fluorescence readings were recorded. Figure 5.3 (iii) (above) shows an image illustrating an intracellular measurement performed in a single MCF-7 cell after micromanipulation.

5.3 In Vitro Determination of Caspase-9 Activity

We performed a calibration measurement of caspase-9 outside the cell using caspase-9 obtained from cytosolic cell extract of cell groups after apoptosis was induced and without the induction of apoptosis. This was done by inducing apoptosis in a group of cells using ALA-PDT and having a control group without ALA-PDT. The cells were harvested and the cytosolic extract placed in picofuge tubes. Optical nanosensors were incubated in the picofuges containing the cytosolic cell extract, one set presumably containing activated caspase-9 while the other set devoid caspse-9.

After incubating MCF-cells using the following treatment groups, experimental group [+]ALA[+]PDT (with ALA-PDT), and the control group [-]ALA[-]PDT (without ALA-PDT), MCF-7 cells were washed with PBS solution, pH 7.4, and then resuspended in lysis buffer (100 mM HEPES, pH 7.4, 10% sucrose, 0.1% 3-[(3-cholamidopropyl)-dimethylammonio]-1-propanesulfonate (CHAPS), 1 mM EDTA, 10 mM dithiothreitol (DTT), 1 mM phenylmethylsulphonyl fluoride (PMSF), 10 mg/ml pepstatin, 10 mg/ml leupeptin) and left on ice for 45 minutes. The cells were then repeatedly passed through a syringe with a 25-gauge needle until most of the cell membrane was disrupted, and centrifuged at 1500 RPM for 10 min. Activity of caspases was measured using fluorogenic substrate peptides; LEHD-AMC for caspase-9 immobilized on the nanotips of the optical nanosensors. The release of AMC was measured after incubating optical nanosensors in picofuge tubes containing the cell lysates from the various treatment groups and using a HeCd laser (excitation 325 nm) to excite AMC. Caspase activity was expressed as fluorescence intensity of

AMC as a function of equivalent nanomoles of LEHD-AMC. We plotted the results of the *in vitro* measurement of caspase-9 activity. The curves for each fluorescent measurement of AMC were plotted for each as a function of nanomoles of AMC. Caspase-9 activity was determined by incubation of optical nanosensors with the substrate LEHD-7-amino-4-methylcoumarin (AMC) in cell lysate ($\sim 10^5$ cells) obtained from the following treatment groups; experimental group (with ALA-PDT), and the control group (without ALA-PDT), and measured the release of AMC. The release of AMC was measured after excitation using HeCd laser (325 nm) and collecting the fluorescence signal using a 380 nm longpass filter. Peak emission wavelength of AMC is about 440 nm.

5.4 In Vivo Determination of Caspase-9 Activity

To perform the intracellular measurements, the optical nanosensor was positioned using the 3-dimensional micromanipulator mounted on the inverted microscope. Using the microscope eyepiece for observation the optical nanosensor was micropositioned within the field of view and, once within the same plane as the cell under investigation, micromanipulated into the cytoplasm of the cell. After incubation at 37°C for 5 min, the HeCd laser excitation source was turned on and fluorescence at λ_{max} 380 nm was measured using a 330nm barrier filter. About 1.5-2.0 h after the induction of apoptosis, the cleavage of LEHD-AMC by caspase-9 occurs and the released AMC molecules were excited at 325nm and the fluorescence emission was measured. The fluorescence signal emitted by AMC was collected by

the fluorescence microscope optics and detected with the PMT. The fluorescence emission was collected as a function of time and the data is transmitted via a HP 53131A (225 MHz) universal counter that serves as an interface, to a PC for data acquisition and processing. Data acquisition and processing is performed using custom software built on LabView platform.

5.5 Results and Discussion

The examination of caspase-9 activity was first performed *in vitro* using cell lysate, and *in vivo*, within single MCF-7 cells using enzyme optical nanosensors. Caspase-9 cleaves the substrate tetrapeptide (LEHD-AMC) between D and AMC, releasing the fluorophore AMC that is measured upon excitation by HeCd laser. Figure 5.4 shows the results *in vitro* study of the experimental group (with ALA-PDT) and the control group (without ALA-PDT). These results show a difference of about an order of magnitude in the mean fluorescence intensity measurements we obtained for the experimental group and the control group. This difference is significant enough to detect and positively identify caspase-9 activity *in vitro*. These results were expected because it is the collective effect of ALA and photoactivation that result in the induction of apoptosis and neither ALA nor photoactivation.

Figure 5.5 shows the background-subtracted results of a series of three intracellular measurements performed with enzyme optical nanosensors using the experimental and control group of MCF-7 cells. This graph consists of the

Measurement of caspase-9 activity
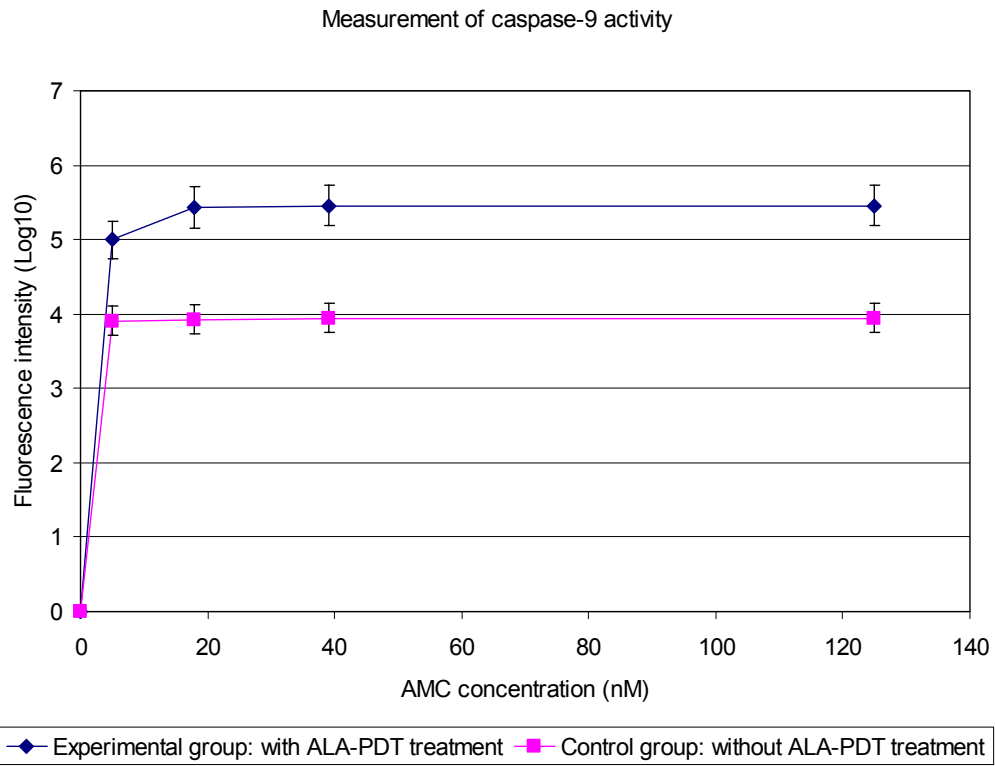
Figure 5.4: shows the background-corrected fluorescence intensity measurements of AMC for the in vitro detection of caspase-9 activity in experimental group of MCF-7 cells, which received both ALA and photoactivation and the control measurements for the in vitro detection of caspase-9 activity in control group of MCF-7 cells, which received neither ALA nor photoactivation. These results represent replicate studies for the measurement of caspase-9 activity with the error bars representing 95% Confidence Interval (CI).
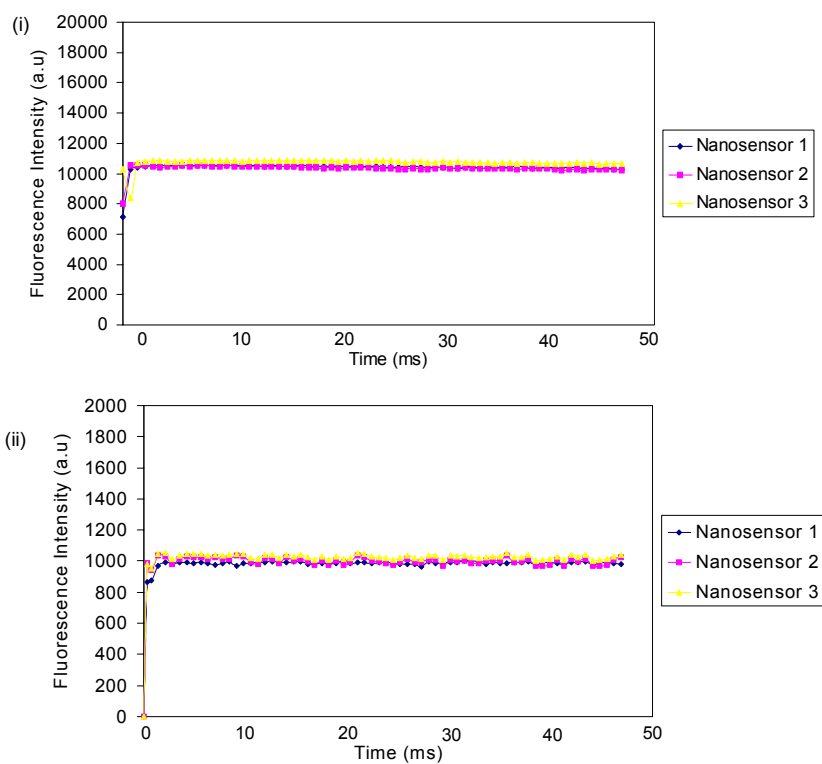
Figure 5.5: (i) Graph showing the background-corrected fluorescence intensity measurements of AMC for the intracellular detection of caspase-9 activity in experimental group of MCF-7 cells, which received both ALA and photoactivation. These results represent replicate studies for the measurement of caspase-9 activity. (ii) Graph showing the background-corrected control measurements for the intracellular detection of caspase-9 activity in control group of MCF-7 cells, which received neither ALA nor photoactivation. These results represent replicate studies for the control measurement of caspase-9 activity

fluorescence intensity of AMC fluorescence as a function of time. The results show that for the control group of cells, the fluorescence signal relative to the experimental group was not significant enough to confound the determination of AMC. Moreover, there are no other molecules that appear to interfere with the fluorescence measurements that would confound the determination of AMC due to the use of near-field excitation and detection. The application of near-field excitation contributes to the specificity of the nanosensor and virtually diminishes any background effects that may confound the determination of AMC because excitation of AMC occurs only in the evanescent-wave component of near-field excitation. Furthermore, the likelihood of interfering species existing within the near field is extremely small in comparison to AMC. Accordingly, the nanosensor used to monitor the experimental group of cells transduced a higher fluorescent signal as a result of the detection of AMC molecules momentarily sequestered at the tip of the optical nanosensor.

Figure 5.6 shows the results of intracellular measurements performed using the enzyme optical nanosensors on the treated control groups of MCF-7 cells. The first treatment group received ALA without photoactivation while the second group received photoactivation without ALA. These graphs consist of the fluorescence intensity of AMC acquired as a function of time using three optical nanosensors toperform three independent measurements on MCF-7 cells. The results show that for the treated control groups, the fluorescence signal detected relative to the
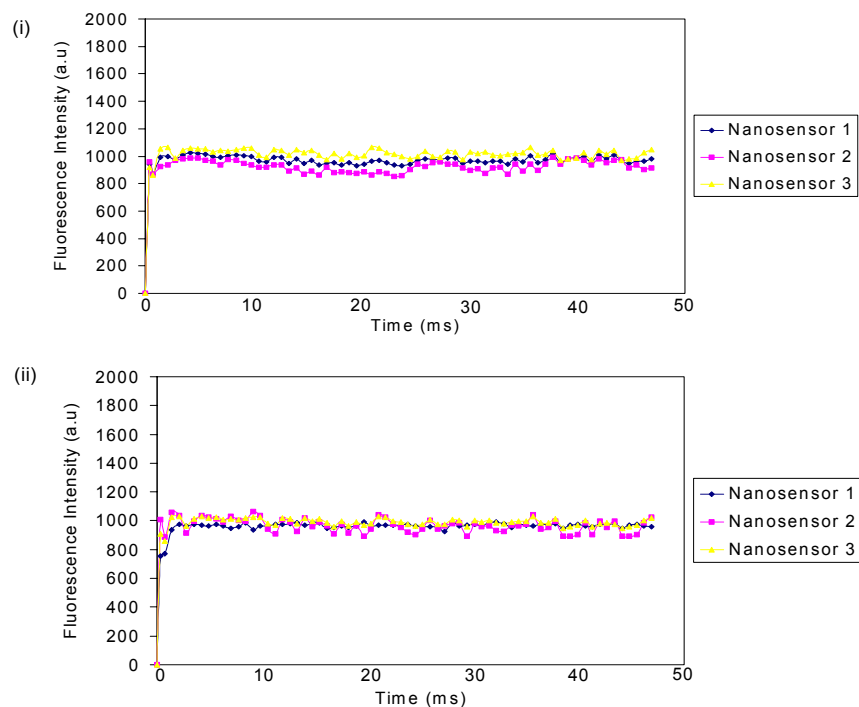
Figure 5.6: (i) shows the background-corrected treated control measurements for the intracellular detection of caspase-9 activity in MCF-7 cells, which received ALA without photoactivation. These results represent replicate studies for the treated control measurement of caspase-9 activity within single live MCF-7 cells. (ii) Graph showing the background-corrected treated control measurements of for the intracellular detection of caspase-9 activity in MCF-7 cells, which did not receive ALA but were photoactived. These results represent replicate studies for the treated control measurement of caspase-9 activity within single live MCF-7 cells.

experimental group was not significant enough to confound the determination of AMC. Once again, these results affirm the excellent degree of reproducibility achieved using optical nanosensors for the intracellular detection of AMC.

Excellent reproducibility was achieved as a result of optimization of the input parameters of the laser-based micropipette-pulling device. For instance, after determining the optimum heating temperature as well as tension applied to pull the fiber, we successfully produced reproducible tip diameters from nanofiber to nanofiber (Figure 5.7). This was confirmed by acquiring several scanning electron microscope (SEM) images of the pulled fibers using a Hitachi S-4700 field emission SEM. The optimization of the input parameters of the micropipette pulling device enables very good batch-to-batch reproducibility, which is especially essential for a technology aimed to single-use nanosensors.

For the *in vivo* studies, caspase-9 activities were analyzed in ALA-PDT treated cells (Experimental group 1 in Figure 5.7) by measuring the fluorescence signal from AMC generated after the cleavage of the peptide substrate LEHD-AMC. Likewise, the same was done for the control groups (Experimental group 2, 3, 4 in Figure 5.7) of cells which received either [+]ALA[-]PDT, [-]ALA[+]PDT or [-]ALA[-]PDT. Figure 5.7 (ii) shows the background-subtracted results of the intracellular determination of caspase-9 activity using six replicate nanosensors, one for each measurement. The graph consists of the fluorescence intensity of AMC
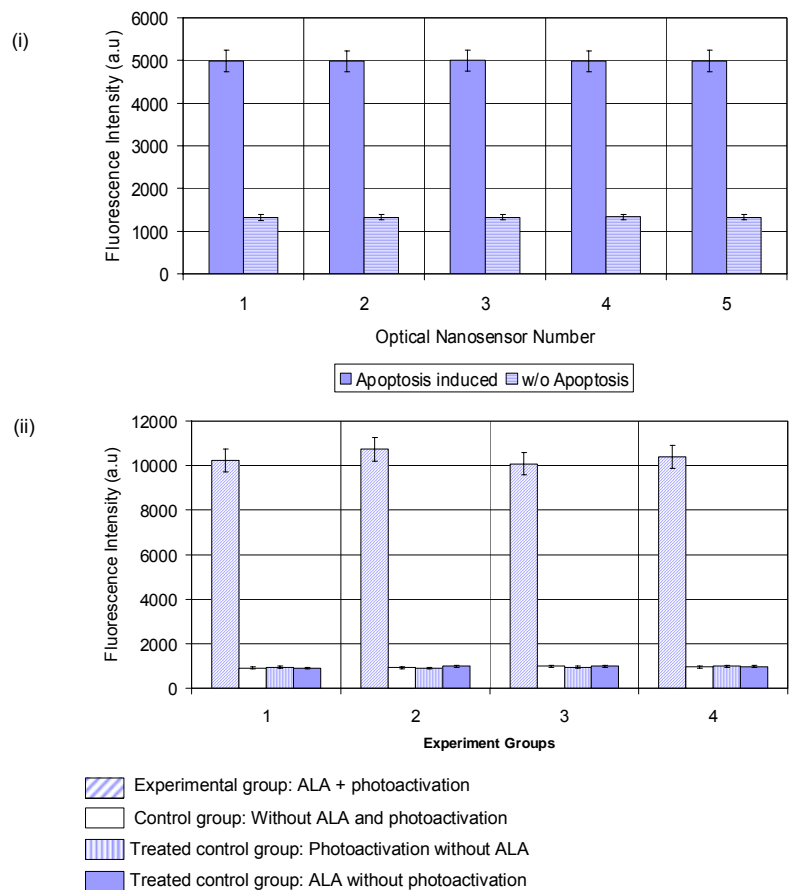
Figure 5.7: (i) shows the reproducibility study performed using optical nanosensors. The calculated percent variability from optical nanosensor to optical nanosensor is within 10%. (ii) Graph showing a side-by-side comparison of intracellular measurement of caspase-9 activity in experimental group of MCF-7 cells and control groups.

fluorescence as a function of illumination time. The fluorescent intensity measurements obtained for these treatment groups were then compared. As shown in Figure 5.7, in untreated cells, [-]ALA[-]PDT, no level of LEHD-AMC cleavage activity was detected. Likewise, the same was observed for the treated control groups, [+]ALA[-]PDT and [-]ALA[+]PDT. However, in treated cells, [+]ALA[+]PDT, significant LEHD-AMC cleavage activity via the measurement of AMC fluorescence was detected. As shown in Figure 5.7, the initiator substrates (LEHD-AMC) of caspase-9 were cleaved into the fluorogenic AMC forms in cells treated with ALA-PDT. This demonstrates the involvement of caspase-9, a member of the family of cysteine proteases that cleave after aspartic acid, in mediating apoptosis. The results obtained here demonstrated the presence of active pathways of caspase-9 during ALA-PDT induced apoptosis in MCF-7 cells.

The fluorescence signals obtained from the cells that were both incubated with ALA and photoactivated were much higher than the signal obtained from both control groups. Statistical analysis was performed on the three sets of results. The mean value of these analyses revealed that the fluorescence signal obtained using the nanosensors used to probe cells incubated with photoactivated ALA was much higher than the signal obtained by nanosensors used to probe untreated and treated control cell groups. A larger mean value for the experimental group affirms the detection of AMC and hence the detection of caspase-9 activity.

The results obtained in this work demonstrate measurements performed inside single living cells using an enzyme substrate-based optical nanosensor and the

potential application of such a nanosensor in protein-protein profiling in biochemical pathways.

We have prepared enzyme substrate-based optical nanosensors using covalent coupling of enzyme substrate to nanotips and demonstrated the application of these sensors for the determination of the cleavage product of LEHD-AMC, AMC, in single live MCF-7 cells. The presence and detection of cleaved AMC in single live MCF-7 cells as a result of this design is representative of caspase-9 activity and a hallmark of apoptosis. These results indicate that AMC, and hence apoptosis, can be monitored and measured using optical nanosensors within single living cells. These results also show the possibility of cataloging cellular components, which can play an important role in understanding the role of these components, and how they work together in a cell.

The studies performed in this work show the possibility of studying individual cells without having to disrupt their physiological make-up, which in the process can negatively interfere with cellular biochemistry. Mechanical and electrical manipulations such as cell lysis that can lead to cell disruption prior to the time of sampling may interfere with measurements of cellular biochemistry by initiating cellular repair mechanisms. Since many cellular signaling pathways act on timescales of a few seconds, there is critical need for single cell measurement techniques with time resolution to perform intracellular measurements. The optical nanosensor is a suitable technology that can be applied to solitary cells and has great potential for intracellular measurement of biological entities as demonstrated in this work.

In this work, an optical nanosensor enabled the measurement of a cellular process, in this case the functioning of an apoptosis enzyme, caspase-9, in its native environment. This work demonstrated a tool that has the potential to shed light on the principles that govern cell-signaling organization. Future work will involve studies that will attempt to carry out similar analysis on other proteins involved in biochemical cellular pathways.

References

1. Robinson, G., *Optical Immunosensors: An Overview*, in *Advances in Biosensors*, T. APF, Editor. 1991, JAI Press Inc: London. p. 230-252.
2. Brasuel, M., Kopelman, R., Miller, TJ., Tjalkens, R., Philbert MA.,, *Fluorescent nanosensors for intracellular chemical analysis: decyl methacrylate liquid polymer matrix and ion-exchange-based potassium PEBBLE sensors with real-time application to viable rat C6 glioma cells.* Anal Chem., 2001. **73**(10): p. 2221-8.
3. Luzzi, V., Lee, C.L., Allbritton, N.L., *Localized sampling of cytoplasm from Xenopus oocytes for capillary electrophoresis.* Anal Chem, 1997. **69**(23): p. 4761-4767.
4. Vo-Dinh, T., and, Allain, L, *CRC Handbook for Biomedical Photonics.* Biosensors for Medical Applications, ed. T. Vo-Dinh. 2003, New York: CRC Press. 31.
5. Cullum, B., Griffin, GD., Miller, GH., Vo-Dinh, T., *Intracellular measurements in mammary carcinoma cells using fiber-optic nanosensors.* Anal Biochem, 2000. **277**(1): p. 25-32.
6. Kasili, P.M., Cullum, B.M., Griffin, G.D., and Vo-Dinh, T., *Nanosensor for In-Vivo Measurement of the Carcinogen Benzo [a] Pyrene in a Single Cell.* Journal of Nanoscience and Nanotechnology, 2003. **2**(6): p. 653-658.
7. Vo-Dinh, T., Alarie, JP., Cullum, BM., Griffin, GD., *Antibody-based nanoprobe for measurement of a fluorescent analyte in a single cell.* Nat Biotechnol, 2000. **18**(7): p. 764-767.
8. Vo-Dinh, T., *Nanobiosensors: Probing the Sanctuary of Individual Living cells.* J Cellular Biochemistry, Supp 161, 2002. **39**: p. 154.
9. Mehmet, H., *Apoptosis: Caspases find a new place to hide.* Nature, 2000. **403**(6765): p. 29-30.
10. Liu, X., Kim, CN., Yang, J., Jemmerson, R., and Wang, X., *Induction of apoptotic program in cell-free extracts: Requirement for dATP and Cytochrome c.* Cell, 1996. **86**(1): p. 147-157.
11. Li, P., Nijhawan, D., Budihardjo, I., Srinivasula, SM., Ahmad, M., Alnemri, ES., Wang, X., *Cytochrome c and dATP-Dependent Formation of Apaf-1/Caspase-9 Complex Initiates an Apoptotic Protease Cascade.* Cell, 1997. **91**: p. 479-489.
12. Deveraux, Q.L., Roy, N., Stennicke, H.R., Van Arsdale T, Zhou Q, Srinivasula, S.M., Alnemri, E.S., Salvesen, G.S., Reed, J.C., *IAPs block apoptotic events induced by caspase-8 and cytochrome c by direct inhibition of distinct caspases.* EMBO J, 1998. **17**(8): p. 2215-23.
13. Sun, X., MacFarlane, M., Zhuang, J., Wolf, BB., Green, DR., Cohen, GM., *Distinct caspase cascades are initiated in receptor-mediated and chemical-induced apoptosis.* J Cell Biol, 1999. **274**(8): p. 5053-5060.
14. MacFarlane, M., Cain, K., Sun, XM., Alnemri, ES., Cohen, GM., *Processing/activation of at least four interleukin-1beta converting enzyme-like*

proteases occurs during the execution phase of apoptosis in human monocytic tumor cells. J Cell Biol, 1997. **137**(2): p. 469-79.

15.   Hengartner, M.O., *Apoptosis. DNA destroyers.* Nature, 2001. **412**(6842): p. 27.

16.   Cullum, B., Vo-Dinh, T., *The development of optical nanosensors for biological measurements.* Trends Biotechnol, 2000. **18**(9): p. 388-393.

17.   Hilf, R., Havens, JJ., Gibson, SL., *Effect of Aminolevulinic Acid on Protoporphyrin IX Accumulation in Tumor Cells Transfected with Plasmids Containing Porphobilinogen Deaminase DNA.* Photochemistry and Photobiology, 1999. **70**(3): p. 334-340.

18.   Sportsman, J., Wilson, GS., *Chromatographic properties of silica-immobilized antibodies.* Anal Chem, 1980. **52**(13): p. 2013-2018.

19.   Lin, J., Herron, J., Andrade, JD., IEEE Trans. Biomed. Eng, 1988. **35**: p. 466-471.

Part Six

Optical Nanosensor for Measuring Apoptosis in a Single Cell

6.0 Abstract

This work demonstrates the application of tetrapeptide-based optical nanosensors for bioanalysis and measuring apoptosis in single living cells. The activation of caspases is one of the earliest biomarkers of apoptosis, making caspases an early and ideal target for measuring apoptosis. Tetrapeptide-based optical nanosensors are a new class of biosensors that are capable of reporting the activity of specific caspases with high sensitivity and specificity. These properties make them promising for the detection and visualization of target caspases in single living cells during apoptosis. By detecting and identifying specific caspases, we confirm proteins involved in the regulation of apoptosis at the lowest possible levels. This article focuses on our recent research in exploring the potential of using tetrapeptide-based optical nanosensors for monitoring of apoptosis in single living cells.

6.1 Introduction

In the past decade, we have witnessed unprecedented advances in fields such as biosciences and optical biosensor technology. Although advances in each of these fields have provided exciting new insights and capabilities, it is the integration of these fields that revolutionary advances are being made. This work is an amalgamation of these fields and focuses on the development of novel optical nanosensors for single cell analysis. These biosensors are devices having cross-section of less than 250 nm and are capable of detecting a chemical or biological event using an optical signal. Furthermore, they are capable of monitoring single live

cells with the potential for subcellular analysis. They consist of nanoscale optical fiber equipped with covalently immobilized profluorescent tetrapeptide biorecognition molecules. At this scale, optical nanosensors are capable of playing a significant role in single cell analysis for example, analyzing proteins or protein-protein interactions within living cells, thereby enabling minimally invasive dynamic monitoring and visualization of molecular events within single living cells. This advantage is important because we can only obtain the most representative information of a cell as a system *in vivo* when the intracellular machinery is intact. In this context, optical nanosensors can play a significant role in helping to understand cell signaling and transduction and, in so doing, advancing the capability and technologies available for single cell analysis.

As we have gained a better understanding of bulk cell assays over time, and achieved a greater understanding of many macroscopic biological processes, we have been driven to rethink the purpose of an increasingly smaller entity -the single cell. Technologies for performing sensitive and selective biochemical analyses of single living cells still remain one of the key challenges in cell biology. Monitoring key cellular events and conquering functional biochemical pathways of a single cell, as heterogeneous as it is, would be an accomplishment in itself at this present time. This is mainly because of the scale required for analysis, and second, for the inability to achieve spatial and temporal resolution at the single cell level scale. The development of new technologies for single cell analysis is important because native biochemical events and reactions within living cells can be deciphered only if we have access to

their cellular distribution and location in a non-destructive and minimally invasive manner. Similarly, as our desire to visualize and decipher biochemical events progresses from bulk cell assays to single cell studies, high demands are placed on measurement technologies. Perhaps no recent technology has greater potential for this application than optical nanosensors. Previous work in our group has demonstrated the functionality and suitability of optical nanosensors for performing measurements in single living cells based on such figures of merit as sensitivity, reproducibility and selectivity [17-19]. These characteristics are important mainly for applications in areas of protein detection, protein-protein interaction profiling, and possibly measurement of critical cellular processes such as apoptosis.

The overall nature of apoptosis in bulk cell assays has been studied over time and is a fairly well understood process *in vitro* [108, 126, 129, 132]. It is also well known and widely accepted that cells in a population behave asynchronously to external stimuli such as chemically induced apoptosis. This is a result of the operation of the cell cycle, and the fact that the single-cell growth rates and cell division rates depend on cellular content; each cell contains different quantities of proteins, DNA, and RNA. Consequently, cell properties are distributed among the cells of the population leading to asynchronous behavior [133]. Hence, a cell population is a heterogeneous system and to study the nature of apoptosis *in vivo* in single living cells requires a measurement technology capable of performing minimally-to-non-invasive analysis of single cells with their biochemical pathways intact. Optical nanosensors are capable of minimally-to-non-invasive analysis of single living cells

as demonstrated in their application in the measurement of carcinogenic compounds within single living cells [17, 18]. This work will involve the application of a similar nanosensor though with a different type of immunochemical format. We adapted the previously used antibody-based optical nanosensor and developed a second-generation tetrapeptide-based optical nanosensor to measure apoptosis in single MCF-7 cells. The focus of this work is in exploring the potential of the second-generation tetrapeptide-based optical nanosensor for measuring apoptosis in single living MCF-7 cells.

In the classical model of apoptosis [134], caspases are divided into initiator caspases and effector caspases according to their function and their sequence of activation. Initiator caspases include caspase-8, -9, while effector caspases include, caspases-3, -6 and −7 [127, 135]. The activation of caspases is one of the earliest biomarkers of apoptosis making caspases an early and ideal target for measuring apoptosis. Apoptosis, or programmed cell death, is a mode of cell death characterized by specific morphological and biochemical features. It is both a normal and abnormal component of the development and health of multi-cellular organisms. Cells die in response to a variety of stimuli and during apoptosis they do so in a controlled, regulated fashion. This makes apoptosis distinct from another form of cell death called necrosis in which uncontrolled cell death leads to lysis of cells, inflammatory responses and, potentially, to serious health problems. Apoptosis, by contrast, is a process in which cells play an active role in their own death, which is why apoptosis is often referred to as cell suicide. Over the past decade, the importance of apoptosis

has been appreciated, and it is now thought to be the main mode of cell death in liver diseases, and neuronal cell death in neurodegenerative disease. Apoptosis has been found to have a role in one mechanism leading neuronal cell death associated with Alzheimer's disease and in liver disease. [86, 87, 136]. On the other hand, the loss of ability of cells to undergo apoptosis is one of the causes of uncontrollable cell growth leading to cancer. Tumor growth is determined not only by increased cell division, but also by decreased tumor-cell attrition. Therefore most, if not all, cancer cells acquire resistance to the various mechanisms that lead to apoptosis. In this context, optical nanosensors would open the way to monitoring caspase activity and in the process measure apoptosis in single living cells. This would be especially useful for a number of reasons. For example, we will be treating the cell as a system and not as a component of a system. Since the single cell is in its own capacity an individual entity, we will be able to obtain more representative information about intracellular biochemical events as opposed to if the cell was part of a population of cells. In addition, we will be analyzing proteins in their native form and environment. This is essential for cataloging the functional and hierarchical organization of proteins in various cellular pathways such as caspases in apoptosis. The results obtained in these experiments can be used to complement data obtained from *in vitro* studies or computational modeling studies.

Since caspases play a central role in the induction of apoptosis, tetrapeptide-based optical nanosensors were used to determine their role in response to a photodynamic therapy (PDT) agent, δ-aminolevulinic acid (ALA) in the well-

characterized human breast carcinoma cell line, MCF-7. MCF-7 cells were exposed to the photosensitizer ALA to explore ALA-PDT induced apoptosis by monitoring caspase-9 and caspase-7 activity. Caspase-9 and caspase-7 protease activity was assessed in single living MCF-7 cells with the known caspase-9 and caspase-7 substrates, Leucine-aspartic-histidine-glutamic acid 7-amino-4-methylcoumarin (LEHD-AMC) and aspartic-glutamic acid-valine-aspasrtic acid 7-amino-4-methylcoumarin (DEVD-AMC) respectively, covalently immobilized to the nanotips of optical nanosensors. Upon the induction of apoptosis, activated target caspases recognize the tetrapeptide sequence it specifically cleaves. The recognition of substrate by caspases is immediately followed by a cleavage reaction yielding the fluorescent AMC which can be excited with a Helium-Cadmium (HeCd) laser to generate a measurable fluorescence signal (Figure 6.1). By comparing the fluorescence signal generated from AMC within cells with activated caspases and from those with inactive caspases, we are able to successfully detect caspase activity within a single living MCF-7 cell.

6.2 Material and Methods

6.2.1 Chemicals and Reagents

δ-aminolevulinic acid (ALA), phosphate buffered saline (PBS), hydrochloric acid (HCl), nitric acid (HNO$_3$), Glycidoxypropyltrimethoxysilane (GOPS), 1,1'-Carbonyldiimidazole (CDI), and anhydrous acetonitrile were purchased from Sigma-Aldrich, St. Louis, MO. Caspase-9 substrate, Leucine-Glutamate-Histidine-Aspartate-

Induction of Apoptosis

Caspase activation

Si-GOPS-O-C-NH—**LEHD** — **AMC**

Si-GOPS-O-C-NH — **LEHD** **AMC**

λ_{em} 325nm

Si-GOPS-O-C-NH — **LEHD** — **AMC**

λ_{em} 380nm
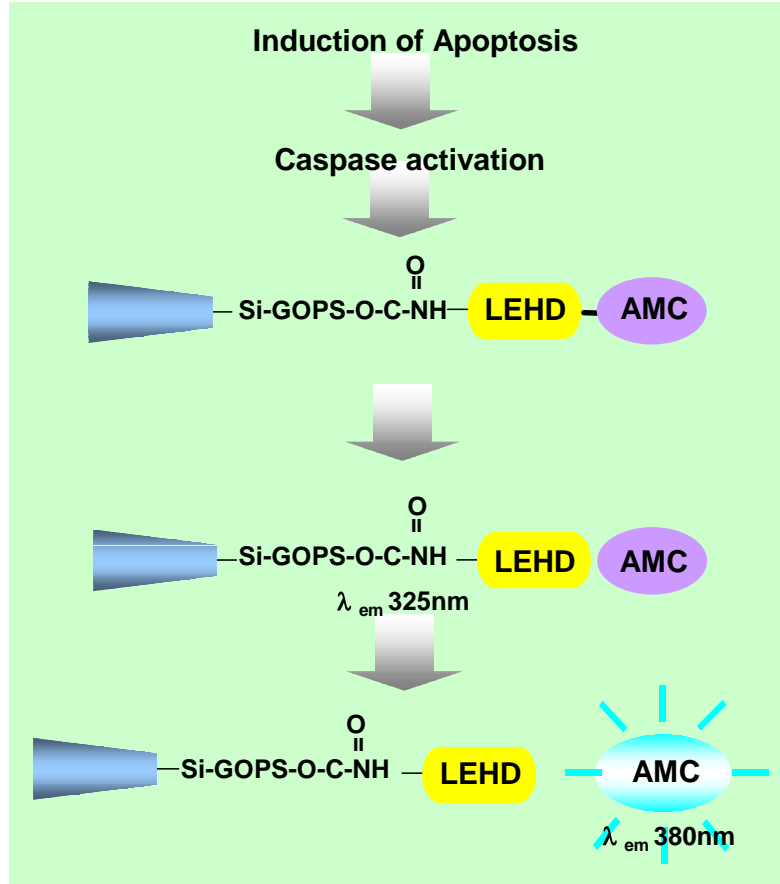
Figure 6.1 shows an illustration of caspase-9 substrate, Leucine-Glutamate-Histidine-Aspartate-7-amino-4-methylcoumarin (LEHD-AMC), and caspase-7 substrate, Aspartate-Glutamte-Valine-Aspartate-7-amino-4-methylcoumarin (DEVD-AMC) cleavage reaction. Free AMC can be excited and the fluorescence emitted is representation of the enzymatic cleavage reaction

7-amino-4-methylcoumarin (LEHD-AMC), Caspase-7 substrate, Aspartate-Glutamte-Valine-Aspartate-7-amino-4-methylcoumarin (DEVD-AMC), 2x reaction buffer, dithiothreitol (DTT), and dimethylsulfoxide (DMSO) were purchased from BD Biosciences, Palo Alto. CA.

6.2.2 Cell Lines

Human breast cancer cell line, MCF-7, was obtained from American Type Culture Collection (Rockville, MD, USA, Cat-no. HTB22). MCF-7 cells were grown in Dulbecco's Modified Eagle's Medium ((DMEM) (Mediatech, Inc., Herndon, VA)) supplemented with 1 mM L-glutamine (Gibco, Grand Island, NY) and 10% fetal bovine serum (Gibco, Grand Island, NY). Baseline cell culture was established in growth medium (described above) in standard T25 tissue culture flasks (Corning, Corning, NY). The flasks were incubated in a humidified incubator at 37°C, 5% CO_2 and 86% humidity. Cell growth was monitored daily by microscopic observation until a 60–70% state of confluence was achieved. The growth conditions were chosen so that the cells would be in log phase growth during photosensitizer treatment with ALA, but would not be so close to confluence that a confluent monolayer would form by the termination of the chemical exposure [18]. In preparation for experiments, cells were harvested from the T25 flasks and 0.1ml (10^5 cells/ ml) aliquots were seeded into 60 mm tissue culture dishes (Corning Costar Corp., Corning, NY) for overnight attachment. The MCF-7 cells were studied as four separate groups with the first group, Group I, being the experimental, exposed to 0.5 mM ALA for 3 h

followed by photoactivation ([+]ALA[+]PDT) [120, 129]. This involved incubating the cells at 37° C in 5% CO_2 for 3 h with 0.5mM ALA. Following incubation the MCF-7 cells were exposed to red light from a HeNe laser (λ 632.8 nm, <15mW, Melles Griot, Carlsbad, CA) positioned about 5.0 cm above the cells for five minutes at a fluence of 5.0 mJ/cm^2 to photoactivate ALA and subsequently induce apoptosis. The second and third groups, Group II and III respectively, served as the "treated control" and were exposed to 0.5 mM ALA for 3 hours without photoactivation ([+]ALA[-]PDT) and photoactivation without 0.5 mM ALA ([-]ALA[+]PDT]) respectively. The fourth group, Group IV was the "untreated control," which received neither ALA nor photoactivation ([-]ALA[-]PDT).

6.3 Experimental Protocol

6.3.1 Preparation of Enzyme Substrate-based Optical Nanosensors

Preparation of similar optical nanosensors has been previously described [16, 36, 61, 123]. Briefly, this process involved cutting and polishing plastic clad silica (PCS) fibers with a 600-μm-size core (Fiberguide Industries, Stirling, New Jersey). The fibers were pulled to a final tip diameter of 50 nm and then coated with ~100 nm of silver metal (99.999% pure) using a thermal evaporation deposition system (Cooke Vacuum Products, South Norwalk, CT) achieving a final diameter of 150 nm. The fused silica nanotips were acid-cleaned followed by several rinses with distilled water. Finally, the substrates were allowed to air dry at room temperature in a dust free environment. The nanotips were then silanized and treated with an organic

coupling agent, 10% Glycidoxypropyltrimethoxysilane (GOPS) in distilled water. The silanization agent covalently binds to the silica surface of the nanotips modifying the hydroxyl group to a terminus that is compatible with the organic cross-linking reagent, 1'1, Carbonyldiimidazole (CDI). The use of CDI for activation introducing an imidazole-terminal group was particularly attractive since the protein to be immobilized could be used without chemical modification. Proteins bound using this procedure remained securely immobilized during washing or subsequent manipulations in immunoassay procedures, as opposed to procedures that use adsorption to attach proteins [130, 131]. The silanized and activated nanotips for measuring caspase-9 activity were immersed in a solution containing DMSO, 2X reaction buffer, PBS, and LEHD-AMC, and allowed to incubate for 3 h at 37°C, while those for measuring caspase-7 activity were immersed in a solution containing DMSO, 2X reaction buffer, PBS, and DEVD-AMC, and allowed to incubate for 3 h at 37°C.

6.3.2 Measurement System and Procedure

A schematic representation of the experimental setup used in this work is shown in Figure 6.2 .The components included a HeCd laser (Omnichrome, <5mW laser power) for excitation, an optical fiber for delivery of excitation light to the optical nanosensor, a Nikon Diaphot 300 inverted fluorescence microscope (Nikon, Inc., Melville, NY), a photon counting photomultiplier tube (PMT) and a PC for data

(ii)

15.0kV x SE(M)　　10μm

Tip size ~ 150 nm

HeCd Laser

Nanosensor

197319792003

HP Universal counter

Data PC

High voltage

PMT

Inverted microscope

(i)
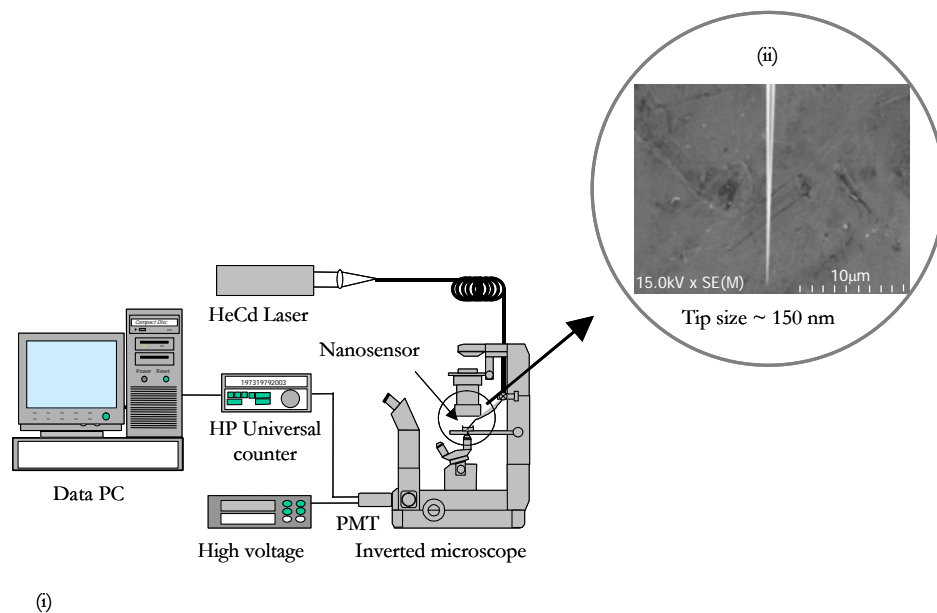
Figure 6.2 (i) Laser-induced fluorescence measurement system used for fluorescence signal acquisition, data recording and processing. (ii) Scanning electron micrograph of optical nanosensor after coating with ~100nm of silver metal.

acquisition and processing. This experimental set-up, used to probe single cells, was adapted for this purpose from a standard micromanipulation and microinjection apparatus. The Nikon Diaphot 300 inverted microscope was equipped with a Diaphot 300/Diaphot 200 Incubator to maintain the cell cultures at 37°C on the microscope stage, during these experiments. The micromanipulation equipment consisted of MN-2 (Narishige Co. Ltd., Tokyo, Japan) Narishige three-dimensional manipulators for coarse adjustment, and Narishige MMW-23 three-dimensional hydraulic micromanipulators for fine adjustments. The optical nanosensor was gently mounted on a micropipette holder (World Precision Instruments, Inc., Sarasota, FL). The 325 nm laser line of a HeCd laser was focused onto a 600-μm-delivery fiber that is terminated with a subminiature A (SMA) connector. The enzyme substrate-based optical nanosensor was coupled to the delivery fiber through the SMA connector and secured to a Nikon inverted microscope with micromanipulators. To record the fluorescence generated by AMC molecules at the nanotips, a Hamamatsu PMT detector assembly (HC125-2) was mounted in the front port of the Diaphot 300 microscope. The fluorescence emitted by AMC from the measurement made using single live cells was collected by the microscope objective and passed through a 330-380 nm filter set and then focused onto a PMT for detection. The output from the PMT was recorded using a universal counter interfaced to a personal computer (PC) with custom-designed LabView software for data treatment and processing.

6.3.3 In Vitro Determination of Caspase Activity

After incubation using the following treatment groups, group (I) - [+]ALA[+]PDT, group II -[+]ALA[-]PDT, group III -[-]ALA[+]PDT, and group IV - [-]ALA[-]PDT, MCF-7 cells were washed with PBS solution, pH 7.4, and then resuspended in lysis buffer (100 m*M* HEPES, pH 7.4, 10% sucrose, 0.1% 3-[(3-cholamidopropyl)-dimethylammonio]-1-propanesulfonate (CHAPS), 1 m*M* EDTA, 10 m*M* dithiothreitol (DTT), 1 m*M* phenylmethylsulphonyl fluoride (PMSF), 10 mg/ml pepstatin, 10 mg/ml leupeptin) and left on ice for 45 minutes. The cells were then repeatedly passed through a syringe with a 25-gauge needle until most of the cell membrane was disrupted, and centrifuged at 1500 RPM for 10 min. Activity of caspases was measured using fluorogenic substrate peptides; LEHD-AMC for caspase-9 and DEVD-AMC for caspase-7. The release of AMC was measured after incubating optical nanosensors in picofuge tubes containing the cell lysates from the various treatment groups and using a HeCd laser (excitation 325 nm) to excite AMC. Caspase activity was expressed as fluorescence intensity of AMC as a function of equivalent nanomoles of LEHD-AMC and DEVD-AMC respectively.

We plotted the results of the *in vitro* measurement of caspase-9 and caspase-7 activity. The curves for each fluorescent measurement of AMC were plotted for each as a function of AMC concentration. Caspase-9 activity was determined by incubation of optical nanosensors with the substrate LEHD-7-amino-4-methylcoumarin (AMC) in cell lysate ($\sim 10^5$ cells) obtained from the following treatment groups; group I, II, III and IV, described earlier in the article. The release of

AMC was measured after excitation using HeCd laser (325 nm) and collecting the fluorescence signal using a 380 nm longpass filter. The peak emission wavelength of AMC is about 440 nm. Likewise, Caspase-7 activity was determined by incubation in cell lysate ($\sim 10^5$ cells) obtained from the following treatment groups I, II, III, and IV. The release of AMC was measured after excitation using a HeCd laser (325 nm) and collecting the fluorescence signal using a 380 nm longpass filter.

6.3.4 In Vivo Determination of Caspase Activity

Using the treatment group I and the control group IV from above, replicate experiment and control measurements were conducted to measure caspase-9 and caspase-7 activity *in vivo*. Determination of the presence or absence of caspase-9 and -7 activities using the optical nanosensor was carried out using the following procedure. A culture dish with sparsely distributed MCF-7 cells was placed on the pre-warmed microscope stage set at 37°C. The optical nanosensor, mounted on a micropipette holder of a micromanipulation system, was moved into position, in the same plane as the cells, using bright-field phase contrast microscopic illumination, so that the tip was just outside of the cell to be probed. The total magnification was 600×. The optical nanosensor was gently micromanipulated into the cell using the hydraulic fine adjustments, past the cell membrane and extending a short way into the cytoplasm. During these micromanipulations, great care was taken not to penetrate the nuclear envelope and compromise the integrity of the nucleus. Room light and microscope illumination light were switched-off; the laser shutter opened, and laser

light allowed illuminating the optical nanosensor with excitation light being transmitted into the nanotip. First, a signal reading was taken with the nanosensor inside the cell with the laser shutter closed in order to record the dark signal. After five min, the laser shutter was opened, allowing the excitation light to be transmitted to the nanosensor tip, and fluorescence readings were recorded. Figure 6.3 (i-iv) shows images illustrating intracellular measurements performed in a single MCF-7 cell using micromanipulation. Once inside the cell, the nanosensor detects and identifies the activity of caspase-9. The fluorescence signal generated is collected by the objective, and passes through spectral and spatial filters before detection with a photomultiplier tube (PMT). The PMT signal is amplified and recorded via a universal counter on a personal computer. Data acquisition and recording are controlled using a LabView custom-written program. Additionally, the entire experiment is imaged using a CCD camera coupled to the side port of the Nikon inverted fluorescence microscope to verify that individual cells are probed. A typical experiment measurement takes ~ 5 minutes.

6.4 Results and Discussion

The examination of caspase-9 and caspase-7 activity was first performed in vitro using cell lysate, and in vivo, within single MCF-7 cells using optical nanosensors. Caspase-9 cleaves the substrate tetrapeptide (LEHD-AMC) between D and AMC, releasing the fluorophore AMC that is measured upon excitation by the
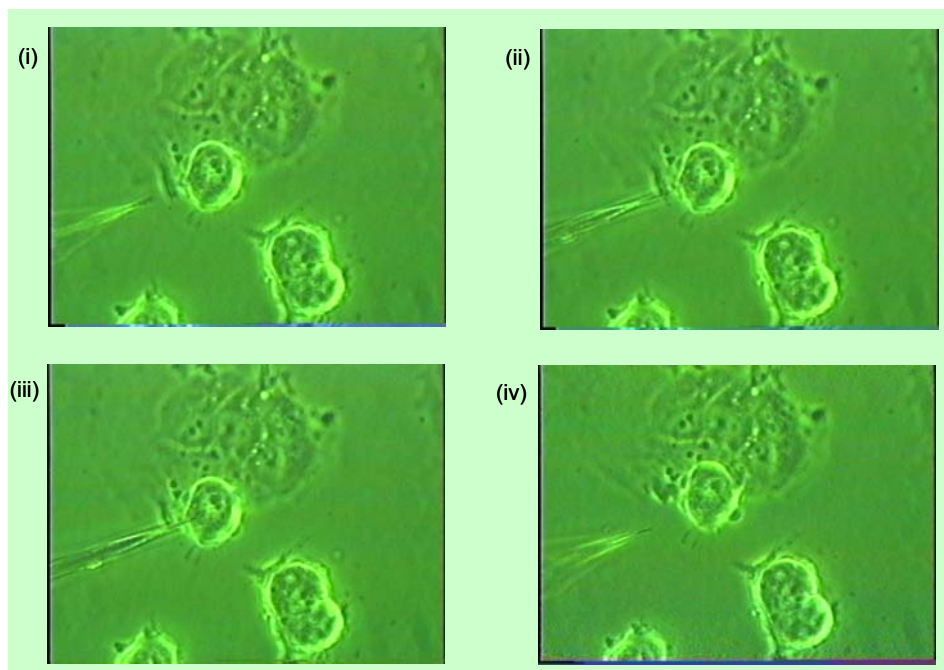
Figure 6.3: shows digital images of the single cell measurement procedure. LEFT TO RIGHT, (i) optical nanosensor outside MCF-7 cell (ii) right before insertion into MCF-7 cell (iii) inserted into MCF-7 cell, and (iv) extracted from MCF-7 cell

HeCd laser. Similarly, caspase-7 cleaves the substrate tetrapeptide (DEVD-AMC) between D and AMC, releasing the same fluorophore AMC for measurement. Apoptotic cells containing activated caspase-9 or caspase-7 yield a fluorescence emission as opposed to non-apoptotic cells, which do not yield a fluorescent signal. Briefly, for the in vitro study, to measure caspase-9 and caspase-7 activity, MCF-7 cells were harvested and centrifuged at 1500 RPM for 10 minutes. The cell suspension ($\sim 10^5$ cells) was mixed with PBS followed by addition of 1:10, 1:20, 1:100 and 1:200 dilutions of 1mM LEHD-AMC and DEVD-AMC respectively, to each cellular reaction. The liberated AMC fluorescence was measured using tetrapeptide-based optical nanosensors.

Figure 6.4 shows the results of the *in vitro* study of caspase-9 and caspase-7 involving the treatment groups, Group I and Group IV. These results show a disparity of an order of magnitude in the mean fluorescent intensity measurements we observed for Group I and IV. This difference is significant enough to determine caspase-9 and caspase-7 activity *in* vitro. Group II and III which were the treated control groups had mean fluorescent measurements similar to the control, Group IV. This result was expected because it is the collective effect of ALA and photoactivation that results in the induction of apoptosis and neither ALA nor photoactivation alone. For the *in vivo* studies, caspase-9 activities were analyzed in ALA-PDT treated cells (group I) by measuring the fluorescence signal from AMC generated after the cleavage of the peptide substrate LEHD-AMC. Likewise, the same was done for the control groups
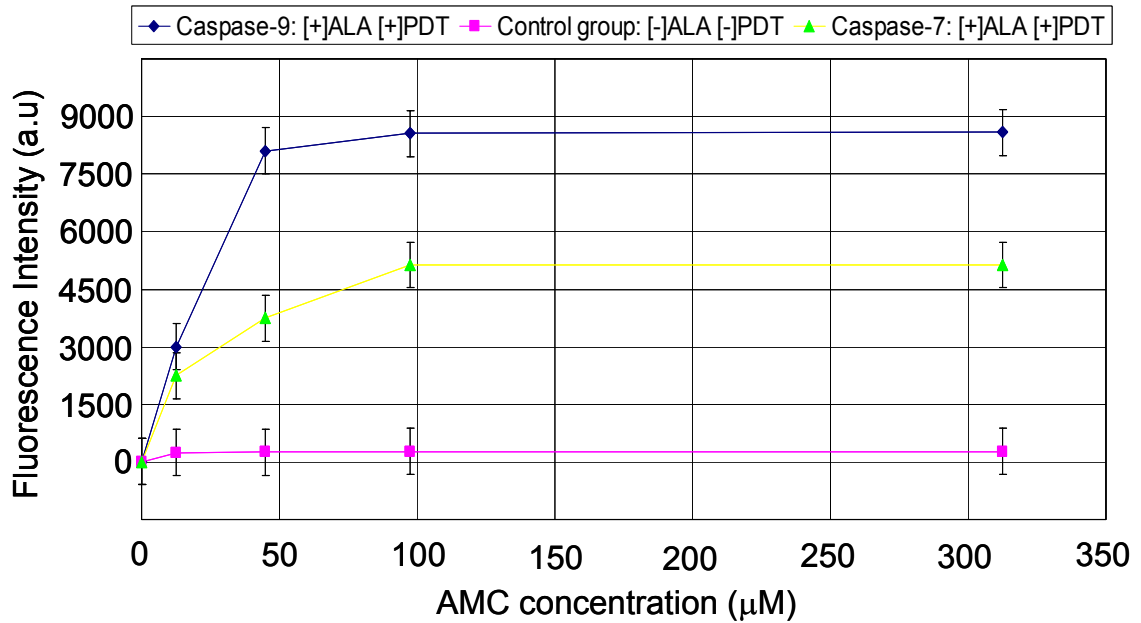
Figure 6.4 shows the results of the *in vitro* study of caspase-9 and caspase-7 involving the treatment groups, Group I: [+]ALA [+]PDT, and Group IV: [-]ALA [-]PDT. These results represent Caspase-9 and Caspase-7 activity of MCF-7 cells with aminolevulinic acid (ALA) induced apoptosis. Following ALA treatment and apoptosis induction, MCF-7 cells were harvested and analyzed for caspase activity.

(II, III and IV) of cells which received either [+]ALA[-]PDT, [-]ALA[+]PDT or [-]ALA[-]PDT. The fluorescent intensity measurements obtained for these treatment groups were then compared. As shown in <u>Figure 6.5</u>, there was no level of LEHD-AMC cleavage activity was detected for the untreated cells, [-]ALA[-]PDT. Likewise, the same was observed for the treated control groups, [+]ALA[-]PDT and [-]ALA[+]PDT. However, in treated cells, [+]ALA[+]PDT, significant LEHD-AMC cleavage activity was detected via the measurement of AMC fluorescence. As shown in <u>Figure 6.5</u>, the initiator substrates (LEHD-AMC) of caspase-9 are cleaved into the fluorogenic AMC forms in cells treated with ALA-PDT. This demonstrates the involvement of caspase-9, which cleaves after aspartic acid residue, in mediating apoptosis. The results obtained here demonstrated the presence of active pathways of caspase-9 during ALA-PDT induced apoptosis in MCF-7 cells. The fluorescence signals obtained from the cells that were both incubated with ALA and photoactivated were significantly higher than the signals obtained from the untreated control and the two treated control groups. Statistical analysis was performed on the three sets of results. The mean value of this analysis revealed that the fluorescence signal obtained using optical nanosensors used to probe the experimental group of cells (Group I) was about 4.59 ($\pm$ 0.02). The mean value of these analyses revealed that the fluorescence signal obtained using optical nanosensors used to probe the control group of cells (Group II, III and IV) was about 3.56 ($\pm$ 0.02). The mean value of this analysis revealed that the fluorescence signal obtained using the nanosensors used to probe

Figure 6.5 shows the result of *in vivo* measurement of caspase-9 activity. The Experiment type refers to the four different treatment groups, Group I [+]ALA[+]PDT, Group II [+]ALA[-]PDT, Group III [-]ALA[+]PDT, Group IV [-]ALA[-]PDT. Each bar represents an average of three intracellular measurements of caspase-9 activity in MCF-7 cells done in triplicate. The error bars shown represent a 95% confidence interval (CI).

cells in Group I was up to an order of magnitude higher than the signal obtained by nanosensors used to probe the control (Group IV), untreated (Group II) and treated (Group III) control cell groups. A larger mean value for the experimental group confirms the detection of AMC and hence the detection of caspase-9 activity.

For the *in vivo* studies to assay caspase-7 activity, MCF-7 cells were treated with ALA-PDT, and caspase-7 activity was monitored by measuring the fluorescence generated by AMC after cleavage of DEVD-AMC. After exposure to ALA- PDT, AMC fluorescence was detected and measured using optical nanosensors. As shown in Figure 6.6, in untreated cells, no level of DEVD-AMC cleavage activity was detected with [+]ALA[-]PDT, [-]ALA[+]PDT or [-]ALA[-]PDT. However, a significant DEVD-AMC cleavage activity via the detection of AMC fluorescence was observed after [+]ALA[+]PDT treatment. Figure 6.6 also shows the background-subtracted results of intracellular measurements performed with nanosensors on two treated control groups (Group II and III) of MCF-7 cells. The first group was treated with [+]ALA[-]PDT, while the second was treated with [-]ALA[+]PDT. These results were similar on average meaning that neither of the two treated control groups were capable of inducing apoptosis. This is in total agreement with the expected outcome of this experiment, as photodynamic therapy is a cooperative effort of the photosensitizer and light. When comparing these results to those obtained from the experimental group, [+]ALA[+]PDT, the fluorescence intensity was almost an order of magnitude lower than that of the experimental group. These results clearly demonstrate the determination of caspase-7 activity within single living cells.
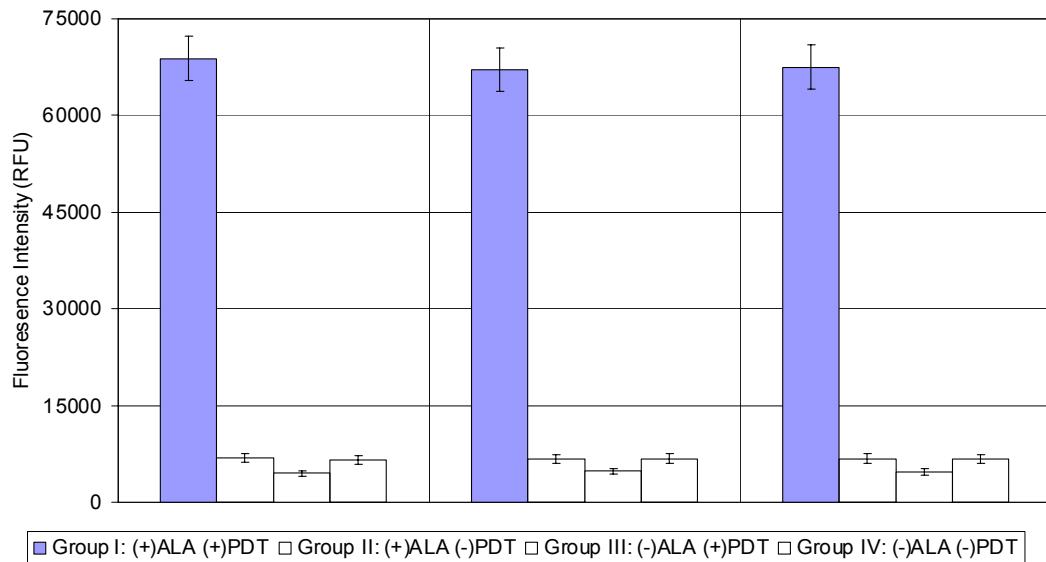
211
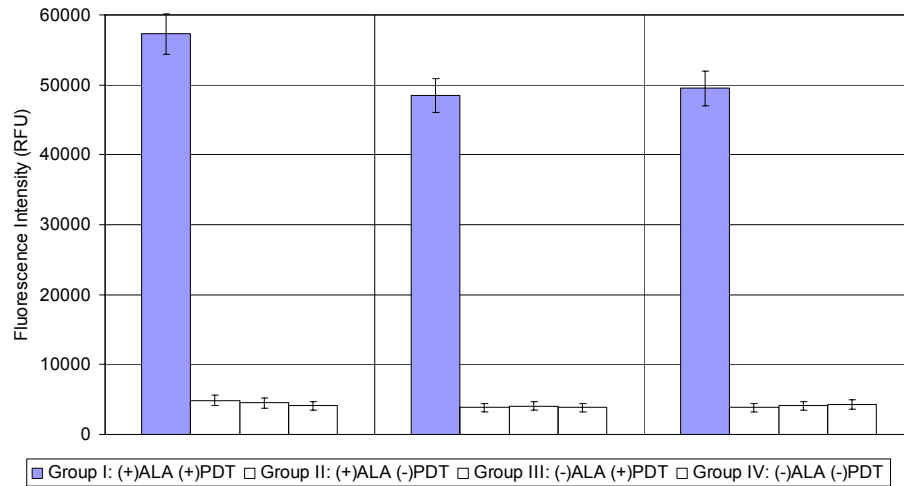
Figure 6.6: shows the result of the *in vivo* measurement of caspase-7 activity. The Experiment type refers to the four different treatment groups, Group I [+]ALA[+]PDT, Group II [+]ALA[-]PDT, Group III [-]ALA[+]PDT, Group IV [-]ALA[-]PDT. Each bar represents an average of three intracellular measurements of caspase-7 activity in MCF-7 cells done in triplicate. The error bars shown represent a 95% confidence interval (CI).

6.5 Summary

We successfully prepared tetrapeptide-based optical nanosensors using a covalent coupling technique to immobilize profluorescent substrates onto nanotips and demonstrated their application in the determination of the cleavage products of LEHD-AMC and DEVD-AMC, AMC, in single living MCF-7 cells. The presence and detection of cleaved fluorogenic AMC in single live MCF-7 cells as a result of this design is representative of caspase-9 and -7 activity, hallmarks of apoptosis or programmed cell death [127]. These results indicate that AMC, and hence apoptosis, can be monitored and measured using optical nanosensors within single living cells during apoptosis. These results also demonstrate the capability of performing measurements inside single living cells consequently with the potential application in protein detection and protein-protein profiling in cellular biochemical pathways.

Due to its nanoscale size, the optical nanosensor does not compromise the integrity of the cell when performing intracellular analysis [123]. This advantage is evident this work which demonstrates the capability of optical nanosensors to study cells without having to disrupt the physiological make-up, thereby not interfering with cellular biochemistry. Mechanical manipulation can lead to cell disruption prior to sampling and this may interfere with measurements of cellular biochemistry. With the optical nanosensors, absence of cell manipulation prior to measurement results in no effects on the cell at the time of sampling. Tetrapeptide-based optical nanosensors are extremely sensitive and have very specific activities, since a single enzyme along

with its respective cofactor or coenzyme can catalyze many reactions and in the process produce a sufficient quantity of the fluorogenic reaction product AMC. This feature together with excitation and detection in the near-field of the optical nanosensor are important because they underline the sensitivity and spatial selectivity conferred by the operating principle of the nanosensor in the sense that only the AMC produced will be excited in the near field of the optical nanosensor. An additional feature of the nanosensor is its biochemical selectivity. Selectivity is dependent upon the selective cleavage capabilities for specific sequences by either caspase-9 or caspase-7.

Tetrapeptide-based optical nanosensors for investigating intact living cells hold promise for minimally invasive dynamic analyses of proteins in biochemical pathways within single living cells. Optical nanosensors provide a new method in cell-based assays offering highly miniaturized, hands-on, nano-scaled devices that make cell-based analysis accessible at the single cell level. Future work will involve studies that will attempt to diversify the application of the optical nanosensor for analysis of protein-protein interactions and similar analyses of other proteins involved in cellular biochemical pathways.

References

1.   Zandonella, C., *Cell Nanotechnology: The Tiny Toolkit.* Nature, 2003. **423**: p. 10-12.
2.   Behbehani, M., *Cell Physiology Source Book*, ed. N. Sperelakis. 1995, San Diego: Academic Press. 490-494.
3.   Morris, C., *Cell Physiology Source Book*, ed. N. Sperelakis. 1995, San Diego: Academic press.
4.   Tsien, R., *Intracellular signal transduction in four dimensions: from molecular design to physiology.* Am J Physiol Cell Physiol, 1992. **263**: p. C723-C728.
5.   Giuliano, K., Post, PL., Hahn, KM., Taylor, DL., *Fluorescent protein biosensors: measurement of molecular dynamics in living cells. .* Annu Rev Biophys Biomol Struct., 1995. **24**: p. 405-34.
6.   Jankowski, J., Tratch, S., Sweedler, JV., *Assaying single cells with capillary electrophoresis.* Trends Anal. Chem., 1995. **14**: p. 170-176.
7.   Luzzi, V., Lee, C.L., Allbritton, N.L., *Localized sampling of cytoplasm from Xenopus oocytes for capillary electrophoresis.* Anal Chem, 1997. **69**(23): p. 4761-4767.
8.   Li, H., Sims, C.E., Wu, H., Allbritton, N.L., *Spatial Control of Cellular Measurements with the Laser-Micropipet.* Anal. Chem., 2001. **73**.
9.   Tan, W., Shi, ZY., Smith, S., Birnbaum, D., and Kopelman, R., *Submicrometer Intracellular Chemical Optical Fiber Sensors.* Science, 1992. **258**(5083): p. 778-781.
10.   Tan, W., Shi, ZY., Smith, S., and Kopelman, R., *Development of Submicron Chemical Optic Sensors.* Anal. Chem, 1992. **64**(23): p. 2985-2990.
11.   Munkholm, C., D.R. Walt, and F.P. Milanovich, *Preparation of Co2 Fiber Optic Chemical Sensor.* Abstracts of Papers of the American Chemical Society, 1987. **193**: p. 183-ANYL.
12.   Munkholm, C., D.R. Parkinson, and D.R. Walt, *Intramolecular Fluorescence Self-Quenching of Fluoresceinamine.* Journal of the American Chemical Society, 1990. **112**(7): p. 2608-2612.
13.   Tan, W.H., et al., *Submicrometer Intracellular Chemical Optical Fiber Sensors.* Science, 1992. **258**(5083): p. 778-781.
14.   Sumner, J., Aylott, JW., Monson, E., Kopelman, R., *A fluorescent PEBBLE nanosensor for intracellular free zinc.* Analyst, 2002. **127**(1): p. 11-16.
15.   Alarie, J.P. and T. VoDinh, *Antibody-based submicron biosensor for benzo a pyrene DNA adduct.* Polycyclic Aromatic Compounds, 1996. **8**(1): p. 45-52.
16.   Vo-Dinh, T., Alarie, JP., Cullum, BM., Griffin, GD., *Antibody-based nanoprobe for measurement of a fluorescent analyte in a single cell.* Nat Biotechnol, 2000. **18**(7): p. 764-767.
17.   Kasili, P.M., Cullum, B.M., Griffin, G.D., and Vo-Dinh, T., *Nanosensor for In-Vivo Measurement of the Carcinogen Benzo [a] Pyrene in a Single Cell.* Journal of Nanoscience and Nanotechnology, 2003. **2**(6): p. 653-658.

18. Cullum, B., Griffin, GD., Miller, GH., Vo-Dinh, T., *Intracellular measurements in mammary carcinoma cells using fiber-optic nanosensors.* Anal Biochem, 2000. **277**(1): p. 25-32.

19. Vo-Dinh, T., and Cullum, BM., *CRC Handbook for Biomedical Photonics.* Nanosensors for Single Cell Analysis, ed. T. Vo-Dinh. 2003, Newyork: CRC Press. 14.

20. Cullum, B.M., et al., *Intracellular measurements in mammary carcinoma cells using fiber-optic nanosensors.* Analytical Biochemistry, 2000. **277**(1): p. 25-32.

21. Cullum, B.M. and T. Vo-Dinh, *The development of optical nanosensors for biological measurements.* Trends in Biotechnology, 2000. **18**(9): p. 388-393.

22. Cullum, B.M. and T. Vo-Dinh, *Optical nanosensors and biological measurements.* Biofutur, 2000. **2000**(205): p. A1-A6.

23. Vo-Dinh, T.G., G. D.; Alarie, J. P.; Cullum, B. M.; Sumpter, B. and Noid, D., *Development of Nanosensors and Bioprobes.* J. Nanoparticle Research, 2000. **2**: p. 17.

24. Vo-Dinh, T., et al., *Antibody-based nanoprobe for measurement of a fluorescent analyte in a single cell.* Nature Biotechnology, 2000. **18**(7): p. 764-767.

25. Cullum, B., Vo-Dinh, T., *The development of optical nanosensors for biological measurements.* Trends Biotechnol, 2000. **18**(9): p. 388-393.

26. Vo-Dinh, T., et al., *Antibody-Based Fiberoptics Biosensor for the Carcinogen Benzo(a)Pyrene.* Applied Spectroscopy, 1987. **41**(5): p. 735-738.

27. Aylott, J., *Optical nanosensors - an enabling technology for intracellular measurements.* Analytst, 2003. **128**(4): p. 309-312.

28. S, U., *Fluorescence Assay in Biology and Medicine.* Vol. 2. 1969, New York, San Francisco, London: Academic Press. 659.

29. http://www.pti-nj.com/, *Fluorescence: The Phenomenon.* 1997, Photon Technology International.

30. Udenfriend, S., *Fluorescence Assay in Biology and Medicine.* Vol. 2. 1969, New York, San Francisco, London: Academic Press. 659.

31. Harrick, N., *Internal Reflection Spectroscopy.* 1967, New York: John Wiley & Sons, Inc.

32. Kröger, K., Jung, A., Reder, S., Gauglitz, G., *Versatile biosensor surface based on peptide nucleic acid with label free and total internal reflection fluorescence detection for quantification of endocrine disruptors.* Analytica Chimica Acta, 2002. **469**(1): p. 37-49.

33. Axelrod, D., *Total Internal Reflection Fluorescence Microscopy in Cell Biology.* Traffic, 2001. **2**(11): p. 764-774.

34. Potyrailo, R., Hobbs, SE., Hieftje, GM., *Optical waveguide sensors in analytical chemistry: today's instrumentation, applications and trends for future development.* FRESENIUS JOURNAL OF ANALYTICAL CHEMISTRY, 1998. **362**(4): p. 349-373.

35.   Guo, Z., Guilfoyle, RA., Thiel, AJ., Wang, R., and Smith, LM., *Direct fluorescence analysis of genetic polymorphisms by hybridization with oligonucleotide arrays on glass supports. Nucleic Acids Res., 22, 5456–5465.* Nucleic Acids Res., 1994. **22**: p. 5456–5465.

36.   Alarie, J., VoDinh, T., *Antibody-based submicron biosensor for benzo[a]pyrene DNA adduct.* Polycyclic Aromatic Compounds, 1996. **8**(1): p. 45-52.

37.   Kumar, A., Larsson, O., Parodi, D., and Liang, Z., *Silanized nucleic acids: a general platform for DNA immobilization.* Nucleic Acids Res., 2000. **28**(14): p. 71e-71.

38.   Lamture, J., Beattie, KL., Burke, BE., Eggers, MD., Ehrlich, DJ., Fowler, R., Hollis, MA., Kosicki, BB., Reich, RK., Smith, SR., *Direct detection of nucleic acid hybridization on the surface of a charge coupled device.* Nucleic Acids Res., 1994. **22**(11): p. 2121-2125.

39.   Alarie, J., Sepaniak, MJ., Vo-Dinh T., *Evaluation of Antibody Immobilization Techniques for Fiber Optic-based Fluoroimmunosensing.* Anal. Chim Acta, 1990. **229**(2): p. 169-176.

40.   Tromberg, B., Sepaniak, MJ., Alarie, JP., Vo-Dinh, T., Santella, RM., *Development of Antibody-Based Fiber-Optic Sensors for Detection of Benzo[a]Pyrene Metabolite.* Anal. Chem., 1988. **60**(18): p. 1901-1908.

41.   Dakubu, S., Ekins, R., Jackson, T., Marshall, NJ., *Chapter 4*, in *Practical Immunoassays: The State of the Art.*, W. Butt, Editor. 1984, Dekker: New York.

42.   Wessendorf, M., Brelje, T. C., *Which fluorophore is brightest? A comparison of the staining obtained using*

fluorescein, tetramethylrhodamine, lissamine rhodamine, texas red, and cyanine 3.18. Histochemistry, 1992. **98**: p. 81-85.

43.   Harms, G.S., Sonnleitner, M., Schütz, GJ., and H.J. Gruber, and Schmidt, T., *Molecule Anisotropy Imaging.* Biophys. J., 1999. **77**: p. 2864-2870.

44.   Sako, Y., Minoguchi, S., and Yanagida, T., *Single molecule imaging of EGFR signalling on the surface of living cells.* Nature Cell Biol., 2000. **2**: p. 168-172.

45.   Schütz, G.J., Kada, G., Pastushenko, VP., and and H. Schindler, *Properties of lipid microdomains in a muscle cell membrane visualized by single molecule microscopy.* EMBO J., 2000a. **19**: p. 892-901.

46.   Hoh, J., and Hansma, PK., *Atomic force microscopy for high resolution imaging in cell biology.* Trends Cell Biol., 1992. **2**: p. 208-213.

47.   Binnig, G., Quate, CF., and Gerber, C., *Atomic Force microscope.* Phys. Rev. Lett., 1986. **56**: p. 930-933.

48.   Turner, A., Karube, I., Wilson, GS., ed. *Biosensors – Fundamentals and Applications.* 1987, Oxford University Press: Oxford.

49.   Schmid, R., and Karube, I., *Biotechnology*, in *Biosensors and Bioelectronics*, H. Rehm, and Reed G., Editor. 1998, VCH Verlagsgesellschaft: Weinheim-Basel-Cambridge-Newyork.

50.   Updike, S., and Hicks, GP., *The Enzyme Electrode.* Nature, 1967. **214**: p. 986-988.

51.   Guilbault, G., and Montalvo, JGJ., *A Urea specific enzyme electrode.* Journal of The American Chemical Society, 1969. **9**: p. 2164-2167.

52.   Bilitewski, U., and Schmid, RD. *Alcohol determination by modified carbon paste electrodes*. in *The GBF International Workshop on Biosensors*. 1989. Braunschweig, Germany.

53.   Kulys, J., Bilitweski, U., and Schmid, RD. *Biosensors based on chemically modified electrodes*. in *The GBF International Workshop on Biosensors*. 1989. Braunschweig, Germany.

54.   Robinson, G., *Optical Immunosensors: An Overview*, in *Advances in Biosensors*, T. APF, Editor. 1991, JAI Press Inc: London. p. 230-252.

55.   B.M. Cullum , T.V.-D., *The development of optical nanosensors for biological measurements.* Trends Biotechnol, 2000. **18**(9): p. 388-393.

56.   M. Shortreed, R.K., M. Kunh, B. Hoyland, *Fluorescent fiber-optic calcium sensor for physiological measurements.* Anal Chem., 1996. **68**(8): p. 1414-8.

57.   S.L. Barker, R.K., Anal Chem., 1998. **70**(23): p. 49062-6.

58.   M. Brasuel, R.K., T.J. Miller, R. Tjalkens, M.A. Philbert, *Fluorescent nanosensors for intracellular chemical analysis: decyl methacrylate liquid polymer matrix and ion-exchange-based potassium PEBBLE sensors with real-time application to viable rat C6 glioma cells.* Anal Chem., 2001. **73**(10): p. 2221-8.

59.   H. A. Clark, R.K., R. Tjalkens, M.A. Philbert, *Optical nanosensors for chemical analysis inside single living cells. 2. Sensors for pH and calcium and the intracellular application of PEBBLE sensors.* Anal Chem, 1999. **71**(21): p. 4837-43.

60.   H. A. Clark, M.M., M.A. Philbert, R. Kopelman, *Optical nanosensors for chemical analysis inside single living cells. 1. Fabrication, characterization, and methods for intracellular delivery of PEBBLE sensors.* Anal Chem, 1999. **71**(21): p. 4831-6.

61.   T. Vo-Dinh, J.P.A., B.M. Cullum, G.D. Griffin, *Antibody-based nanoprobe for measurement of a fluorescent analyte in a single cell.* Nat Biotechnol, 2000. **18**(7): p. 764-767.

62.   B.M. Cullum , G.D.G., G.H. Miller, T. Vo-Dinh, *Intracellular measurements in mammary carcinoma cells using fiber-optic nanosensors.* Anal Biochem, 2000. **277**(1): p. 25-32.

63.   T. Vo-Dinh, B.M.C., G.D. Griffin, Radiat. Res, 2001. **156**(4): p. 437-438.

64.   Vo-Dinh, T., *Chemical Analysis of Polycyclic Aromatic Compounds*. 1989, New York: Wiley.

65.   http://www.city.toronto.on.ca/health/pdf/cr_appendix_b_pah.pdf.

66.   A.V. Castellano, J.L.C., M.C. Hernandez, P.S. Aleman, J.C. Jimenez, *Benzo(a)pyrene levels in Jinamar Valley: preliminary results.* AFINIDAD, 1999. **56**(480): p. 113-120.

67. L. Shriver-Lake, B.D., R. Edelstein, K. Breslin, S. Bhatia, F. Ligler, *Antibody immobilization using heterobifunctional crosslinkers.* Biosen. and Bioelect., 1997. **12**(11): p. 1101-1106.

68. J.R. Sportsman, G.S.W., Anal Chem, 1980. **52**: p. 2013-2018.

69. J.H. Lin, J.H., J.D. Andrade, IEEE Trans. Biomed. Eng, 1988. **35**: p. 466-471.

70. G.D. Griffin, K.R.A., R.N. Thomason, C.M. Murchison, M. Mcmanis, P.G. Wecker, T. Vo-Dinh. *Polynuclear Aromatic Hydrocarbons.* in *Polynuclear Aromatic Hydrocarbons, Tenth International Symposium.* 1985. Columbus, OH: Battelle Press.

71. T. Kuljukka-Rabb, K.P., S. Isotalo, S. Mikkonen, L. Rantanen, K. Savela, *Time- and dose-dependent DNA binding of PAHs derived from diesel particle extracts, benzo[a]pyrene and 5-methylchrysene in a human mammary carcinoma cell line (MCF-7).* Mutagenesis, 2001. **16**(4): p. 353-358.

72. D.C. Spink, B.H.K., M.M. Hussain, B.C. Spink, S.J. Wu, N. Liu, R. Pause, L.S. Kaminsky, *Induction of CYP1A1 and CYP1B1 in T-47D human breast cancer cells by benzo[A]pyrene is diminished by arsenite.* DRUG METABOLISM AND DISPOSITION, 2002. **30**(3): p. 262-269.

73. Sethi, R., *Transducer Aspasects of Biosensors.* Biosensors & Bioelectronics, 1994. **9**: p. 243-264.

74. Hall, E., *Biosensors.* 1990, Buckingham: Open University Press.

75. Byfield, M., Abuknesha, RA., *Biochemical Aspects of Biosensors.* GEC J. Res., 1991. **9**: p. 97 – 117.

76. Vo-Dinh, T., et al., *Evaluation of the Fiberoptic Antibody-Based Fluoroimmunosensor for DNA Adducts in Human Placenta Samples.* Clinical Chemistry, 1991. **37**(4): p. 532-535.

77. Vo-Dinh, T.G., G. D. and Sepaniak, M. J., in *Fiber Optic Chemical Sensors and Biosensors*, O.S. Wolfbeis, Editor. 1991, CRC Press: Boca Raton. p. 217 - 257.

78. Kienle, S., et al., *Electropolymerization of a phenol-modified peptide for use in receptor-ligand interactions studied by surface plasmon resonance.* Biosensors & Bioelectronics, 1997. **12**(8): p. 779-786.

79. Pathak, S.S. and H.F.J. Savelkoul, *Biosensors in immunology: the story so far.* Immunology Today, 1997. **18**(10): p. 464-467.

80. Regnault, V., et al., *Both kinetic data and epitope mapping provide clues for understanding the anti-coagulant effect of five murine monoclonal antibodies to human beta(2)-glycoprotein I.* Immunology, 1999. **97**(3): p. 400-407.

81. Huber, A., S. Demartis, and D. Neri, *The use of biosensor technology for the engineering of antibodies and enzymes.* Journal of Molecular Recognition, 1999. **12**(3): p. 198-216.

82. Van Regenmortel, M.H.V., et al., *Measurement of antigen-antibody interactions with biosensors.* Journal of Molecular Recognition, 1998. **11**(1-6): p. 163-167.

83. Tromberg, B.J., et al., *Fiberoptic Chemical Sensors for Competitive-Binding Fluoroimmunoassay.* Analytical Chemistry, 1987. **59**(8): p. 1226-1230.

84.   Velander, W., Subramanian, A., Madurawe, RD., Orthner, C., *The use of Fab masking antigens to enhance the activity of immobilized antibody.* Biotechnology and Bioengineering, 1992. **39**: p. 1013-1023.

85.   Cohen, G.M.A.P.-. *Caspases: the executioners of apoptosis.* Biochem J., 1997. **326**(Pt 1): p. 1-16.

86.   Su, J., Anderson, AJ., Cummings, BJ., Cotman, CW., *Immunohistochemical evidence for apoptosis in Alzheimer's disease.* Neuroreport., 1994. **5**(18): p. 2529-2533.

87.   Casey, C., Nanji, A., Cederbaum, AI., Adachi, M., Takahashi, T., *Alcoholic liver disease and apoptosis.* Alcohol Clin Exp Res., 2001. **25**(5 Suppl ISBRA): p. 49S-53S.

88.   Yang, J., Liu, X., Bhalla, K., Kim, CN., Ibrado, AM., Cai, J., Peng, TI., Jones, DP., Wang, X., *Prevention of apoptosis by Bcl-2: release of cytochrome c from mitochondria blocked.* Science, 1997. **275**(5303): p. 1129-1132.

89.   Kluck, R., Bossy-Wetzel, E., Green, DR., Newmeyer, DD., *The release of cytochrome c from mitochondria: a primary site for Bcl-2 regulation of apoptosis.* Science, 1997. **275**(5303): p. 1132-1136.

90.   Nagata, S., *Apoptosis by Death Factor.* Cell, 1997. **88**: p. 355-365.

91.   Nakagawa, T., Zhu, H., Morishima, N., Li, E., Xue, J., Yanker, BA., Yuan, J., *Caspase-12 mediates endoplasmic-reticulum-specific apoptosis and cytotoxicity by amyloid-beta.* Nature, 2000. **403**: p. 98-103.

92.   Morishima, N., Nakanishi, K., Takenouchi, H., Shibata, T., Yasuhiko, Y., *An ER stress-specific caspase cascade in apoptosis: cytochrome c- independent activation of caspase-9 by caspase-12.* J. Biol. Chem., 2002. **277**: p. 34287-34294.

93.   Nicholson, D., and Thornberry, NA., *Caspases: killer proteases.* Trends Biochem Sci., 1997. **8**: p. 299-306.

94.   Kluck RM, B.-W.E., Green DR, Newmeyer DD,, *The release of cytochrome c from mitochondria: a primary site for Bcl-2 regulation of apoptosis.* Science, 1997. **275**(5303): p. 1132-6.

95.   Wang G.Q, G.B.R., Wieckowski E, Goldstein L.A, Gambotto A, Kim T.H, Fang B, Rabinovitz A, Yin X, Rabinowich H,, *A Role for Mitochondrial Bak in Apoptotic Response to Anticancer Drugs.* J. Biol. Chem., 2001. **276**: p. 34307-34317.

96.   Li P, N.D., Budihardjo I, Srinivasula S.M, Ahmad M, Alnemri E.S, Wang X,, *Cytochrome c and dATP-Dependent Formation of Apaf-1/Caspase-9 Complex Initiates an Apoptotic Protease Cascade.* Cell, 1997. **91**(4): p. 479-489.

97.   Zamzami N, M.P., Castedo M, Zanin C, Vayssiere JL, Petit PX, Kroemer G., *Reduction in mitochondrial potential constitutes an early irreversible step of programmed lymphocyte death in vivo.* J Exp Med, 1995. **181**(5): p. 1661-72.

98.   Fletcher GC, X.L., Passingham SK, Tolkovsky AM., *Death commitment point is advanced by axotomy in sympathetic neurons.* J Cell Biol, 2000. **150**(4): p. 741-754.

99.   Liu X, K.C., Yang J, Jemmerson R, Wang X., *Induction of apoptotic program in cell-free extracts: requirement for dATP and cytochrome c.* Cell, 1996. **86**(1): p. 147-57.

100.   Budihardjo I, O.H., Lutter M, Luo X, Wang X,, *Biochemical pathways of caspase activation during apoptosis.* Annu Rev Cell Dev Biol, 1999. **15**: p. 269-90.

101.   Dougherty, T., Gomer, CJ., Henderson, BW., Jori, G., Kessel, D., Korbelik, M., Moan, J., and Peng, Q., *Photodynamic therapy.* J. Natl. Cancer Inst., 1998. **90**: p. 889-905.

102.   Bissonnette, R., and Lui, H., *Current status of photodynamic therapy in dermatology.* Dermatol. Clin., 1997. **15**: p. 507-519.

103.   Kessel, D., Luo, Y., *Photodynamic therapy: a mitochondrial inducer of apoptosis.* Cell Death Differ., 1999. **6**: p. 28-35.

104.   Inoue S, S.-E.A.E., Omoteyama,, Human Cell, 2001. **14**(3): p. 211-221.

105.   Hinnen, P., de Rooij, FWM., van Velthuysen, MLF., Edixhoven, A., van Hillegersberg, R., Tilanus, HW . *Biochemical basis of 5-aminolaevulinic acid-induced protoporphyrin IX accumulation: a study in patients with (pre) malignant lesions of the oesophagus.* Br. J. Cancer, 1998. **78**: p. 679-682.

106.   Henderson, B., and Dougherty, TJ., *How does photodynamic therapy work?* Photochem Photobiol., 1992. **55**(1): p. 145-157.

107.   Vaux, D., Haecker, G., Strasser, A., *An evolutionary perspective on apoptosis.* Cell, 1994. **76**(5): p. 777-779.

108.   Kerr, J., Wyllie, AH., and Currie, AR., *Apoptosis: a basic biological phenomenon with wide-ranging implications in tissue kinetics.* Br. J. Cancer, 1972. **26**(4): p. 239-257.

109.   Hornung R, W.H., Crompton NE, Keefe KA, Jentsch B, Perewusnyk G, Haller U, Kochli OR,, *m-THPC-mediated photodynamic therapy (PDT) does not induce resistance to chemotherapy, radiotherapy or PDT on human breast cancer cells in vitro.* Photochemistry and Photobiology, 1998. **68**(4): p. 569-574.

110.   Hajri, A., Coffy, S., and Vallat, F., *Human pancreatic carcinoma cells are sensitive to photodynamic therapy in vitro and in vivo.* Br. J. Surg., 1999. **86**(7): p. 899-906.

111.   Noodt, B., Berg K., and Stokke T., *Apoptosis and necrosis induced with light and 5-aminolaevulinic acid-derived protoporphyrin IX.* Br. J. Cancer, 1996. **74**(1): p. 22-29.

112.   Teiten, M.-H., Marchal, S., D'Hallewin, MA., Guillemin, F., and Bezdetnaya, L., *Primary Photodamage Sites and Mitochondrial Events after Foscan® Photosensitization of MCF-7 Human Breast Cancer Cells.* Photochemistry and Photobiology, 2003. **78**(1): p. 9.

113.   Schmitt, E., *Activation and role of caspases in chemotherapy-induced apoptosis.* Drug Resistance Updates, 1999. **2**: p. 21-29.

114.   Li, P., Nijhawan, D., Budihardjo, I., Srinivasula, SM., Ahmad, M., Alnemri, ES., Wang, X., *Cytochrome c and dATP-Dependent Formation of Apaf-*

1/Caspase-9 Complex Initiates an Apoptotic Protease Cascade. Cell, 1997. **91**: p. 479-489.

115. Kolárová, H., Kubínek, R., Lenobel, R., Bancírová, M., Strnad, M., Jírová, D., Lasovský, J., *In vitro photodynamic therapy with phthalocyanines on the MCF7 cancer cells.* Internet Journal of Photochemistry and Photobiology., 1999: p. http://www.photobiology.com/photo99/contrib/kolarova/index.htm.

116. Bachmann-Moisson, N., Vandoeuvre-les, N., Barberi-Heyob, M., Gramain, MP., Bour, C., Marchal, S., Parache, RM., Guillemin, FH., Merlin, JL. *Evaluation of interacellular tamoxifen-induced fluorescence in tamoxifen-resistant human breast adenocarcinoma cells, pp.308-312.* in *SPIE: Optical Biopsies and Microscopic Techniques II.* 1997. San Remo, Italy: SPIE--The International Society for Optical Engineering.

117. Sasai K, Y.H., Suzuki F,, Jpn. J. Cancer Res, 2002. **93**: p. 275-283.

118. McNeil, P., *Cellular and molecular adaptations to injurious mechanical stress.* Trends Cell Biol., 1993. **3**(9): p. 302-307.

119. Ghosh, A., Greenberg, ME., *Calcium Signaling in Neurons: Molecular Mechanisms and Cellular Consequences.* Science, 1995. **268**(5208): p. 239-247.

120. Hilf, R., Havens, JJ., Gibson, SL., *Effect of Aminolevulinic Acid on Protoporphyrin IX Accumulation in Tumor Cells Transfected with Plasmids Containing Porphobilinogen Deaminase DNA.* Photochemistry and Photobiology, 1999. **70**(3): p. 334-340.

121. Tikkanen, M., Carter, DJ., Harris, AM., Le, HM., Azorsa, DO., Meltzer, PS., and Murdoch, FE., *Endogenously expressed estrogen receptor and coactivator AIB1 interact in MCF-7 human breast cancer cells.* PNAS, 2000. **97**(23): p. 12536-12540.

122. Brasuel, M., Kopelman, R., Miller, TJ., Tjalkens, R., Philbert MA.,, *Fluorescent nanosensors for intracellular chemical analysis: decyl methacrylate liquid polymer matrix and ion-exchange-based potassium PEBBLE sensors with real-time application to viable rat C6 glioma cells.* Anal Chem., 2001. **73**(10): p. 2221-8.

123. Vo-Dinh, T., *Nanobiosensors: Probing the Sanctuary of Individual Living cells.* J Cellular Biochemistry, Supp 161, 2002. **39**: p. 154.

124. Mehmet, H., *Apoptosis: Caspases find a new place to hide.* Nature, 2000. **403**(6765): p. 29-30.

125. Liu, X., Kim, CN., Yang, J., Jemmerson, R., and Wang, X., *Induction of apoptotic program in cell-free extracts: Requirement for dATP and Cytochrome c.* Cell, 1996. **86**(1): p. 147-157.

126. Deveraux, Q.L., Roy, N., Stennicke, H.R., Van Arsdale T, Zhou Q, Srinivasula, S.M., Alnemri, E.S., Salvesen, G.S., Reed, J.C., *IAPs block apoptotic events induced by caspase-8 and cytochrome c by direct inhibition of distinct caspases.* EMBO J, 1998. **17**(8): p. 2215-23.

127. Sun, X., MacFarlane, M., Zhuang, J., Wolf, BB., Green, DR., Cohen, GM., *Distinct caspase cascades are initiated in receptor-mediated and chemical-induced apoptosis.* J Cell Biol, 1999. **274**(8): p. 5053-5060.

128. MacFarlane, M., Cain, K., Sun, XM., Alnemri, ES., Cohen, GM., *Processing/activation of at least four interleukin-1beta converting enzyme-like proteases occurs during the execution phase of apoptosis in human monocytic tumor cells.* J Cell Biol, 1997. **137**(2): p. 469-79.

129. Hengartner, M.O., *Apoptosis. DNA destroyers.* Nature, 2001. **412**(6842): p. 27.

130. Sportsman, J., Wilson, GS., *Chromatographic properties of silica-immobilized antibodies.* Anal Chem, 1980. **52**(13): p. 2013-2018.

131. Lin, J., Herron, J., Andrade, JD., IEEE Trans. Biomed. Eng, 1988. **35**: p. 466-471.

132. Dragovich T, R.C., Thompson CB., *Signal transduction pathways that regulate cell survival and cell death.* Oncogene, 1998. **17**(25): p. 3207-3213.

133. Mantzaris, N., Daoutidis, P., Srienc, F., and Fredrickson, AG. *Growth Processes in a Cascade of Bioreactors: Comparison of Modeling Approaches.* in *AIChE J.* 1999.

134. Thornberry, N., Lazebnik, Y., *Caspases: Enemies within.* Science, 1998. **281**: p. 1312-1316.

135. Budihardjo, I., Oliver, H., Lutter, M., Luo, X., and Wang, X., *Biochemical Pathways of caspase activation during apoptosis.* Annu. Rev. Cell. Dev. Biol., 1999. **15**: p. 269-290.

136. Mattson, M., Guo, Q., Furukawa, K., Pedersen, WA., *Presenilins, the endoplasmic reticulum, and neuronal apoptosis in Alzheimer's disease.* J Neurochem., 1998. **70**(1): p. 1-14.

VITA

Paul Misiko Kasili was born on May 2nd 1973 to Prof. Edward G. Kasili and Speranza K. Kasili in Nairobi, Kenya. He obtained his primary education at Flora Hostel Nursery and Consolata School respectively, and his secondary education at Lenana School. After completing his secondary school education, he was accepted to the College of Physical and Biological Sciences, University of Nairobi-Kenya where he majored in Chemistry and Zoology. After completing two years at the University of Nairobi, Paul transferred to a liberal arts college, Coe College in Cedar Rapids, Iowa where he majored in Chemistry and minored in Biochemistry. At the spring 1998 commencement ceremony, Paul was awarded a B.A. degree in Chemistry and Biochemistry from Coe College where he graduated *cum laude*. In the fall of 1998, he was accepted to the Graduate School of Arts and Sciences, University of Tennessee-Knoxville, to pursue a Ph.D. in Biomedical Sciences with the great opportunity to be involved in cutting edge biomedical research and work with Dr. Tuan Vo-Dinh. The cutting edge biomedical research performed in Dr. Vo-Dinh's research group matched perfectly with Paul's interest in multidisciplinary research involving the application of analytical techniques and technologies to the solution of biological problems. On December 2nd 2003, Paul successfully defended his doctoral dissertation, entitled, "*The Development of Optical Nanosensor Technology for Single Cell Analysis.*" He will receive a Doctor of Philosophy degree in Biomedical Sciences, which will be awarded at the University of Tennessee-Knoxville commencement ceremony in the spring of 2004.